이학박사학위논문

고추의 C3HC4 형 RING Zinc Finger Protein 의 기능 연구

Functional Characterization of C3HC4-type RING Zinc Finger Protein Gene from Hot Pepper

2017년 8월

서울대학교 대학원

생명과학부

마히팔 싱

Functional Characterization of C3HC4-type RING Zinc Finger Protein Gene from Hot Pepper

by
Mahipal Singh
under the supervision of
Professor Choo Bong Hong

A Thesis Submitted in Partial Fulfillment
of the Requirements for the Degree of
Doctor of Philosophy

August, 2017

School of Biological Sciences
Graduate School
Seoul National University

Abstract

RING finger is a cysteine-rich domain (40–60 residues) in which cysteine and histidine residues ligated with two zinc ions in a cross-brace manner to stabilize the domain structure. RING finger proteins play a crucial role in diverse biological processes such as transcriptional activation, recombination of DNA, translational processes, signal transduction, programmed cell death, membrane association, and protein folding and assembly. RING finger proteins have also been implicated in various and fundamental functions in plant growth and development. Although, RING finger proteins have been closely and repeatedly involved in the development of multiple organisms, however, cases reported in plants are comparatively limited. *Capsicum annuum RING Zinc Finger Protein 1* (*CaRZFP1*) is a C3HC4-type RING zinc finger protein gene previously isolated from a cDNA library of heat-stressed hot pepper. Expression of *CaRZFP1* was also induced by diverse abiotic stresses including cold, dehydration and high salinity in hot pepper. Transcript induction kinetics of *CaRZFP1* was distinct in different plant parts of hot pepper. In our previous work elucidating *in vivo* function of *CaRZFP1*, we transferred *CaRZFP1* into tobacco (*Nicotiana tabacum*); transgenic tobacco exhibited enhanced growth and tolerance to abiotic stresses. As further analysis of *CaRZFP1* ectopic expression in a heterologous host plant, this study, I mobilized and constitutively overexpressed *CaRZFP1* into lettuce (*Lactuca sativa*). In contrast to tobacco, transgenic lettuce exhibited poorer growth and delayed flowering compared with vector-only controls; characteristics included weakened leaf growth, shorter plant height, and stunted root growth. Thus, ectopic expression of *CaRZFP1* caused pleiotropic

developmental changes in the *CaRZFP1*-transgenic lettuce plants. In addition, I found a significant correlation between *CaRZFP1* expression and the degree of diminished growth of *CaRZFP1*-transgenic lettuce plants. Starting from T_2, I categorized transgenic lettuce lines according to *CaRZFP1* transcript expression levels (low, medium, and high). The correlation between *CaRZFP1* transcript level and a negative phenotypic effect was repeatedly maintained through the next generations of *CaRZFP1*-transgenic lettuce plants. Overall, *CaRZFP1* expression impeded the growth and development of *CaRZFP1*-transgenic lettuce plants in a dose-dependent fashion. The weaken growth of *CaRZFP1*-transgenic lettuce plants continued to the late stage of development. At full growth, *CaRZFP1*-transgenic lettuce was shorter than vector-only plants. *CaRZFP1*-transgenic lettuce delayed in flowering and inflorescence size was smaller compared to vector-only plants. Flower size did not differ significantly between the transgenic and control lines, but the former head significantly fewer flowers per inflorescence.

To examine the retarded growth of *CaRZFP1*-transgenic lettuce and the robust growth of *CaRZFP1*-transgenic tobacco at the cellular level, I analyzed leaf, stem, and root sections of both plants and compared them with vector-only controls. The cross sections of leaves and stems of *CaRZFP1*-transgenic lettuce and vector-only lettuce were not distinguishable in terms of morphology, cell size, or tissue organization. However, the development of endodermis and vascular bundles was significantly hampered by *CaRZFP1* expression in transgenic lettuce roots. Remarkably, I observed a strong correlation, albeit negative, between the expression level of *CaRZFP1* and the degree of disruption of internal root morphology. The overall root morphology and tissue patterns were preserved in *CaRZFP1*-transgenic tobacco roots. *CaRZFP1* over-expression effect on the abiotic stress tolerance in *CaRZFP1*-transgenic lettuce plants was also examined, but no significant

differences were observed between the *CaRZFP1*-transgenic lettuce and vector-only plants. To identify genes that might be involved in this phenotypic effect, transcriptome analyses on transgenic plants of both species were performed, uncovering dozens of genes that reflect the different outcomes between tobacco and lettuce. In particular, the strong negative correlation between *CaRZFP1* expression and growth in lettuce helped us isolate genes most likely involved in the phenotypic differences. These included protein kinase, transcriptional factor, transporter protein, hormone and metabolism-related genes, and some unannotated genes. I separated the up- and down-regulated genes into two groups: "Group 1" included genes with correlative changes in expression level among the four *CaRZFP1*-transgenic lettuce lines (#6, #14, #16 and #12), while "Group 2" included only genes with significant expression-level changes mainly in line #12 (highest *CaRZFP1* expression). To validate the transcriptome profiling results, nine genes were randomly selected for oligo-RNA blot analysis either significantly up- or down-regulated in transgenic lettuce lines. Oligo-RNA blot results showed that the trends of the differentially expressed genes were generally consistent across the two different approaches. Therefore, collectively these results showed that a gene with a specific function in one organism can yield completely different effects depending on the host species it is moved into and address concerns of unexpectedly different outcome of a gene in different genetic environments.

Key Words*;* ZFPs, RING finger protein, *Lactuca sativa*, abiotic stresses, transgenic lettuce plants, over-expression, RNA blot analyses, *in situ* hybridization, transcriptome profiling, endodermis and vascular bundles

Student Number: 2010-31292

Contents

Abstract i

Contents iv

List of figures viii

List of tables ix

Abbreviation x

Chapter I. Introduction 1

I.1. Role of zinc in biology 5

I.2. Zinc Finger motif 5

I.3. Zinc finger domains structure and classification 8

I.4. Biological functions of ZFPs 12

I.4.1. ZFPs implicated in nucleic acid interactions 13

I.4.1.1. ZFPs interact with DNA 13

I.4.1.2. ZFPs interact with RNA 16

I.4.2. ZFPs interact with protein and lipid 18

I.5. RING finger proteins 20

I. 6. Aims of this study. 25

Chapter II. Materials and Methods 26

II.1. Plant material and growth condition 27
II.2. Abiotic stresses treatment 27
II.3. Generation of transgenic lettuce plants overexpressing *CaRFZP1* 28
II.4. RNA and DNA blot analyses 29
II.5. Phenotypic assay 31
II.6. Thermotolerance assay 32
II.7. Cold tolerance assay 32
II.8. Drought tolerance assay 32
II.9. Histological and *in situ* hybridization analyses 33
II.10. Transcriptome analysis 35
II.11. Multiple sequence alignment and phylogenetic analysis 36

Chapter III. Results……37

III.1. Sequence homology and phylogenetic analyses of hot pepper CaRZFP1 with other zinc finger protein genes 38
III.2. Expression of *CaRZFP1* was induced widely in different tissues of hot pepper plants in response to various abiotic stresses 43
III.3. Genomic DNA blot analysis of hot pepper 46
III.4. Generating transgenic lettuce plants overexpressing *CaRFZP1* 48

III.5. Growth of *CaRZFP1*-transgenic lettuce plants were retarded 51

III.6. Root growth of *CaRZFP1*-transgenic lettuce plants was impeded 56

III.7. *CaRZFP1*-transgenic lettuce plants were shorter in full growth and flowering was delayed 58

III.8. Development of endodermis and vascular bundle was impaired in the *CaRZFP1*-transgenic lettuce roots 62

III.9. *CaRZFP1*-transgenic lettuce plants were intolerant to abiotic stress 71

III.10. Transcriptome profiles of *CaRZFP1*-transgenic lettuce plants 77

Chapter IV. Discussion……....99

Conclusion……..……...121

References……..……...123

Abstract in Korean……..……...145

List of Figures

Figure 1. Different structural motif of DNA binding domains 4
Figure 2. Three-dimensional structure of classical C2H2 zinc finger motif 7
Figure 3. Topologies and structures of different zinc finger domain containing proteins 9
Figure 4. Schematic representations of a C2H2 zinc finger domain interact with stretch of DNA target site 14
Figure 5. Overview of the ubiquitin-mediated protein degradation pathway 23
Figure 6. Sequence comparison of CaRZFP1 with other zinc finger proteins 39
Figure 7. Phylogenetic analysis of CaRZFP1 with other zinc finger proteins 41
Figure 8. Predicted transmembrane domain in CaRZFP1 protein 42
Figure 9. Temporal expression patterns of *CaRZFP1* transcript in response to diverse environmental stresses in different tissues of hot pepper plants 44
Figure 10. Genomic DNA blot analysis of hot pepper genome 47
Figure 11. Generation of *CaRFZP1* over-expressed transgenic lettuce plants 49
Figure 12. *CaRZFP1* over-expressing transgenic lettuce plants showed hampered growth and development 53

Figure 13. Phenotype and root development of the *CaRZFP1*-transgenic lettuce and vector-only plants.....57
Figure 14. Hampered growth and development *CaRZFP1* over-expressing transgenic lettuce plants extended to the reproductive stage.....59
Figure 15. Cytological comparisons of *CaRZFP1*-transgenic and vector-only lettuce plants. 64
Figure 16. Abiotic tolerance assay of transgenic lettuce plants. 73
Figure 17. Comparison of relative expression levels of transcripts induced or suppressed in *CaRZFP1*-transgenic lettuce and vector-only lines. 80
Figure 18. Differentially expressed genes in *CaRZFP1*-transgenic lettuce and tobacco plants were categorized into several groups according to their putative functions.....94
Figure 19. Overlap of differentially expressed genes in *CaRZFP1*-transgenic lettuce line #6, #14 and #12. 95
Figure 20. Possible function of *CaRZFP1* in impaired development of endodermis and vascular bundle development as well as in retarded growth and development of *CaRZFP1*-transgenic lettuce plants.....96
Figure 21. RNA blot hybridization results using oligonucleotides for the differentially expressed transcripts in the *CaRZFP1*-transgenic and vector-only lettuce plants to confirm transcriptome profile data produced by microarray analysis 97

List of tables

Table 1. Classification and structural properties of various ZFPs 11

Table 2. Genes up-regulated in *CaRZFP1*-overexpressing T_4 generation lettuce plants 82

Table 3. Genes down-regulated in *CaRZFP1*-overexpressing T_4 lettuce plants 89

Table 4. Oligonucleotides used in RNA blot analyses 93

Table 5. Up-regulated genes in *CaRZFP1*-overexpressing T_2 tobacco plants 115

Table 6. Down-regulated genes in *CaRZFP1*-overexpressing T_2 tobacco plants 117

Abbreviations

aa	**amino acids**
CaRZFP1	***Capsicum annuum RING Zinc Finger Protein 1***
bp	**base pairs**
BSA	**bovine serum albumin**
cDNA	**complementray DNA**
cRNA	**complementray RNA**
Cys	**cysteine**
dATP	**deoxyadenosine triphosphate**
dCTP	**deoxycytidine triphosphate**
DEPC	**diethyl pyrocarbonate**
DNA	**deoxyribonucleic acid**
DNase	**deoxyribonuclease**
dNTP	**deoxynucleotide triphosphate**
dsDNA	**double stranded DNA**
DTT	**dithiothreitol**
EDTA	**ethylenediaminetetraacetic acid**
His	**histidine**
Kan	**kanamycin**
kb	**kilobase pair**
Leu	**leucine**
LiCl	**lithium chloride**
NaCl	**sodium chloride**
nt	**nucleotide**

NTP	**nucleoside 5-triphosphates**
MS	**murashige-skoog**
PEG	**polyethylene glycol**
PBS	**Phosphate-buffered saline**
PCR	**polymerase chain reaction**
Phe	**phenylalanine**
RNA	**ribonucleic acid**
RNase	**ribonuclease**
RT-PCR	**reverse transcriptase polymerase chain reaction**
SDS	**sodium dodecyl sulfate**
SSC	**saline sodium citrate**
SSPE	**saline sodium phosphate-EDTA**
TE	**Tris.HCL/EDTA**
tRNA	**transfer RNA**
Tyr	**tyrosine**
µg	**microgram**
µm	**micrometer**
UV	**ultraviolet**
Zn	**zinc**

CHAPTER I

INTRODUCTION

Developmental processes are regulated by cooperative interactions between DNA, RNA, and protein throughout the evolution of life. Intricate regulatory gene network establishes the spatiotemporal pattern which determines the different morphogenetic events in multicellular organisms during growth and development. Gene expression is mainly regulated at the point of transcriptional initiation in all living known organisms. Transcription factors (TFs) play a critical role in gene regulation. The expression of all genes requires binding of general transcription machinery at promoter regions and gene specific TFs at the *cis*-regulatory sequence of the adjacent DNA to the regulated gene (Wray *et al.*, 2003; Lee & Young, 2000). The binding of TFs on these specific DNA regions affects the rate of transcription initiation either in the activation or repression of gene expression (Howard and Davidson, 2004). TF contains several different types of functional domains, for instance, DNA-binding domains, protein-protein interaction domains, nuclear localization signals, and ligand-binding domains. These domains play a crucial role in the gene regulation (Lee & Young, 2000). TFs are classified into different families based on their DNA binding domains with characteristic amino acid sequences and three-dimensional structures (Figure 1). Cro, CAP, and λ–repressor were first TFs identified, containing a helix-turn-helix DNA-binding domain (Anderson *et al.*, 1981; Mckay and Steitz, 1981; Pabo and Lewis, 1982). Later other structural motifs were identified as the zinc finger (Miller *et al.*, 1985), helix-loop-helix (Littlewood & Evan, 1995), homeodomain protein (Gehring *et al.*, 2002; Burglin & Affolter, 2016), leucine zipper (Vinson *et al.*, 2002) and several other motifs (Figure 1). Most of the DNA binding domain use of a two-fold symmetric to bind DNA double helix and form a dimer or tetramer complex for DNA-binding. However, the zinc finger domain has recently received much attention

because of its different mode of DNA recognition (Pavletich & Pabo, 1991; Klug, 2010). Zinc fingers can be connected linearly in tandem fashion to recognize nucleic acid (DNA or RNA) sequences of variable length. This modular usage of each finger with a different nucleic acid binding specificity, offer a large number of combinatorial possibilities for sequence-specific recognition of nucleic acids. Therefore, it may explain why do ZFPs ubiquitously exist in nature, including 3%, 2.3%, 2.2% and 1.5% all genes of the human, mouse drosophila and Arabidopsis genome (Papworth *et al.*, 2006; Klug, 2010).

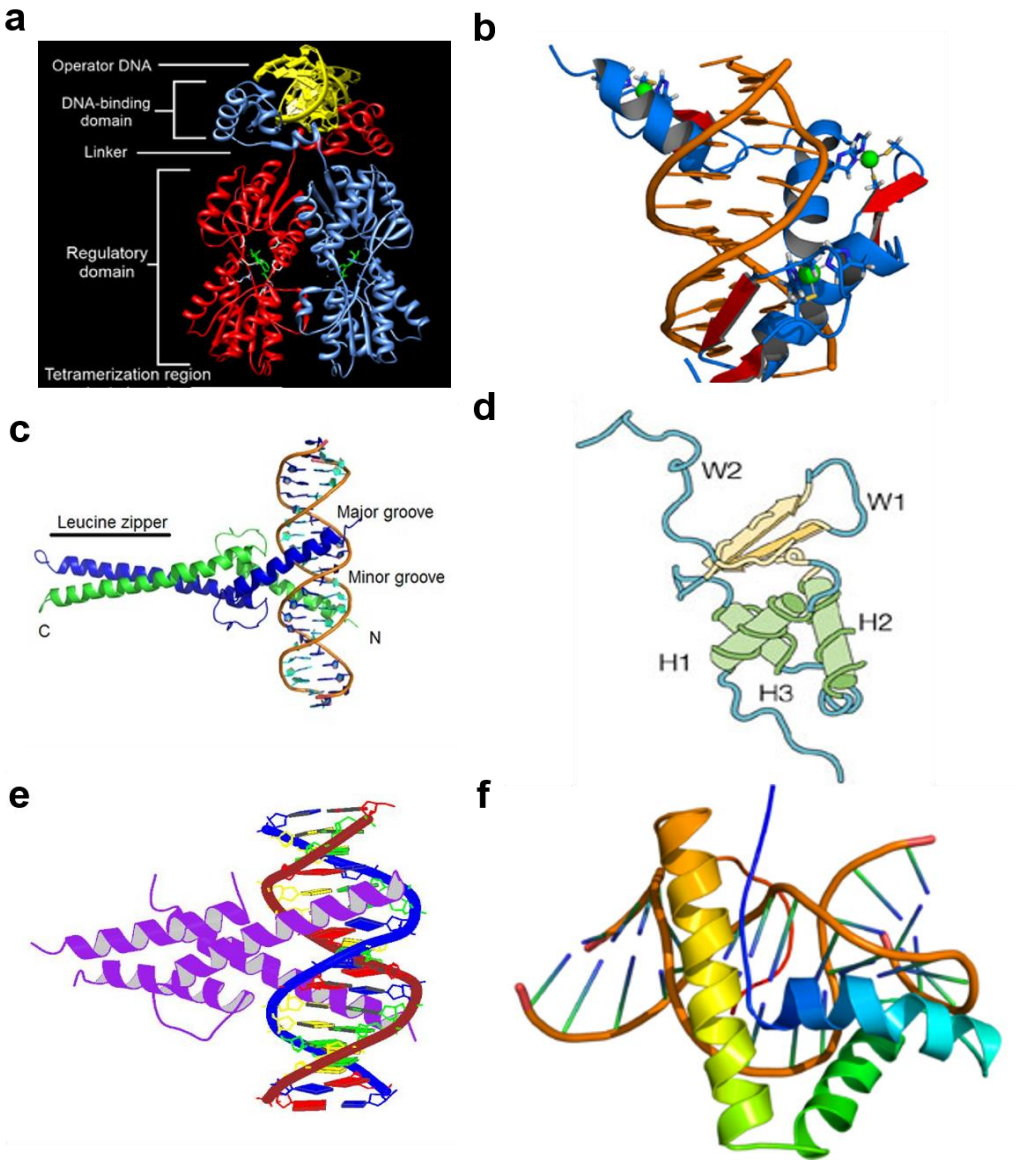

Figure 1. Different structural motif of DNA binding domains. Transcription factors classified into different families based on their DNA binding domain. **a.** The helix-turn-helix motif with DNA. **b.** zinc finger motif. **c.** leucine zipper motif. **d.** Winged helix motif. **e.** helix-loop-helix motif. **f.** HMG box motif (Deplancke *et al.,* 2016).

I.1. Role of zinc in biology

Zinc is an essential metal element has been implicated in a wide variety of cellular processes including cellular metabolism, signal transduction, gene expression, apoptosis, growth and development (Frassinetti *et al*., 2006; Meyer & Kieffer, 2015). Zinc ion consist specific chemical properties: (1) zinc has flexible coordination sphere which can accommodate numerous geometries such as tetrahedral, pentahedral and octahedral depending on the protein and metal binding site (2) zinc is redox inactive (3) its exchange kinetics faster in a negatively charged environment and also influenced by different coordination sites. Owing to these unique characteristic of zinc, selected as the cofactor by evolution to perform efficient enzymatic reactions and stabilize the structure in many proteins (Meyer & Kieffer, 2015). Moreover, histidine, cysteine, glutamate and aspartate are mostly found within the zinc coordination sphere in numerous proteins. Zinc coordination is crucial for folding, structural stability, functional and catalytic activity of metalloproteins (Houben *et al.,* 2005). The human proteome also contains 10% zinc binding proteins while bacteria and archaeans hold only 6%, indicating that zinc plays a critical role in fundamental processes of life (Andreini *et al*., 2006).

I.2. Zinc finger motif

The zinc finger domain in zinc finger proteins (ZFPs) consists of 20–100 residues and is found ubiquitously from prokaryotes to eukaryotes (Takatsuji, 1999; Krishna *et al.,* 2003; Matthews *et al.,* 2009). The term "zinc finger" refers to a type of protein structure held together by one or more zinc ion in order to stabilize the domain structure which resembles finger-like shape and originated the birth certificate of a large family of proteins named

ZFPs (Takatsuji, 1998; Kielbowicz-Matuk 2012). ZFP was first identified as a repeated motif in transcription factor IIIA (TFIIIA) in the African clawed (*Xenopus laevis*) oocytes (Miller *et al.,* 1985). Amino acid sequencing of TFIIIA revealed nine tandem sequences of 30 amino acids and existence of several zinc ions. This domain often described as a consensus amino acid sequence, (Tyr, Phe)-X-Cys-X2-4-Cys-X3-Phe-X5-Leu-X2-His-X3-5-His, where Tyr represents tyrosine; Phe, phenylalanine; Cys, cysteine; Leu, leucine while X represents any amino acids (Wolfe *et al.,* 1999). Later, three-dimensional structures showed that two invariant of cysteine on the β-sheet hairpin and two histidines in the α-helix bound to a zinc ion which is required for the protein fold and structure stability (Pavletich & Pabo, 1991). Each domain folds into the left-handed ββα secondary structures. Thus, this type of ZFP also called classical C2H2 (Figure 2). In addition, three other conserved amino acids tyrosine, phenylalanine and leucine also have been involved to form a hydrophobic structural core to the adjacent zinc binding site of the folded structure. Cysteine, histidine and hydrophobic amino acids highly conserved in the ZFPs while other residues show great sequence diversity (Gamsjaeger *et al.*, 2007).

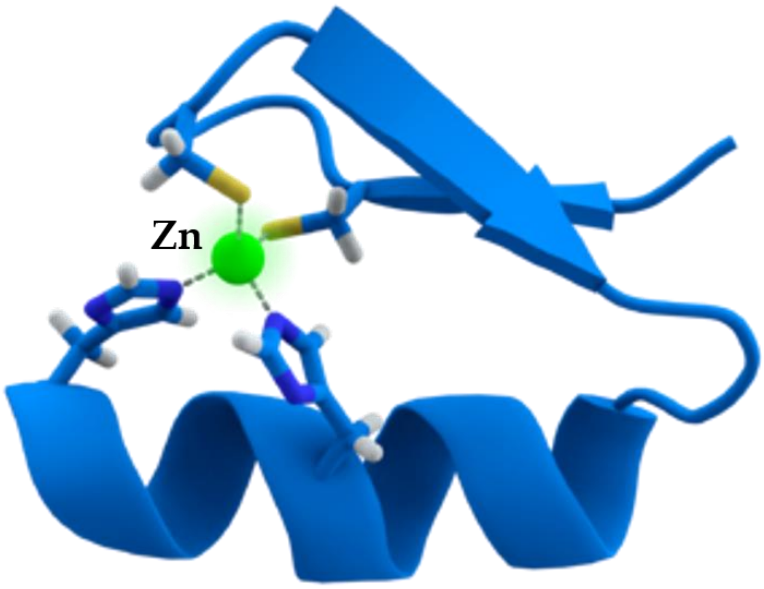

Figure 2. Three-dimensional structure of classical C2H2 zinc finger motif. The C2H2 ZFP contains an α-helix and an antiparallel β-sheet. The zinc ion (green) is coordinated by two histidine and two cysteine amino acids to stabilize functional domain of C2H2 (Splettstoesser, 2007).

I.3. Zinc finger domains structure and classification

ZFPs comprise a large and diverse gene family with considerable variation in structure and recognition sequences (Laity *et al.,* 2001). Originally, zinc fingers were classified based on the number and order of the cysteine and histidine residues that brought the types of Cys_2His_2, Cys_4, Cys_6, and so on. Recent grouping of ZFPs uses characteristics of the folded domain of the protein backbone (Laity *et al.,* 2001; Krishna *et al.,* 2003; Gamsjaeger *et al.,* 2007; Matthews *et al.,* 2009). Different classes of ZFPs have different structural features (Figure 3; Table 1). The most common "fold groups" of zinc fingers are the Cys_2His_2-like (the classic zinc finger), treble clef, and zinc ribbon. The classical C2H2 ZFP composed of antiparallel β-sheet and α-helix to form a ββα structure which is coordinate by a zinc ion in either a Cys-Cys-His-His or a Cys-Cys-His-Cys manner (Figure 3a). In this protein, individual zinc finger motifs are often found in contiguous as tandem repeats with two, three, or more fingers. Some classes of ZFPs such as nuclear hormone receptors (GATA) and LIM ZFPs contain a common core fold structure called the treble-clef motif. The treble-clef motif made up of a β- hairpin at the N-terminus containing the sequence Cys-x-x-Cys, followed by a connecting β-hairpin and an α-helix at C-terminal containing Cys-x-x-Cys sequence (Figure 3b and c). Each domain binds to the two zinc ions, although a loop and a second β-hairpin of varying length and conformation. These zinc fingers found in numerous proteins; however, these ZFPs do not share sequence or functional similarity with each other. Another class of ZFPs belongs to zinc ribbon fold group contain two beta-hairpins making two structurally similar zinc-binding sub-sites (Figure 3d).

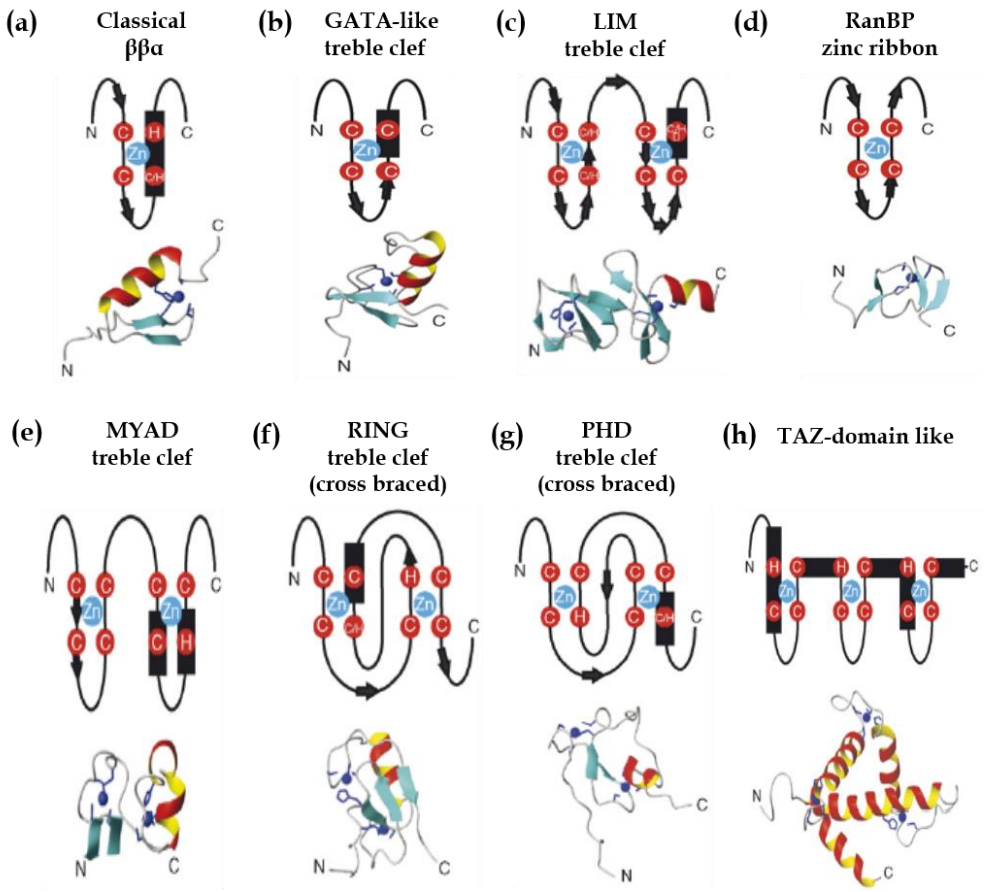

Figure 3. Topologies and structures of different zinc finger domain containing proteins a. representative example of classical ββα (C2H2). **b.** treble clef (GATA-like). **c.** treble clef (LIM). **d.** zinc ribbon (RanBP). **e.** treble clef (MYND). **f.** cross-braced-treble clef (RING). **g.** cross-braced-treble clef (PHD). **h.** TAZ-domain like (Gamsjaeger *et al.,* 2007).

The zinc ribbons are the largest fold group of ZFPs found in a diverse group of proteins and showed limited sequence similarity. This restricted sequence conservation is reflected in the structural variability of zinc ribbons (Krishna *et al.,* 2003). All ZFPs needed one or more zinc ions to bound by Cys, His and occasionally with aspartate or glutamate amino acids to fold the domain into finger-like shape. The numbers of zinc ions coordinated in different ZFPs are variable (Figure 3; Table 1). Some ZFPs coordinate with only a one zinc ion for instance, C2H2, GATA, A20, ZnF UBP, and RanBP ZFPs, whereas LIM (Lin-11, Isl-1, Mec-3), MYND (myeloid, Nervy, DEAF-1), RING (Really interesting new gene) and PHD (Plant homology domain) coordinate with two zinc ions (Freemont *et al.,* 1991; Lovering *et al.,* 1993; Ansieau & Leutz, 2002; Kadrmas & Beckerle, 2004; Spadaccini *et al.,* 2006; Dul and Walworth, 2007). LIM domains comprise two sequential zinc-binding modules that resemble the treble-clef GATA-type fold (Figure 3c). The consensus sequence is rather variable: cysteine, histidine, aspartate and glutamate residues are all known to be involved in zinc coordination, and the loops between zinc ligands differ in length. LIM proteins have been implicated in a wide range of biological functions, including cell adhesion, gene expression, cytoskeleton organization, growth and development (Kadrmas & Beckerle, 2004). MYND domains also bound by two zinc ions, but they are smaller domain (~40 amino acids) compared to the LIM domains (~55 amino acids). The first zinc-binding module contains only a short β hairpin, whereas the second zinc-binding module forms two short α helices (Figure 3e). MYND domains mostly involved in protein-protein interaction and found in transcriptional regulators (Spadaccini *et al.,* 2006).

Table 1. Classification and structural properties of various zinc finger proteins

Zinc finger class	Zinc ion ligation	Protein fold	Interacting biomolecules
C_2H_2	CC-H (C/H)	classical ββα,	DNA, RNA, protein
GATA	CC-CC	treble clef	DNA, protein
Nuclear hormone receptor	CC_A-CC_A-CC_B-CC_B	treble clef	DNA
RanBP	CC-CC	zinc ribbon	Ubiquitin, RNA
ZnF UBP	CC-CH	treble clef	Ubiquitin
A20	CC-CC	treble clef	Ubiquitin
LIM	CC_A-$(C/H)(C/H)_A$-CC_B-$C(C/H/D/E)_B$	treble clef	Protein
MYND	CC_A-CC_A-CC_B-HC_B	treble clef	Protein
RING	CC_A-CH_B-$(C/H)C_A$-CC_B	treble clef (cross braced	Protein
PHD	CC_A-CC_B-HC_A-$C(C/H)_B$	treble clef (cross braced)	Histone protein, ubiquitin
FYVE	CC_A-CC_B-CC_A-CC_B	treble clef (cross braced)	Lipid
Protein Kinase C	H_A-CC_B-CC_A-$(H/D)C_B$-C_A	treble clef (cross braced)	Diacylglycerol, phorbol ester
TAZ	HC_A-CC_A-HC_B-CC_B-HC_C-CC_C	TAZ-domain-like	Protein

C represents cysteine; H, histidine; D, aspartate; E, glutamate while subscript A, B, C symbolize different zinc ions bound in a zinc finger domain

RING finger is a cysteine-rich domain in which cysteine and histidine residues ligated with two zinc ions in a cross-brace manner. RING finger domain composed of single three stranded anti-parallel β-sheet and an α-helix associated by long loops (Figure 3f). RING motif plays key role ubiquitin-mediated protein degradation. PHD domains are structurally related to RING finger. PHD domain composed of a two-stranded β-sheet and an α-helix bound by two zinc ions to stabilize the PHD domain and also support by the hydrophobic amino acid which is highly conserved tryptophan (Trp335) in all PHD domains (Figure 3g). PHD domain has been involved in the regulation of gene transcription (Dul and Walworth, 2007). The transcriptional adaptor zinc-binding (TAZ) domain is the only ZFP that bound with three zinc ions (Ponting *et al.,* 1996). TAZ domain found in transcriptional coactivator CBP and p300 in which two copies of TAZ domains fold into the peculiar way. The three zinc ions bound to one histidine and three cysteine ligands in an HCCC motif, while each zinc ion exists in the intervening loop region of the two antiparallel α-helixs and the next helix (Figure 3h). TAZ domain has been interacted with various transcription factors and viral oncoproteins (Blobel, 2000).

I.4. Biological functions of ZFPs

ZFPs comprise a large and diverse gene family with considerable variation in structure and recognition sequences due to their structural diversity. ZFPs were first discovered as a DNA-binding domain in TFIIIA from *Xenopus laevis*, however, now they have been linked to various important biological functions by interacting with DNA, RNA, and proteins (Laity *et al.,* 2001; Matthews & Sunde, 2002; Gamsjaeger *et al.,* 2007).

I.4.1. ZFPs implicated in nucleic acid interactions

ZFPs well defined for their different binding abilities to DNA, RNA, protein and small biomolecules (Gamsjaeger *et al.,* 2007). However, ZFPs are best known for sequence-specific nucleic acid binding proteins. ZFPs are often occurring in clusters with two, three or more fingers and each finger have different binding specificities. ZFPs demonstrated considerable versatility in binding style even among the members of the same class; some of them bind to DNA while others bind to RNA, protein and lipid indicated that ZFPs evolved with diverse functions.

I.4.1.1. ZFPs interact with DNA

ZFPs are well known for its ability to interact with specific DNA sequence to activate or repress gene expression (Klug, 2010). To understand, how do ZFPs bind to specific DNA sequence? The breakthrough came in 1991 about this interaction, when the first crystal structure of a DNA–ZFP complex (Zif268, an early response gene) was resolved by Pavletich & Pabo (1991). Most of the C2H2 ZFPs functions as transcription factors bind to specific DNA sequences. Each finger interacts (α-helix also called as recognition helix) to the major groove of DNA helix through hydrogen bonds using amino acid residues in α-helix at the positions −1, 3, and 6 to typically space at 3-bp intervals on one strand of the DNA while on the other strand of the DNA at position 2 (Figure 4). Other interactions were also observed there on the invariant His and the 5′ phosphate DNA backbone, however, these interactions not involved in specific recognition of DNA sequences. Although amino acid residues in the recognition α-helix determine the DNA binding specificities, but inter-finger linker sequence (TGEKP) also contribute to increase their DNA-binding affinity. Once ZFPs bind to the correct DNA sequence, the linkers adopt a helix-capping structure to hold fingers in the proper orientation for optimal interactions and stabilization of DNA-ZFP

complexes.

Site-directed mutagenesis studies revealed that single nucleotide mutation can reduce the ZFPs binding affinity up to 20-fold (Choo and Klug, 1993). ZFPs are often found in contiguous tandem repeats to accomplish higher recognition specificity of a longer sequence of DNA. Each finger have different sequence specificity as well as act as independently, hence, fingers with different triplet sequence can be linked to binding specific DNA sequence. This typical characteristic of the ZFPs has endorsed the *de novo* design of DNA-binding proteins for specific DNA sequences, alter the key amino acids in the α-helical to modulate the DNA-binding specificity of individual zinc fingers. However, to avoid the chance to bind to the nonspecific sequence in the genome, increase the length of the DNA sequence targeted and its degree of rarity (Klug, 2010).

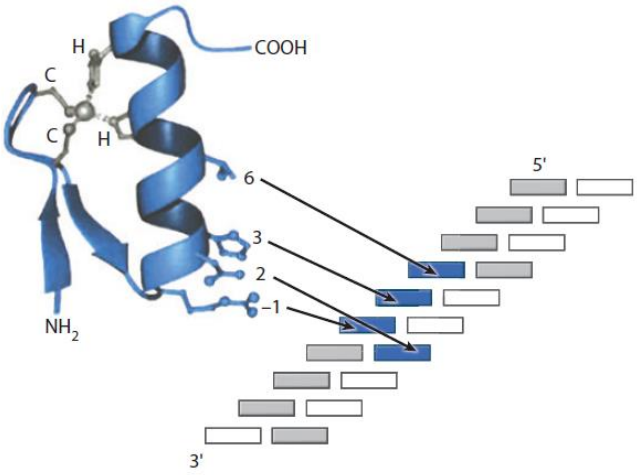

Figure 4. Schematic representations of a C2H2 zinc finger domain interact with the stretch of DNA. Specific amino acids of C2H2 zinc finger associate with a fragment of DNA at positions −1, 3, and 6 on the major groove of DNA and position 2 to the other strand of DNA. Thus, the contacting residue for a finger is not simply a 3-bp of three consecutive bases, however, a 4-bp site overlapping. C, cystine; H, histidine (Klug, 2010).

In subsequent studies, several other ZFP-DNA structures have been resolved, including GLI (Pavletich and Pabo, 1993), Tramtrak (Fairall *et al*., 1993), YY1 (Houbaviy *et al*., 1996) and TFIIIA (Nolte *et al*., 1998). In earlier studies, it was reported that multiple zinc fingers are required for sequence-specific DNA recognition (Matthews *et al*., 2000). However, to date, there are no general rules for ZFPs to DNA recognition. The sequences bound by a series of ZFP turned out not to be completely distinct from each other but instead overlapped: the same DNA triplet can be contacted by amino acids from more than one finger (Pearson, 2008). *AtRING1A* regulates flowering by repressing the expression of *MAF4* and *MAF5* genes in Arabidopsis (Shen *et al*., 2014). *AtZAT6* alter the expression of stress-related genes to bind on TACAAT motif in the promoter region of pathogen-related genes such as PR1, PR2, PR5 and abiotic stress-responsive genes including CBF1, CBF2, and CBF3 (Shi *et al*., 2014). *Cm-BBX24* encodes a zinc finger transcription factor functioned as a repressor of flowering by negatively regulating the expression of genes participated in photoperiod flowering pathway including GI, PRR5, CO, FT, and SOC1 and gibberellin biosynthesis genes GA20 and GA3. Cm-BBX24 also regulates the genes involved in stress responses (cold and drought) through gibberellin biosynthesis (Yang *et al*., 2014). Zinc finger protein ZNF658 regulates the transcription of genes implicated in zinc homeostasis and affects the expression of multiple ribosomal proteins and ribosome biogenesis by orchestrated the zinc transcriptional regulatory network (Ogo *et al*., 2015). *aslA* gene encodes for C2H2-type zinc finger transcription factor negatively regulate the genes involved in K^+ stress tolerance and vacuolar biogenesis in Aspergillus (Park *et al*., 2015). The stem cell zinc finger 1 (SZF1)/ZNF589, specifically expressed in CD34+ hematopoietic cells, suggesting functions in the epigenetic control of gene expression in hematopoietic stem/progenitor cells (Venturini *et al*., 2015).

ZMYND8 (zinc finger MYND8) a key player in transcription regulatory network. ZMYND8 is a novel chromatin reader of H3.1K36Me2/H4K16Ac marks. ZMYND8 has been regulating the subsets of genes involved in cell proliferation epithelial-mesenchymal transition and invasion of cancer cells possibly through its chromatin reader function (Basu *et al.,* 2017).

I.4.1.2. ZFPs interact with RNA

Besides ZFPs ability to interact with DNA, however, some of the ZFPs have also been involved in RNA binding with high affinity (Brown, 2005). In most of the cases, ZFP-RNA interaction demonstrated no sequence specificity and binding targets include different types and structures of RNA, for instance, dsRNA, ssRNA, and DNA-RNA heteroduplexes. Thus, the ZFPs can recognize the different structure and RNA sequence. Additionally, several ZFPs can interact with RNA as well as DNA but perform distinct functions. However, a ZFP-RNA interaction has been an enigma. How do ZFPs interact to RNAs exactly? This has been cracked by the crystal structure of ZFP-RNA (TFIIIA-5S rRNA) complex resolved, in which three fingers bind to 5S rRNA and form a 7S ribonucleoprotein particle to stabilize the RNA (Guddat *et al.,* 1990)**.** This structure analysis revealed that ZFPs specifically recognize individual bases positioned in the loop regions of the RNA. Zinc finger domain in JAZ protein bind specifically to RNA-DNA hybrids over DNA which is required for JAZ nuclear localization (Yang *et al.,* 1999). Two CCCH zinc fingers bind to AU-rich elements in the Nup475 transcript and mediate destabilization of the Nup475 transcript (Blackshear, 2002). Two ZFPs (*PIE-1* and *POS-1I*) in *C. elegans* regulate the germ cell fate by inhibiting transcription or translation of maternal RNAs (Ogura *et al.,* 2003). The C2H2 finger protein also plays a crucial role in the maturation of mRNA. The C2H2 like finger in U1C protein has been implicated in mRNA splicing via

recognizing the 5′ splice site of pre-mRNA transcript (Muto *et al.,* 2004). Transcription factor Wilm's tumor protein 1 export from the nucleus to cytoplasm binding specifically to RNA via its C2H2 finger domain and mediating RNA metabolism (Niksic *et al.,* 2004). The mammalian protein tristetraprolin consists two CCCH zinc fingers domain which is interacts with adenine-uridine rich elements within the 3′-untranslated region of the target mRNA to drives its degradation (Baou *et al.,* 2009). The mouse *Zfp36l2* is RNA-binding protein plays an essential role in female fertility at early embryo development through the mRNA stability in the life cycle of hematopoietic stem and progenitor cells (Stumpo *et al.,* 2009). AtTZF1 facilitate the target mRNA degradation in a sequence dependent fashion (Qu *et al.,* 2014). AtC3H14 ZFP interacts with target transcript in a sequence-specific manner and affects cell elongation and secondary wall biosynthesis in Arabidopsis (Kim *et al.,* 2014). A FYVE ZFPs specifically links mRNA transport to endosome trafficking. FYVE domain binds to endosomal lipids, PAM2-like domain and a key RNA-binding protein MLLE. However, loss of FYVE domain leads to specific defects in mRNA, ribosome, and septin transport without affecting the functions of the endosomal component and their movement (Pohlmann *et al.,* 2015). RanBP2 type ZFP required for chloroplast RNA editing in plants (Sun *et al.,* 2015). Zinc finger antiviral protein, ZAP, overexpression of ZAP in HeLa cells inhibits the retrotransposition of engineered human LINE (L1), mouse L1, zebrafish LINE-2 and Alu elements. However, siRNA-mediated suppression of ZAP in HeLa cells increase the ~2-fold retrotransposition of human L1 (Moldovan & Moran, 2015). Suppressor of pas1 (SOP1), a zinc-finger protein has been implicated in nuclear RNA degradation. The sop1 mutation suppresses the developmental phenotype of a splice site mutation in the essential a splicing-defective allele of PASTICCINO2 (PAS2) gene. SOP1 protein is required for

the nuclear exosome functions in Arabidopsis (Hematy *et al.,* 2016). ZC3H14 is RNA-binding proteins which modulate pre-mRNA processing of selected mRNA transcript and plays an important role in regulating cellular energy levels (Wigington *et al.,* 2016). CPSF30 selectively recognizes the AU-rich hexamer (AAUAAA) sequence exist in α-synuclein pre-mRNA in a cooperative manner with the high affinity which demonstrated that RNA recognition involves a metal-dependent cooperative binding mechanism (Shimberg *et al.,* 2016). Several CCCH type ZFPs have been identified in humans and mice such as tristetraprolin (TTP), roquin 1 and MCPIP1 are critical for many aspects of immune regulation by targeting mRNA splicing, polyadenylation, transportation, translation, degradation of mRNA and modulation of signaling pathways (Fu & Blackshear, 2017). In summary, zinc finger is small, however, seems to be quite versatile. ZFPs can be used for sequence-specific recognition of nucleic acids

I.4.2. ZFPs bind to protein and lipid

Although the majority of the ZFPs identified to date are involved in nucleic acid binding, however, over the past decades more and more ZFPs have been characterized, it has shown the ability to mediate protein-protein interactions to achieve a specific dimerization (Sanchez and Zhou, 2011). Many ZFPs have different kinds of fingers in the single protein, some of which interact with DNA while others bind to RNA or in protein-protein interactions. The combinations of diverse ZFPs allow proteins to bind many different ligands at the same time (Klug, 2010). Ikaros, a protein plays a crucial role in gene silencing and activation during lymphoid differentiation. Ikaros protein composed by six C2H2 ZFPs which are split into two clusters, its four N-terminal fingers can mediate sequence-specific DNA binding while two C-terminal clusters implicated in protein-protein interactions (McCarty *et al.,* 2003). Numerous ZFPs such as LIM, MYND, RING, A20, TAZ, and PHD

fingers exclusively act in protein-protein interactions (Sanchez and Zhou, 2011). Binding partners of these ZFPs generally belong to certain families, indicating that these ZFPs may be involved in modulating specific biological pathways. For example, the A20 ZFPs have been participating in ubiquitin binding to regulate ubiquitin ligase activity (Feng *et al*., 2016). PHD finger has been involved in identification of histones modification in the sequence-dependent manner to regulate gene expression. FYVE fingers are a specific group of ZFPs have been implicated in the recognition of the lipid phosphatidylinositol-3-phosphate (PtdIns3P) and usually located in the cell membrane. ZFPs in protein kinase C specifically interact with small ligands, for instance, phorbol esters and diacylglycerol which act in signal transduction (Matthews and Sunde, 2002). Multiple melanoma antigen (MAGE) family proteins are the binding partner of E3 RING ubiquitin ligases. Biochemical analysis revealed that MAGE family proteins increase the ubiquitin ligase activity of RING proteins (Doyle *et al*., 2010). EIRP1 encodes a C3HC4-type RING finger protein that tends to possess E3 ligase activity, EIRP1 interact to VpWRKY11 through the RING domain. EIRP1 targeted VpWRKY11 to degradation via 26S proteasome mediating proteolysis (Yu *et al*., 2013). DELLA-RING finger protein complex binds to the promoters of a subset of gibberellin responsive genes and represses their expression in Arabidopsis (Park *et al*., 2013). Rice RING finger E3 ligase (OsHCI1), OsHCI1 interacted with multiple substrate proteins to drives export of nuclear proteins to the cytoplasm via monoubiquitination and its heterologous ectopic expression also enhanced the thermotolerance in Arabidopsis (Lim *et al*., 2013). DUF581 is plant specific FCS-Like zinc finger domain has been implicated in protein-protein interaction (K & Laxmi, 2014). RNF114 interacts with A20 in T cells and modulates A20 ubiquitylation. RNF114 is stabilizing the A20 protein; regulate the nuclear factor-κB activity that involved in the

signaling pathways modulating T cell-mediated immune response (Rodriguez *et al.*, 2014). E3 ligase SDIR1 (SALT- AND DROUGHT-INDUCED REALLY INTERESTING NEW GENE FINGER1) interacts with SDIRIP1 (SDIR1-INTERACTING PROTEIN1) to modulate SDIRIP1 stability through ubiquitin-mediated protein degradation pathway. The SDIR1/SDIRIP1 complexes modulate the salt stress response and ABA signaling in Arabidopsis (Zhang *et al.,* 2015). Auxin-responsive genes OsCYP2 interact with a C2H2-type zinc finger protein (OsZFP), participate in IAA signal pathways regulating the lateral root development in rice (Cui *et al.,* 2017). Therefore, collectively above studies demonstrated that ZFPs have been diverse binding abilities from DNA to RNA, protein and lipid. Single ZFPs can interact with various molecules, while the surface used for contacting with DNA often differs from that involved in RNA or protein–protein interactions, however, mediate the distinct functions.

I.5. RING finger proteins

RING finger is a small zinc-binding domain was first identified in the human gene RING1 (Really Interesting New Gene 1) which is located in the major histocompatibility region on chromosome 6 and subsequently found in various key regulatory proteins (Berg & Shi, 1996). The RING finger protein was originally named by the initial letters of the RING1 (Freemont *et al.,* 1991; Lovering *et al.*, 1993). They have been further grouped into several classes (C2H2, C2C2, C2C2C2C2, C2HCC2C2, C2HC, C2HC5, C3HC4, C3H2C3, C3H, C3HDC3, C3HGC3, C3H2SC2, C4HC3, C4, C4C4, C5HC2, C6, and C8) according to the number of conserved cysteine and histidine residues, the spacing between them, and their specific molecular functions (Laity *et al.,* 2001; Krishna *et al.,* 2003; Stone *et al.*, 2005; Alam *et al.*, 2016). C3HC4-type zinc-finger also called RING-HC finger, a cysteine-rich domain of 40 to 60

residues that ligated with two zinc ions. C3HC4-type RING motif has consensus sequence Cys-X2-Cys-X9-39-Cys-X1-3-His-X2-3-Cys/His-X2-Cys-X4-48-Cys-X2-Cys where Cys, represent cysteine; His, histidine; X can be any amino acid (Laity *et al.*, 2001; Krishna *et al.*, 2003; Stone *et al.*, 2005).

Most of the RING finger-containing proteins posses E3 ubiquitin ligase activity. Ubiquitin-mediated protein degradation plays a crucial role in fundamental cellular processes, including differentiation, cell division, signaling, hormonal responses, growth, and biotic and abiotic stress responses (Vierstra, 2009; Jang *et al.*, 2015; Park *et al.*, 2015). Three sets of enzymes are required for ubiquitination of a targeted substrate: ubiquitin-activating (E1) enzyme, ubiquitin-conjugating (E2) enzyme, and ubiquitin-ligase (E3). Ubiquitin is activated by the ubiquitin-activating enzyme E1 in an ATP-dependent reaction and forms a thioester bond with the E1 enzyme. Activated ubiquitin is then transferred to a Cys residue of the ubiquitin-conjugating enzyme E2. Finally, ubiquitin formed an isopeptide bond to a Lys residue of a target substrate through an ubiquitin ligase E3. E3 ubiquitin ligases confer specificity to ubiquitination by transfer from an E2 enzyme to a specific substrate. These three steps are then repeated to attach multiple ubiquitin molecules to the target protein (Vierstra, 2009). Finally, the polyubiquitinated target proteins are degraded by the 26S proteasome (Figure 5).

Ubiquitin ligases are a large and diverse family of proteins. There are a larger number of E3 ubiquitin ligases than E1 and E2 enzymes in the eukaryotic genome. In fact, the Arabidopsis genome encodes only two E1 isoforms, approximately 40 E2 enzymes, and over 1, 400 putative E3 ligases (Vierstra, 2009). There are two main classes of E3 ubiquitin ligase: homology to E6-AP carboxy terminus (HECT); and RING finger/U-box. The RING-finger E3 ligases are the largest family and contain ligases such as a complex

of Skp1-Cullin-F-box protein (SCF) and the anaphase-promoting complex (APC) (Nakayama & Nakayama, 2006). E3 ubiquitin ligase also classified into two different types based on their structure (single-subunit or multi-subunit) and the mechanism of ubiquitin transfer action (Vierstra 2009; Hua and Vierstra, 2011). The majority of RING ubiquitin E3 ligases function as either a single subunit E3s wherein the RING protein provides both the substrate binding site and an E2 binding site, or as multisubunit E3s wherein the RING protein provides an E2 binding site and other components provide the substrate binding sites (Stone *et al.*, 2005; Guerra *et al.*, 2013). The existence of such a large number of E3 ligases diversity suggests that E3 ubiquitin ligase possesses high specificity of their target substrate recognition and different possible E2-E3 combinations further increase the level of specificity to modulate the specific biological pathways (Vierstra 2009; Sharma *et al.*, 2016).

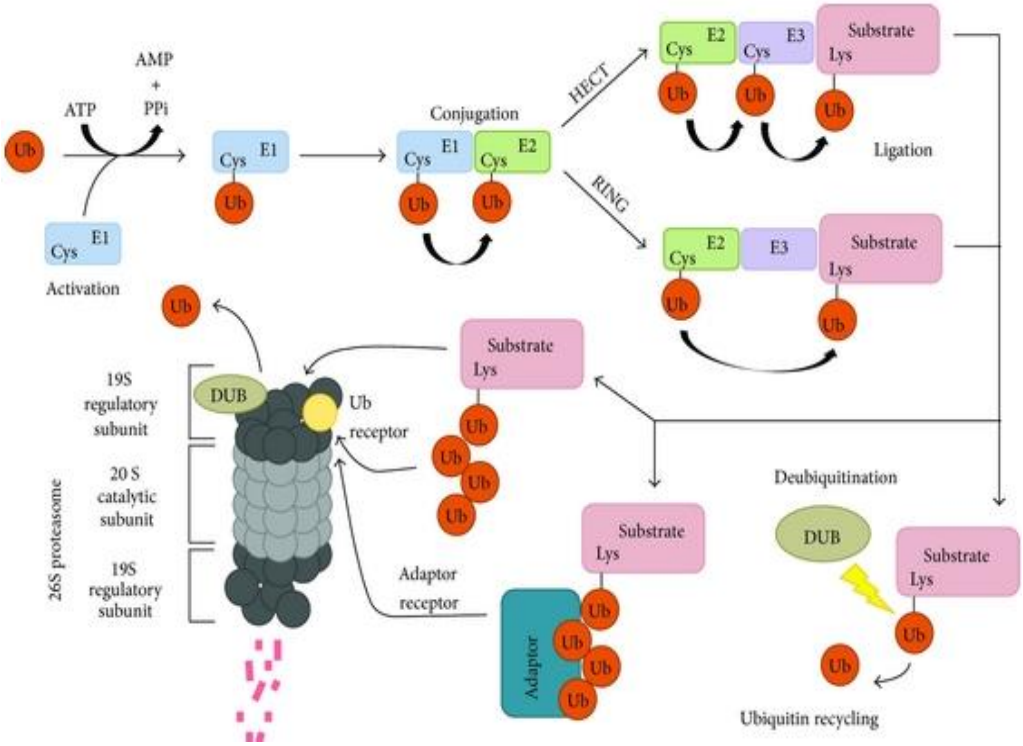

Figure 5. Overview of the ubiquitin-mediated protein degradation pathway. Ubiquitin-mediated protein degradation is carried out by three set of enzymes: ubiquitin-activating (E1), ubiquitin-conjugating (E2), and ubiquitin-ligase (E3) enzymes. Ubiquitin is activated by a E1. Activated ubiquitin is transferred to a E2. Ubiquitin is subsequently conjugated to target proteins in a process mediated by an E3 ubiquitin ligase. There are two main classes of E3 enzymes, HECT and RING/U box, which is differ in the manner by transfer ubiquitin to a target substrate. Finally, the polyubiquitylated substrate protein is degraded by the 26S proteasome. The proteasome is composed of a catalytic 20S core particle structure and two 19S regulatory caps which together called the 26S proteasome (Lin and Man, 2013).

Although RING zinc-finger proteins have been implicated in diverse functions including transcriptional activation, recombination of DNA, translational processes, signal transduction, programmed cell death, membrane association, and protein folding and assembly (Laity *et al.,* 2001; Krishna *et al.,* 2003; Gamsjaeger *et al.,* 2007; Matthews *et al.,* 2009; Font and Mackay, 2010). RING zinc-finger proteins have been closely and repeatedly involved in the development of multiple organisms (Xie *et al.,* 2002; Zhang *et al.,* 2005; Gamsjaeger *et al.,* 2007; Duggan *et al.,* 2008; Font and Mackay, 2010; Montano *et al.,* 2013; Waltzer *et al.,* 2016; Zhou *et al.,* 2016), however, cases reported in plants are comparatively limited including auxin signaling (SINAT5) (Xie *et al.*, 2002), ABA signaling (Zhang *et al.*, 2005), PEX10 (C3HC4 RING finger) is required for photorespiration and peroxisome contact with chloroplasts (Schumann *et al.,* 2007), a RING finger E3 ligase (*OsDSG1*) gene control seed germination and stress response in Rice (Park *et al.*, 2010), DELLA proteins and their interacting RING finger proteins repress gibberellin responses by binding to the promoters of a subset of gibberellin-responsive genes in Arabidopsis (Park *et al.*, 2013), a zinc finger protein (*CmBBX24*) regulates flowering time and abiotic stress in chrysanthemum by modulating gibberellins biosynthesis (Yang *et al.*, 2014), Arabidopsis *ZFP3* interferes with abscisic acid and light signaling in seed germination and plant development (Joseph *et al.*, 2014), a FYVE zinc finger domain protein transport mRNA to endosome trafficking (Pohlmann *et al.,* 2015), The ectopic expression of *AtC3H17* caused pleiotropic effects on vegetative development such as enhanced seedling growth, early flowering, seed germination, seed development, and acts as a nuclear transcriptional activator in Arabidopsis (Seok *et al.*, 2016). Auxin-responsive genes OsCYP2 interact with a C2HC-type zinc finger protein (OsZFP), participate in IAA signal pathways regulating the lateral root development in rice (Cui *et al.*, 2017).

1.6. Aims of this study

Previously, we isolated a C3HC4-type RING zinc finger protein gene, *CaRZFP1*, from a cDNA library of heat-stressed hot pepper (*Capsicum annuum*). Various environmental stresses (e.g., heat, cold, dehydration, and high salinity) induce *CaRZFP1* transcription in hot pepper. When the *CaRZFP1* open reading frame (ORF) was transformed into tobacco (*Nicotiana tabacum*) and ectopically expressed, transgenic tobacco plants showed enhanced growth and abiotic stress tolerance (Zeba *et al.,* 2009). In this study, we mobilized and expressed *CaRZFP1* in lettuce (*Lactuca sativa*) to further analyze the effect of *CaRZFP1* ectopic expression in a heterologous host plant. Contrasting with tobacco, transgenic lettuce exhibited poorer growth than vector-only controls, specifically delayed flowering, weakened leaf growth, shorter plant height, and stunted root growth. **To elucidate the molecular mechanisms underlying the totally different effects caused by the same RING zinc finger protein gene expressed in transgenic lettuce versus transgenic tobacco, the following questions will be pursued:**

- How does *CaRZFP1* negatively regulate the growth and development of *CaRZFP1*-transgenic lettuce plants?
- How does *CaRZFP1* act differently in transgenic-tobacco and lettuce plants at the cellular level?
- Is CaRZFP1 function in the abiotic tolerance mechanism in transgenic lettuce plants?
- What could be the target genes regulated by *CaRZFP1* in the *CaRZFP1*-transgenic lettuce plants?

CHAPTER II

MATERIALS AND METHODS

II.1. Plant material and growth condition

Seeds of hot pepper (*C. annuum* L. cv. Bu Gang), tobacco (*N. tabacum* L. cv. Wisconsin 38) and lettuce (*L. sativa* L. cv. Chung Chima) were sown on soil in plastic pots and reared in a growth chamber under controlled conditions of 25°C, 60% relative humidity, and a 16-h photoperiod from white fluorescent lamps (200 μmol photons m^{-2} s^{-1}). Vector-only or *CaRZFP1*-transgenic tobacco and lettuce plants were further grown in a greenhouse insulated with a dual door at 25±2°C under natural lighting with additional fluorescent lighting to maintain a 16 h photoperiod. Transgenic tobacco and lettuce plants carrying recombinant expression construct of *CaRZFP1* and the vector-only were self-fertilized, and T_1 generation seeds were harvested. T_1 generation seeds with the transgene expressed were selected on a kanamycin-containing medium, raised for flowering, and self-fertilized again to obtain T_2 generation seeds. This selection, self-fertilization and rearing in a green house was repeated to get further generations, up to T_5 generation. For the growth assay, transgenic lines were transferred to soil in plastic pots and reared in a growth chamber as described above. Four to five weeks old plants were used for nucleic acid extraction.

II.2. Abiotic stresses treatment

To examine the expression profiles of *CaRZFP1* under abiotic stress conditions, the young hot pepper plants with four to six leaves were subjected to various environmental stresses, i.e., high-temperature, dehydration, high salinity, and cold. For the high-temperature stress, the plants were placed in an incubator (Robbins Scientific) at 42°C for 0.5, 1, 2, and 4 h with the relative humidity higher than 90%. For the dehydration stress, the young plants were carefully transferred from their pots onto dry

paper and placed in the growth chamber for 0.5, 1, 2, 4, 8, 12, 24, and 48 h. For the high salinity stress, the young plants were removed from the soil, washed with distilled water, and soaked for 0.5, 1, 2, 4, 8, 12, 24, and 48 h in 250 mM NaCl solution. For the cold stress, the young plants were exposed to 4°C in a cold room for 1, 2, 4, 8, 12, 24, and 48 h. The stressed plant tissues were frozen in liquid nitrogen immediately after stress treatments and subjected to RNA extraction.

II.3. Generation of transgenic lettuce plants overexpressing *CaRFZP1*

The open reading frame of *CaRZFP1* was amplified by PCR with a primer pair covering both termini. The 5′ primer was 5′-ATATGGATCCATGCAGAAGTCAACTGCTACG-3′ and the 3′ primer was 5′-ATATGGATCCCTAACCAAACAAATATAGGAATAC-3′ with the underlined *Bam*HI restriction site. PCR was carried out with the initial reaction of 94°C for 5 min; followed by 30 cycles of 94°C for 1 min, 55°C for 30 s, and 72°C for 1 min; with a final reaction of 10 min at 72°C. The amplified PCR product was then digested with *Bam*HI and ligated into the pBKS1-1 plant expression vector (Suh *et al.*, 1994) at the *Bam*HI site to locate the open reading frame under the control of the CaMV 35S promoter. Nucleotide sequence of the cloned coding region in pBKS1-1 was confirmed by an automated DNA sequencer (3730xI DNA Analyzer, Applied Biosystems). The *CaRZFP*-pBKS1-1 plasmid was electroporated into the *Agrobacterium tumefaciens* strain LBA4404 and used for transformation of lettuce. In brief, sterilized hypocotyls of lettuce were cut to 1-2 cm length and infected with the *Agrobacterium* cells carrying the expression construct. After co-cultivation for 24 h, explants were washed with sterilized MS medium, and placed in a shoot induction medium containing 200 mg/ml kanamycin and 100 mg/ml

cefotaxime. Kanamycin-resistant shoots were selected and transferred to a root induction medium containing 200 mg/ml kanamycin (Horsch *et al.,* 1985). The putative *CaRZFP1*-transgenic plants were then transferred to soil and reared in a growth chamber, then in a greenhouse as described above.

II.4. RNA and DNA blot analyses

Total RNA was extracted from plant tissues frozen in liquid nitrogen. Briefly, frozen tissue was ground to powder, homogenized in 3 ml of extraction buffer (100 mM LiCI, 100 mM Tris-CI pH 8.0, 10 mM EDTA, and 1% SDS), a mixture of 3 ml of chloroform-isoamyl alcohol (24:1) was added, followed by vortexing and centrifugation at 10000x*g* for 25 min at 4°C. The supernatant was transferred to a 1.5 ml microcentrifuge tube, extraction was repeated with 1.5 ml chloroform-isoamyl alcohol (24:1) mixture, and precipitated in an equal volume of 4 M LiCI at -70°C for 2 h. After centrifugation, the pellet was washed with cold 70% ethanol and dissolved in DEPC-treated distilled water. Twenty µg of total RNA, for each sample, was loaded onto 1.2% agarose gel with formaldehyde. To check the integrity of the sample, RNA was visualized by staining with ethidium bromide and UV illumination after electrophoresis, and RNA was transferred onto nylon membranes (Hybond-N^+, GE Healthcare Bio-Sciences), followed by crosslinking with UV illumination. To generate *CaRZFP1*-specific probe, the coding sequence of *CaRZFP1* was amplified by PCR and labeled with α^{32}P-dCTP. Pre-hybridization for 2 h and hybridization for 16 to 22 h were done in a solution of 1 M dibasic sodium phosphate (pH 7.2), 14% SDS, and 20 µl of 1 mM EDTA (pH 8.0) at 65°C. For RNA blot analysis using oligonucleotides, 60 mer oligonucleotides were end labeled with γ^{32}P-dATP and polynucleotide kinase. The hybridization procedure was the same as the PCR-generated probe, except the hybridization and washing temperature which was at 58°C.

After hybridization, the membrane was washed twice with 1X SSPE and 0.1% SDS for 15 min, once at room temperature, then at 65°C, and the membrane was washed several times in 0.5X SSPE and 0.1% SDS at 65°C (Sambrook and Russell, 2001). The blots were exposed to a phosphoimager screen and an image was developed in a phosphoimager (Typhoon 8600, Molecular Dynamics). For RT-PCR analysis, total RNA preparation was predigested with DNase I (Takara Bio.) at 37°C for 30 min, and the first cDNA strand was generated by reverse transcribing RNA using AMV reverse transcriptase (Promega) at 42°C for 1 h. cDNA was quantified using a spectrophotometer (ND-1000, NanoDrop Technologies), and subjected to PCR using a primer pair of 5′-ATGCAGAAGTCAACTGCTACG-3′ and 5′-CTAACCAAACAAATATAGGAATAC-3′ covering the open reading frame of *CaRZFP1* in a PCR mixer (Promega) on a DNA thermal cycler (MJ Mini thermal cycler, Bio-Rad) with a following profile: initial step at 94°C for 5 min followed by 30 cycles of 94°C for 1 min, 55°C for 30 s, and 72°C for 1 min, and a final step at 72°C for 10 min. Amplified RT-PCR products were confirmed by DNA nucleotide sequencing. Genomic DNA was extracted from hot pepper leaves according to the CTAB protocol (Doyle and Doyle, 1990). Briefly, hot pepper were ground in liquid nitrogen and then preheated CTAB buffer (1.4 M NaCl, 2% (w/v) hexadecyltrimethyl ammonium bromide, 0.5% β-mercaptoethanol, 100 mM Tris-HCl (pH 8.0), 20 mM EDTA (pH 8.0) was added. The mixture was incubated at 65°C for 30 min. Added 20 μl of 0.1mg/ml RNAse A to the mixture and again incubated at 37°C for 15 min. Then it was extracted twice with an equal volume of 24:1 chloroform:isoamyl alcohol at 12,000xg in a microcentrifuge for 15 min. Genomic DNA was precipitated at -20°C with 0.8 volumes of isopropanol for 2 h. The pellet was made at 12,000xg for 10 min and washed with 70% ethanol and centrifuged at room temperature at 12,000xg for 10 min. Pellets were re-suspended in TE

buffer (10 mM Tris (pH 8.0), 1 mM EDTA (pH 8.0). Genomic DNA blot analysis was carried out according to Sambrook and Russell (2001). Briefly, 20 µg genomic DNA of hot pepper was completely digested with *Hin*dIII, *Eco*RI, and *Xba*I, and fractionated on a 0.8% agarose gel. Subsequently, DNA transfer was done with 20X SSC (3.0 M NaCl, 0.3 M sodium citrate, pH 7.0) after depurination in 0.25 M HCl for 15 min, denaturation in 0.5 M NaOH and 1.5 M NaCl for 30 min, neutralization in 1 M Tris-HCl (pH 8.0) and 1.5 M NaCl for 30 min, and DNA was transferred onto nylon membranes (Hybond-N^+, GE Healthcare Bio-Sciences), followed by crosslinking with UV illumination. Preparation of probes, hybridizations and washing the membrane was carried out as described for RNA blot hybridization. The blots were exposed to a phosphoimager screen and an image was developed in a phosphoimager (Typhoon 8600, Molecular Dynamics). All chemicals used were from Sigma-Aldrich, Becton, Dickinson and Co. and Duchefa Biochemie, otherwise mentioned.

II.5. Phenotypic assay

Seeds of *CaRZFP1*-transgenic and vector-only lettuce plants were sown in plastic pots and reared in a growth chamber or a green house under the controlled conditions as described above for the phenotypic examination during the vegetative growth. The plants were moved to a greenhouse under the controlled conditions as described above to follow the full life cycle. Evaluated parameters were leaf length, leaf width, leaf fresh weight, root mass, root fresh weight, plant height, flowering time, flower size, and seed morphology.

II.6. Thermotolerance assay

T_3 transgenic lettuce lines (#6, #12, #14, #15 and #16) and vector-only lettuce lines (V10, V30, and V38) were transferred to the small plastic pots containing soil mixture and reared in the growth chamber. The seedlings were watered regularly to ensure proper development, were subjected to thermotolerance assay. Young plants of about 7-8 leaves were exposed to high-temperature at 44°C for 1, 2, 3 and 4 h. After exposure to 44°C, plants were returned to the growth chamber at 25°C for recovery. Recovery was monitored and plants were photographed after 7 days. This experiment were repeated three times.

II.7. Cold tolerance assay

T_3 transgenic lettuce lines (#6, #12, #14, #15 and #16) and vector-only lettuce lines (V10, V30, and V38) were transferred to the small plastic pots containing soil mixture and reared in the growth chamber. The seedlings were watered regularly to ensure proper development, were subjected to cold tolerance assay. Young plants of about 7-8 leaves were exposed to cold stress at 4°C for 4 days in the cold room. After the cold stress, plants were returned to the growth chamber at 25°C for recovery. Recovery was monitored and plants were photographed after 7 days. This experiment was repeated independently three times.

II.8. Drought tolerance assay

T_3 transgenic lettuce lines (#6, #12, #14, #15 and #16) and vector-only lettuce lines (V10, V30, and V38) were transferred to the small plastic pots containing soil mixture and reared in the growth chamber. The seedlings were watered regularly to ensure proper development. When the plants were 4 weeks old, plants were stopped with watering for 4 weeks. After 4 weeks of

drought stress, *CaRZFP1*-transgenic lettuce and vector-only plants were re-watered and incubated for two weeks in a growth chamber under normal physiological conditions. Photographs were taken after 2 weeks of re-watering of plants. This experiment was repeated three times.

II.9. Histological and *in situ* hybridization analyses

To examine the effect of ectopic expression of *CaRZFP1* at the cellular level, the *CaRZFP1*-transgenic and the vector-only lettuce and tobacco (Zeba *et al.*, 2009) plants were anatomically assayed. Leaves, stems, and roots of the plants were taken and placed them immediately in 4% paraformaldehyde and vacuum infiltrated until the tissues sank. The samples were washed twice with 1X PBS (130 mM NaCl, 7 mM Na_2HPO_4, and 3 mM NaH_2PO_4, pH 7.0) for 30 min each and dehydrated using increasing concentrations of ethanol series (10%, 30%, 40%, 50%, 60%, 70%, and 85%), 60 min for each step. The samples were then incubated in 95% ethanol plus 0.1% eosin-Y overnight. Next day, samples were incubated in 100% ethanol, histoclear/ethanol series of 25, 50 and 75%, and twice in 100% histoclear, 60 min for each step. Histoclear was replaced with paraplast and kept the samples at 60°C overnight. Paraplast was changed 3 times in a day with fresh molten wax and cool to room temperature to solidify. Samples were cross-sectioned in 6 to 8 µm thickness using a microtome (Microm HM340E, Microm International GmbH). The cross sections were floated on DEPC-treated water and dried overnight at 40°C to fix the sections onto Superfrost Plus Microscope Slides (Thermo Fisher Scientific). The cross sections were deparaffinised by dipping the slides in xylene for 10 min and rehydrated with a graded ethanol series (100%, 95%, 90%, 80%, 60%, and 30%). After rinsing with distilled water, the sections were stained with 1% safranin and observed under light microscopes (Leica DC500, Leica Microsystems; Olympus BX51, Olympus Corporation). *In*

situ hybridization to visualize *CaRZFP1* transcript was carried out as described by Brewer *et al.,* (2006) Briefly, the cross sections were fixed onto Su perfrost Plus Microscope Slides and deparaffinized. The sections were incubated in 1X PBS for 5 min, permeabilized by proteinase K treatment for 30 min, fixed in 4% paraformaldehyde in phosphate buffer (pH 7.0) for 10 min, acetylated twice with 0.5% acetic anhydride in 0.1 M triethanolamine for 10 min each, and the slides were washed in 1X PBS for 5 min. Then the sections were hybridized with *in vitro* transcribed digoxigenin-labeled *CaRZFP1* sense or antisense riboprobes which were synthesized from linearized pBluescript plasmids containing *CaRZFP1* as described in the (SP6/T7) DIG RNA labeling Kit (Roche Applied Science). Briefly, the root sections were hybridized with equal concentrations of either sense or antisense RNA probes in a hybridization buffer [50X Denhardt's, 50% dextran sulphate, 100 mg/ml tRNA, 50% formamide, 10X *in situ* hybridization salts (3 M NaCl, 100 mM Tris-HCl pH 8.0, 100 mM Na-phosphate pH 6.8, and 50 mM EDTA pH 8.0)], covered with parafilm and incubated at 53°C overnight in a humidity chamber. After hybridization, the slides were put into 2X SSC for 60 min to allow parafilm to float off. Then the slides were washed twice in 0.2X SSC at 55°C for 1 h each, equilibrated twice in 1X NTE (2.5 M NaCl, 50 mM Tris-Cl pH 8.0, and 5 mM EDTA pH 8.0) at 37°C with gentle agitation for 5 min each. The slides were then put into 1X NTE buffer with 20 µg/ml RNase A for 30 min at 37°C with gentle agitation, rinsed twice in 1X NTE for 2 min each, washed in 0.2X SSC at 55°C for 1 h, equilibrated in 1X PBS for 5 min at room temperature, incubated in blocking solution [1% blocking reagent (Roche Diagnostics Gmbh), 100 mM Tris-Cl pH 7.5, and 150 mM NaCl] for 45 min at room temperature, and washed with a washing buffer (1% BSA, 100 mM Tris-Cl pH 7.5, 150 mM NaCl, and 0.3% Triton X-100) for 45 min. The anti-digoxigenin antibody (Roche Applied Science) was diluted to 1:1,250

ratio in the washing buffer and 200 µl of anti-digoxigenin antibody solution was directly applied onto the slide carrying the parafilm strips. The slides were incubated in the dark for 2-3 h at room temperature or overnight at 4°C, washed four times in washing buffer for 15 min each on a shaking platform, and the slides were transferred into 1X PBS, incubated for 2 min, and equilibrated in TN buffer (100 mM Tris-HCl pH 9.5 and 100 mM NaCl) twice for 2 min each. The staining solution was prepared immediately before use by adding 20 µl nitro-blue tetrazolium/5-bromo-4-chloro-3-indolyphosphate per 1 ml TN buffer. The slides were covered with the staining solution and kept in a plastic box in the dark at room temperature for 2-3 days. Development of staining was monitored under a light microscope, and once the color reaction was complete, the slides were placed in TE buffer for 5-10 min to stop the staining reaction. The slides were washed in 1X PBS for 5 min, and images were captured with a light microscope (Olympus BX51).

II.10. Transcriptome analysis

Four T_4 generation *CaRZFP1*-transgenic lettuce lines (#6, #12, #14, and #16) and three vector-only control lettuce lines (V10, V30, and V38) were selected for transcriptome analysis using Arabidopsis 44K oligo microarray (Agilent Technology) to maintain the methods used for the transcriptome profiling of *CaRZFP1*-transgenic tobacco (Zeba *et al.*, 2009). Total RNA was extracted from 4 weeks old plants, and genomic DNA was removed by DNase I (Takara Bio Inc.) digestion. Synthesis of cRNA probes and hybridization were carried out using Agilent's low RNA Input linear amplification kit (Agilent Technologies) according to the manufacturer's instructions. Briefly, total RNA 1 µg was mixed with T7 promoter primer mix and incubated at 65°C for 10 min, cDNA master mix (5X first strand buffer, 0.1 M DTT, 10 mM dNTP mix, RNase-Out, and MMLV-RT) was added,

incubated at 40°C for 2 h, and reverse transcription and dsDNA synthesis were terminated by incubating at 65°C for 15 min. Transcription of the dsDNA was done by adding transcription master mix (4x transcription buffer, 0.1 M DTT, NTP mix, 50% PEG, RNase-Out, inorganic pyrophosphatase, T7-RNA polymerase, and cyanine 3-CTP) and incubating at 40°C for 2 h. The labeled cRNA was purified on cRNA cleanup module, and hybridized to the microarrays at 65°C for 17 h. After hybridization, microarrays were washed for 1 min at room temperature with GE Wash Buffer 1, again for 1 min at 37°C with GE Wash buffer 2, and dried immediately by centrifugation at 400x*g* for 2 min at room temperature. The hybridization images were scanned using a DNA microarray scanner and quantified with the feature extraction software 9.3.2.1 (Agilent Technologies). Data normalization and calculation of fold-change were performed using GeneSpringGX 7.3 (Agilent Technologies). Greater than 2 fold changes with $p < 0.05$ was set as the threshold for statistical significance.

II.11. Multiple sequence alignment and phylogenetic analysis

Multiple sequence alignments were performed by the Bioedit program (http://www.mbio.ncsu.edu/bioedit/bioedit.html). The transmembrane domain was predicted at least by one of the four programs is marked (MEMSAT, http://www.sacs.ucsf.edu/cgi-bin/memsat.py; SOSUI, http://bp.nuap.nagoya-u.ac.jp/sosui/; TMHMM, http://www.cbs.dtu.dk/services/TMHMM/; HMMTOP, http://www.enzim.hu/hmmtop/). Phylogenetic analysis was performed with the MEGA6.0 program (Tamura *et al.*, 2013) by the neighbor-joining method (Saitou and Nei, 1987), and the bootstrap test was carried out with 1000 iterations (Brown, 1994).

CHAPTER III

RESULTS

III.1. Sequence homology and phylogenetic analyses of hot pepper CaRZFP1 with other zinc finger protein genes

CaRZFP1 homolog gene sequences were retrieved from the National Centre for Biotechnology Information database (http://www.ncbi.nlm.nih.gov/). We aligned the CaRZFP1 sequence with the RING zinc finger proteins from several organisms, mainly plant species (Figure 6): *Capsicum chinense, Ricinus communis, Vitis vinifera, Populus trichocarpa, Glycine max, Arabidopsis thaliana, Brassica rapa, Oryza sativa, Zea mays, Caenorhabditis elegans, Bombyx mori, Mus musculus, Homo sapiens, Drosophila melanogaster, Selaginella moellendorffii*, and *Sorghum bicolor*. The alignments revealed that *CaRZFP1* shares a highly conserved C3HC4-type RING zinc finger domains which widely distributed in animals and plants. Phylogenetic analysis showed that clustering by each of these species agreed well with their taxonomic classification. Additionally, the amino acid sequences of the *CaRZFP1*-encoded protein and the *C. chinense* zinc finger protein shared 99% homology (Figure 7). To examine the possible transmembrane region of *CaRZFP1*, different transmembrane prediction programs (MEMSAT, SOSUI, TMHMM, TSEG, DAS, and HMMTOP) were used. The most of the program predicted only two transmembrane in *CaRZFP1* (Figure 8a and b) and the length of transmembranes segments is underlined (Figure 6). Therefore, these results suggest that C3HC4-type RING zinc finger domain may generate from the common ancestor and may have functional and evolutionary importance in the plants.

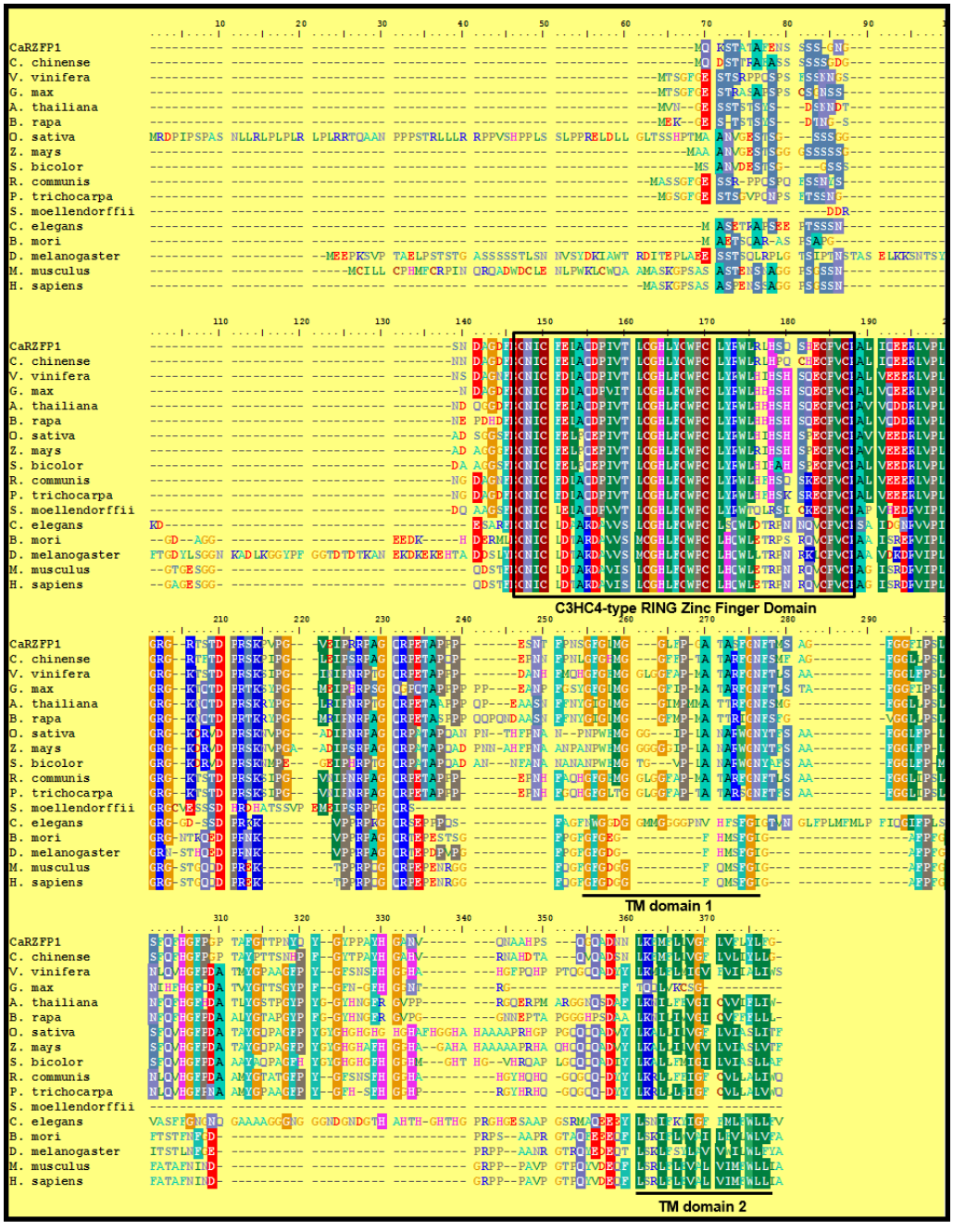
C3HC4-type RING Zinc Finger Domain
TM domain 1
TM domain 2

Figure 6. Sequence comparison of CaRZFP1 with other zinc finger proteins. Deduced amino sequence of CaRZFP1 was aligned with putative zinc finger proteins from *Capsicum chinese, Vitis vinifera, Glycine max, Arabidopsis thailiana, Brassica rapa, Oryza sativa, Zea mays, Sorghum bicolor, Ricinus communis, Populus trichocarpa, Selaginella moellendorffii, Caenorhabditis elegans, Bombyx mori, Drosophila melanogaster, Mus musculus,* and *Homo sapiens*. The number of the amino acid residue was shown above the aligned sequences. Conserved C3HC4-type RING zinc finger domain was boxed. Predicted transmembrane domains, TM Domini 1 and 2, were underlined. Colored and shaded amino acids are chemically similar residues. Dash indicates gaps introduced to maximize homology.

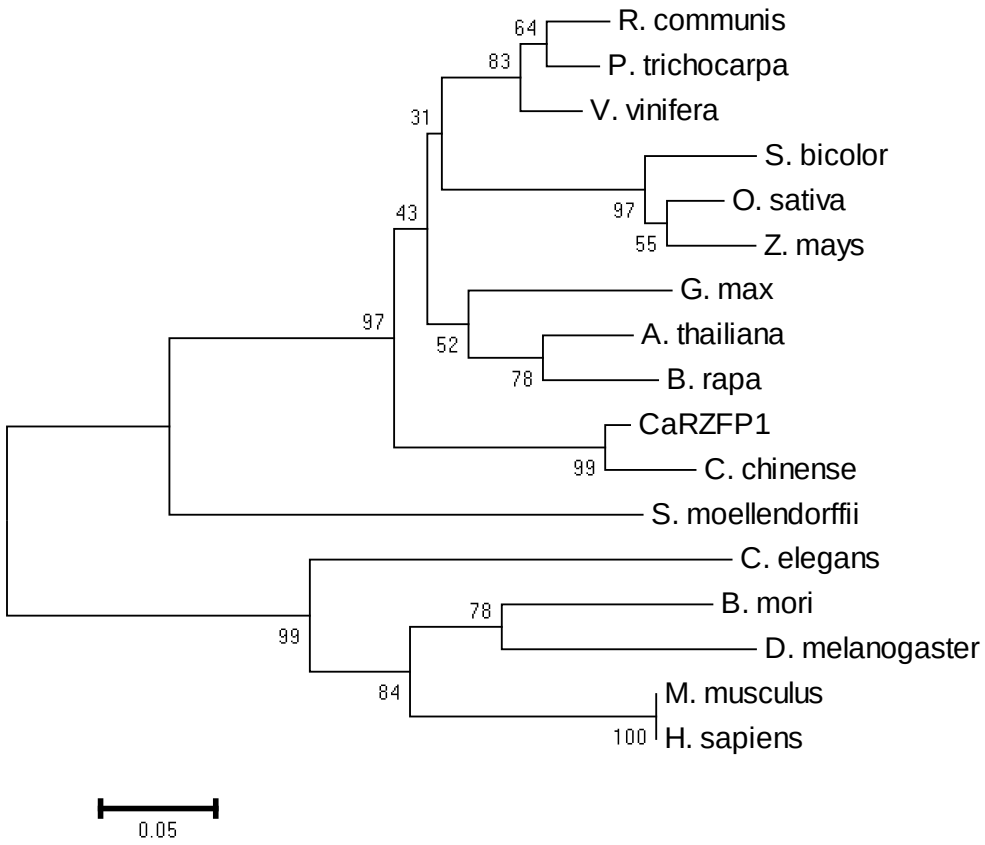

Figure 7. Phylogenetic analysis of CaRZFP1 with other zinc finger proteins. The evolutionary history was inferred using the Neighbor-Joining method. The tree was obtained from amino acid sequences, and phylogenetic analyses were conducted in MEGA6.0 program. The bootstrap consensus tree inferred from 1000 replicates was taken to represent the evolutionary history. *Ricinus communis, Populus trichocarpa, Vitis vinifera, Sorghum bicolor, Oryza sativa, Zea mays, Glycine max, Arabidopsis thailiana, Brassica rapa, Capsicum chinese, Selaginella moellendorffii, Caenorhabditis elegans, Bombyx mori, Drosophila melanogaster, Mus musculus,* and *Homo sapiens*, from the top.

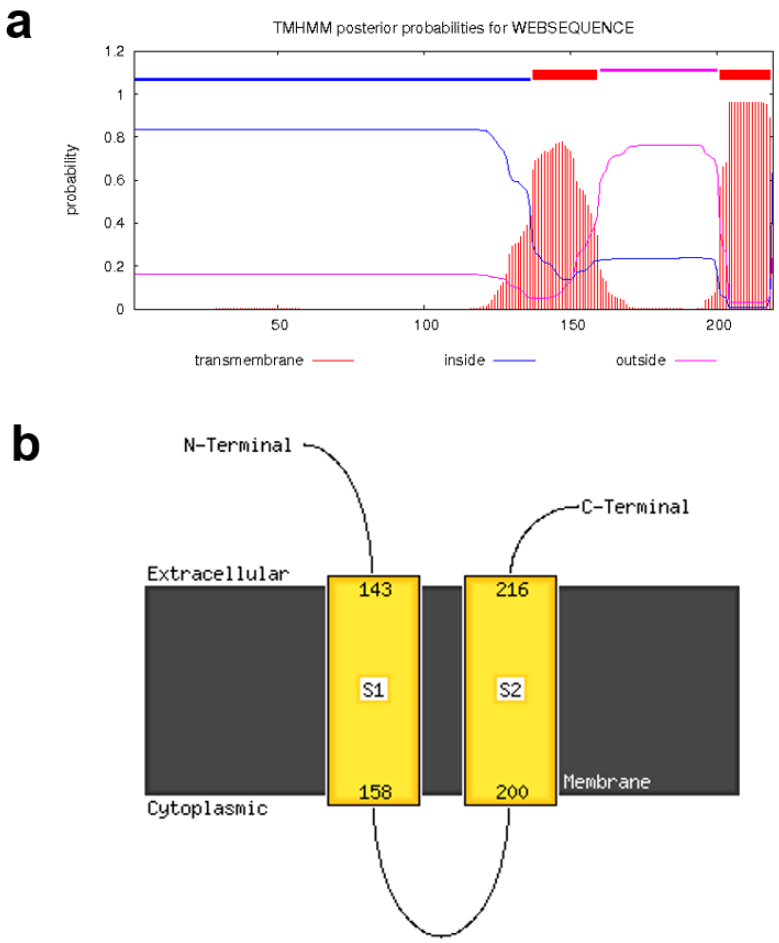

Figure 8. Predicted transmembrane domains in *CaRZFP1* protein. *CaRZFP1* protein sequence was analyzed by five different transmembrane prediction programs (MEMSAT, SOSUI, TMHMM, TSEG and HMMTOP). The transmembrane helix that was predicted at least by one of the five programs is marked (MEMSAT, http://www.sacs.ucsf.edu/cgi-bin/memsat.py SOSUI, http://bp.nuap.nagoya-u.ac.jp/sosui/; TMHMM, http://www.cbs.dtu.dk/services/TMHMM/; TSEG, http://www.genome.jp/SIT/tsegdir/; HMMTOP, http://www.enzim.hu/hmmtop/).

III.2. Expression of *CaRZFP1* was induced widely in different tissues of hot pepper plants in response to various abiotic stresses

To investigate *CaRZFP1* expression patterns in the hot pepper, mRNA accumulation profiles were monitored under diverse abiotic stress conditions in different tissues. The results of RNA blots showed that 30 min of high-temperature stress (42°C) resulted in high *CaRZFP1* transcript levels (Figure 9). Transcript induction kinetics were distinct in different plant parts; for example, *CaRZFP1* expression was highest at 2 h in the leaf (before declining), but at 1 h in the stem and the root (Figure 9). Additionally, *CaRZFP1* transcript levels were higher in the leaf early under dehydration stress and then decreased for the remainder of the treatment. In the stem and root, transcript levels decreased less dramatically from treatment start to end (Figure 9). Under high salinity stress, *CaRZFP1* transcript levels in the leaf and stem steadily increased until the end of treatment, but in the root, transcripts were only weakly present at the beginning and were not apparent thereafter (Figure 9). Cold stress at 4°C induced low *CaRZFP1* expression early in treatment, followed by significant increases in the leaf and stem upon prolonged cold exposure. In the root, however, early exposure to cold-induced weak expression; subsequently, the transcript diminished (Figure 9).

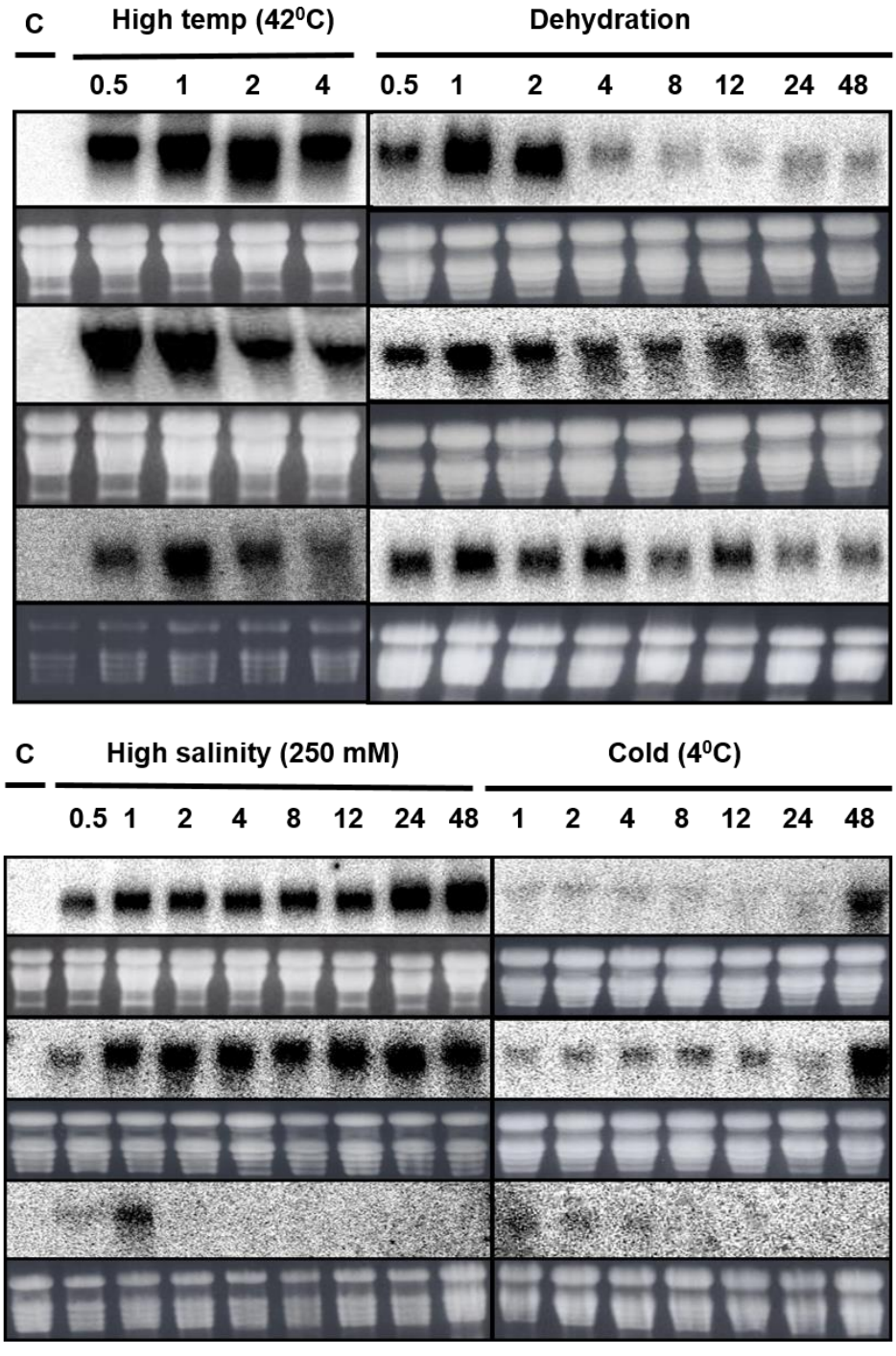
C
High temp (42⁰C)
Dehydration
0.5 1 2 4
0.5 1 2 4 8 12 24 48
C
High salinity (250 mM)
Cold (4⁰C)
0.5 1 2 4 8 12 24 48
1 2 4 8 12 24 48

Figure 9. Temporal expression patterns of the *CaRZFP1* transcript in response to diverse abiotic stresses in different tissues of hot pepper plants. Expression profile of *CaRZFP1* in different tissues of hot pepper plants in response to high-temperature at 42°C, dehydration stress, salinity stress (250 mM), and cold stress at 4°C. Four weeks old hot pepper plants were exposed to various stresses for the different time length in hours, the treated tissues were harvested, and total RNAs were extracted. Total RNAs were separated by electrophoresis on a 1.2%-formaldehyde-agarose gel and blotted to a Hybond –N nylon membrane. The blots were hybridized with the ^{32}P-labelled *CaRZFP1* probe.

III.3. Genomic DNA blot analysis of hot pepper

To examine the family members of *CaRZFP1* in the hot pepper genome, genomic DNA blot analysis was conducted using *CaRZFP1* clone as a probe. Genomic DNA of hot pepper was digested with three different enzymes such as *Hind*III (H), *Eco*RI (E) and *Xba*I (X). DNA blot result of hot pepper genome showed 1 to 2 signals (Figure 10). Therefore, these results indicate that *CaRZFP1* is typically present in one or two genomic copies in hot pepper genome.

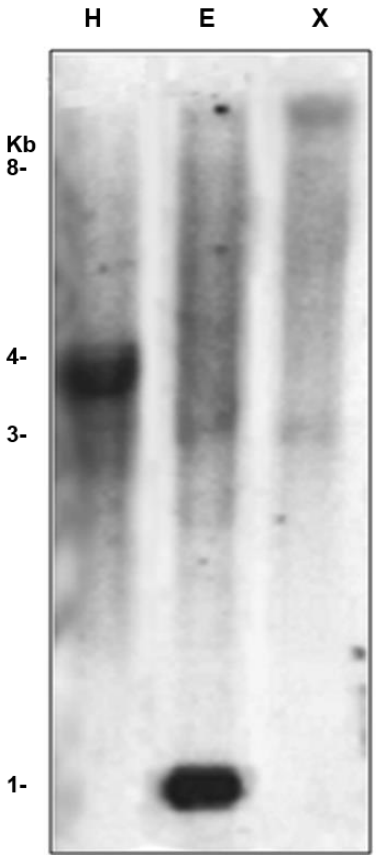

Figure 10. Genomic DNA blot analysis of hot pepper genome. Total genomic DNA of hot pepper was digested with *Hind*III (H), *Eco*RI (E) and *Xba*I (X) and run on a 0.7% agarose gel. The blot was hybridized with the ^{32}P-labeled *CaRZFP1* probe. DNA size marker is indicated in kilobases at the left.

III.4. Generating transgenic lettuce plants overexpressing *CaRFZP1*

To investigate the effect of *CaRZFP1*-ectopic expression, transgenic lettuce was generated, which over-expressed *CaRZFP1* under the control of cauliflower mosaic virus 35S promoter (Figure 11a). This construct and the vector without *CaRZFP1* was introduced into the lettuce genome, respectively. The putative *CaRZFP1*-transgenic lettuce plants were selected on kanamycin-containing medium and planted in soil. Next, T_1-generation lines were screened with RNA blot analysis to evaluate *CaRZFP1* transcript levels and confirm transgenicity (Figure 11b). In the representative examples shown, T_1 transgenic lines #12, #14, #15, and #16 exhibited different but significant levels of ectopically expressed *CaRZFP1* transcript under normal growth conditions. Line #6 expressed very low *CaRZFP1* levels undetectable via RNA blot hybridization; transcripts were thus confirmed with RT-PCR and DNA-blot analyses (Figure 11c and d). Confirmed T_1 lines were reared in a greenhouse and repeatedly self-fertilized to obtain next-generation seeds (T_2 to T_5). Transgenicity of all putative transgenic plants from different generations was confirmed by RNA blot analysis. Along the process, we noticed that most *CaRZFP1*-transgenic lettuce plants with detectable *CaRZFP1* transcript levels exhibited growth impairment, more strongly in some lines than in others. Starting from T_2, we categorized transgenic lettuce lines according to *CaRZFP1* transcript expression levels (low, medium, and high). Five independent T_2 lines were selected based on *CaRZFP1* transcript levels and denoted with numerals 6, 12, 14, 15, and 16. Additionally, three vector-only lines (V10, V30, and V38) with morphology typical of nontransgenic lettuce were also selected for further analyses (Figure 11b).

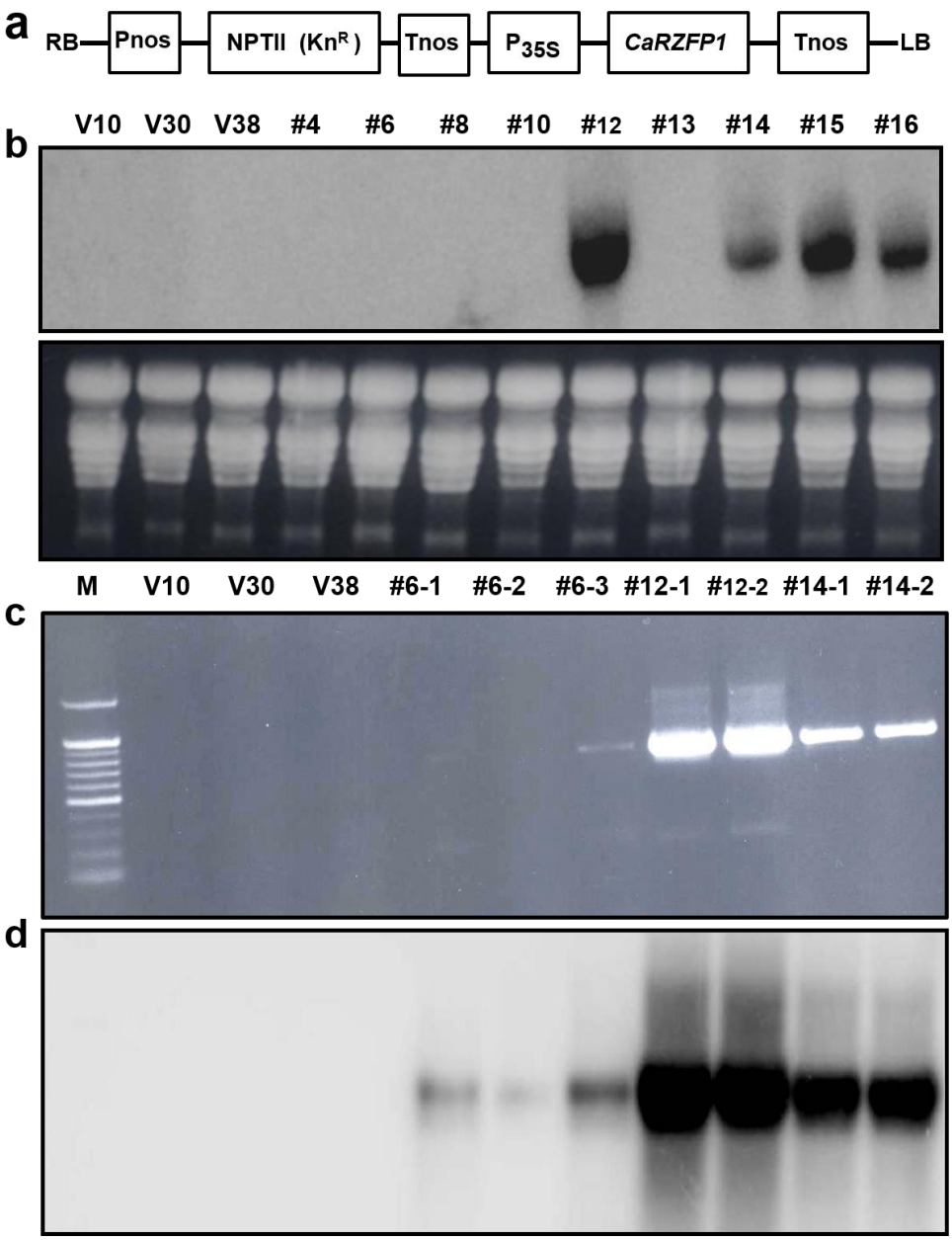
a
RB
Pnos
NPTII (KnR)
Tnos
P35S
CaRZFP1
Tnos
LB
b
V10 V30 V38 #4 #6 #8 #10 #12 #13 #14 #15 #16
c
M V10 V30 V38 #6-1 #6-2 #6-3 #12-1 #12-2 #14-1 #14-2
d

Figure 11. Generation of *CaRFZP1* over-expressed transgenic lettuce plants. **a.** Diagrammatic representation of pBKS1-1-*CaRZFP1* construct employed for lettuce transformation. RB, right border sequence of T-DNA; *Pnos*, promoter of the nopaline synthase gene; *NPT*, neomycin phosphotransferase gene; Kn^R kanamycin resistance gene; *Tnos*, terminator of the nopaline synthase gene; P_{35S}, *35S* promoter of cauliflower mosaic virus, *CaRZFP1,* 657 bp *C. annuum* RING zinc finger protein 1 gene; LB, left border sequence of T-DNA. **b.** RNA blot hybridization results for vector-only and putative T_1 transgenic plant lines. Total RNA was separated by electrophoresis on a 1.2% formaldehyde agarose gel and blotted onto a Hybond-N nylon membrane. Separated RNA was stained with ethidium bromide for visualization with UV illumination. The blots were hybridized to the ^{32}P-labelled *CaRZFP1* probe. **c.** One step RT-PCR analysis for the *CaRZFP1* transcript in the *CaRZFP1*-transgenic lettuce plants. RT-PCR results with a primer pair enclosing the ORF of *CaRZFP1* for three vector-only control lines and several *CaRZFP1*-transgenic lines. **d.** RT-PCR results were further confirmed by DNA blot analysis using the ^{32}P-labeled *CaRZFP1* probe. M, DNA size marker.

III.5. Growth of *CaRZFP1*-transgenic lettuce plants were retarded

Comparison of the growth robustness during the vegetative stage with the transcript level showed a strong negative-correlation between the growth and the transcript level of *CaRZFP1*, i.e. stronger expression of *CaRZFP1* tightly related to the severe retarded in growth. The ectopic expression of *CaRZFP1* caused pleiotropic developmental changes. Growth and development retardation was noticeable soon after germination and continued thereafter; transgenic lettuce exhibited overall poorer growth than vector-only plants, resulting in smaller leaf size, shorter plant height, and lower fresh weight (Figure 12a). Line #12 exhibited the highest *CaRZFP1* expression and the most impeded growth among all transgenic lettuce lines. Lines #14, #15, and #16 were more moderate in terms of both *CaRZFP1* expression and hampered growth. Line #6's very low, near-undetectable *CaRZFP1* expression corresponded to a negligible effect on growth and development; its phenotype was similar to vector-only controls (Figure 12a). Thus, ectopic expression of *CaRZFP1* caused pleiotropic developmental changes. After 28 days of germination, the average leaf lengths of *CaRZFP1*-transgenic lettuce lines #6, #12, #14, #15, and #16 were 13.8 ± 0.47, 9.3 ± 0.19, 11.0 ± 0.62, 10.4 ± 0.74, and 11.5 ± 0.89 cm, while leaves from vector-only V10, V30, and V38 averaged 15.4 ± 0.53, 14.4 ± 0.30, and 14.5 ± 0.32 cm (Figure 12b). Average leaf widths of #6, #12, #14, #15, and #16 were 6.9 ± 0.41, 4.0 ± 0.22, 5.6 ± 0.78, 5.1 ± 0.24, and 5.0 ± 0.74 cm, whereas V10, V30, and V38 leaf widths averaged 9.0 ± 0.25, 8.4 ± 0.31, and 8.6 ± 0.29 cm (Figure 12c). Average fresh weights of #6, #12, #14, #15, and #16 were 4.4 ± 0.23, 1.3 ± 0.34, 2.9 ± 0.15, 2.7 ± 0.21, and 3.4 ± 0.24 g, while those of V10, V30, and V38 were 6.6 ± 0.43, 5.6 ± 0.34, and 5.7 ± 0.20 g (Figure 12d). The correlation between *CaRZFP1*

transcript level and a negative phenotypic effect was repeatedly maintained through the next generations of *CaRZFP1*-transgenic lettuce (Figure 12e, f, and g). Overall, growth of *CaRZFP1*-transgenic lettuce plants was dramatically impeded by *CaRZFP1* expression in a dose-dependent fashion.

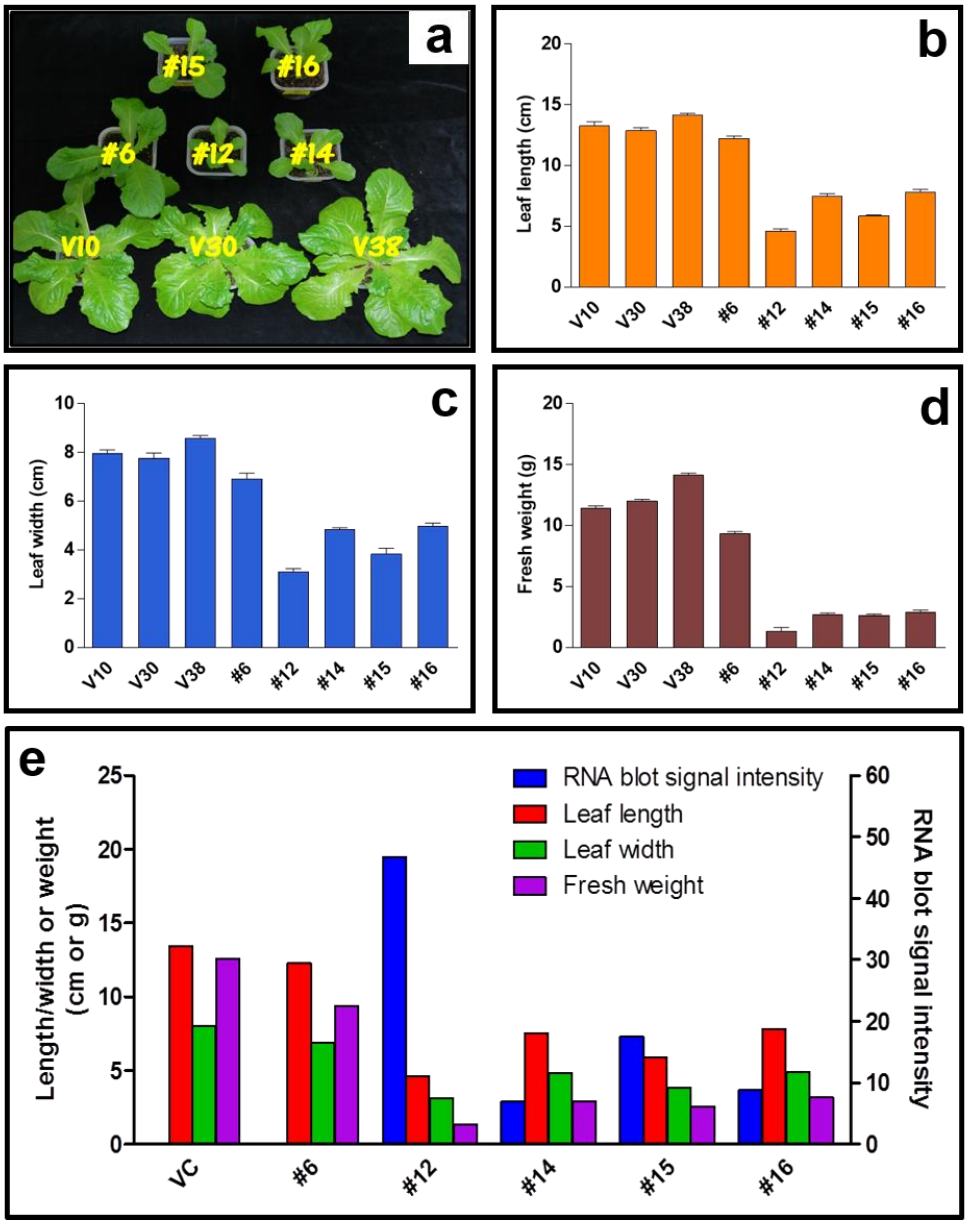
a
#15
#16
#6
#12
#14
V10
V30
V38
b
Leaf length (cm)
0
5
10
15
20
V10
V30
V38
#6
#12
#14
#15
#16
c
Leaf width (cm)
0
2
4
6
8
10
V10
V30
V38
#6
#12
#14
#15
#16
d
Fresh weight (g)
0
5
10
15
20
V10
V30
V38
#6
#12
#14
#15
#16
e
RNA blot signal intensity
Leaf length
Leaf width
Fresh weight
Length/width or weight (cm or g)
RNA blot signal intensity
0
5
10
15
20
25
0
10
20
30
40
50
60
VC
#6
#12
#14
#15
#16

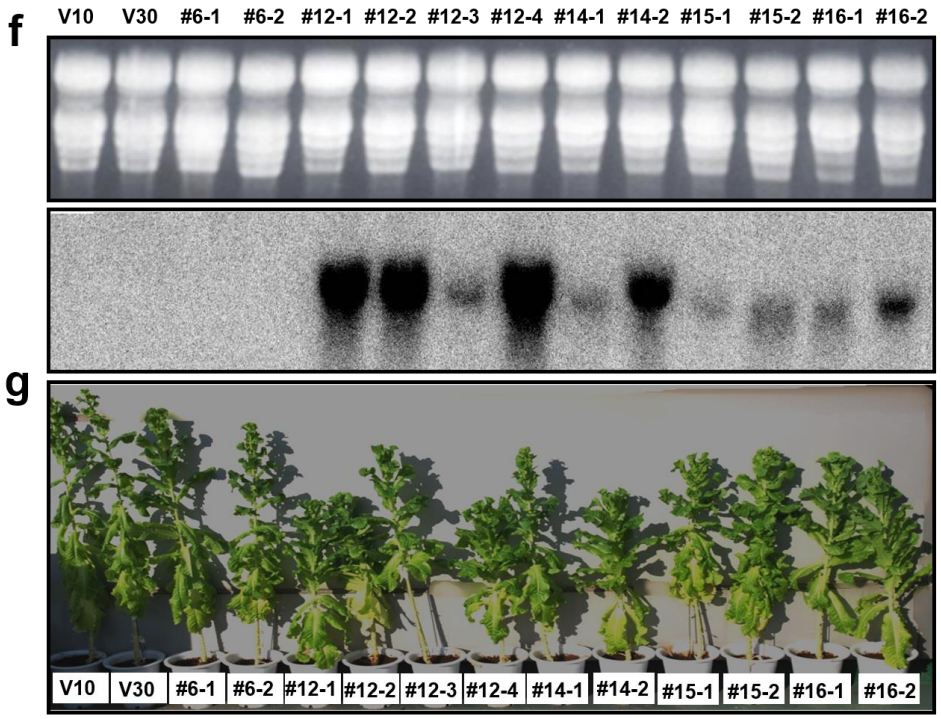
f
V10
V30
#6-1
#6-2
#12-1
#12-2
#12-3
#12-4
#14-1
#14-2
#15-1
#15-2
#16-1
#16-2
g
V10
V30
#6-1
#6-2
#12-1
#12-2
#12-3
#12-4
#14-1
#14-2
#15-1
#15-2
#16-1
#16-2

Figure 12. *CaRZFP1* over-expressing transgenic lettuce plants showed hampered growth and development. a. Typical examples of T_3 transgenic lettuce plant lines #6, #12, #14, #15, and #16 and lettuce plants carrying only the vector after 4 weeks since seed imbibition. **b.** Comparison of leaf length of the plants in **a**. **c.** Comparison of leaf width of the plants in **a**. **d.** Comparison of fresh weight of the plants in **a**. **e.** The data in **b**, **c** and **d** were aligned with *CaRZFP1* transcript level analyzed by RNA blot hybridization. V10, V30 and V38, lettuce plants carrying only the expression vector. Error bars show standard deviation. VC, an average of V10, V30, and V38. **f.** RNA blot hybridization results of vector-only or putative T_3 *CaRZFP1*-transgenic lettuce lines that are shown in **g**. Total RNA was separated by electrophoresis on a 1.2% formaldehyde agarose gel and blotted onto a Hybond-N nylon membrane. Separated RNA was stained with ethidium bromide for visualization with UV illumination. The blots were hybridized to the ^{32}P-labelled *CaRZFP1* probe. **g.** Typical examples of T_3 transgenic lettuce plant lines #6, #12, #14, #15 and #16 and lettuce plants carrying only the vector after 12 weeks since seed imbibition.

III.6. Root growth of *CaRZFP1*-transgenic lettuce plants was impeded

The correlation between the level of *CaRZFP1* expression and the negative effects on the development of *CaRZFP1*-transgenic lettuce plants extended to the root growth. Transgenic lettuce possessed shorter, less-developed roots, and this phenotype was closely correlated to *CaRZFP1* transcript levels. Compared with vector-only plants, primary root growth, as well as total root-system length and lateral/adventitious root formation, were strongly decreased in line #12, mildly impaired in lines #14, #15, and #16, but only slightly affected in line #6 (Figure 13a). Average root fresh weights in lines #6, #12, #14 #15, and #16 were 1.05 ± 0.15, 0.17 ± 0.01, 0.55 ± 0.09, 0.39 ± 0.04, and 0.52 ± 0.08 g, while those in V10, V30, and V38 were 1.71 ± 0.20, 1.64 ± 0.28, and 1.40 ± 0.28 g (Figure 13b). Thus, *CaRZFP1* expression was strongly correlated with decrease in root biomass (Figure 13b and c). Again, *CaRZFP1* expression in line #6 was very low in the root and required confirmation with RT-PCR and DNA blot analysis (Figure 13d and e).

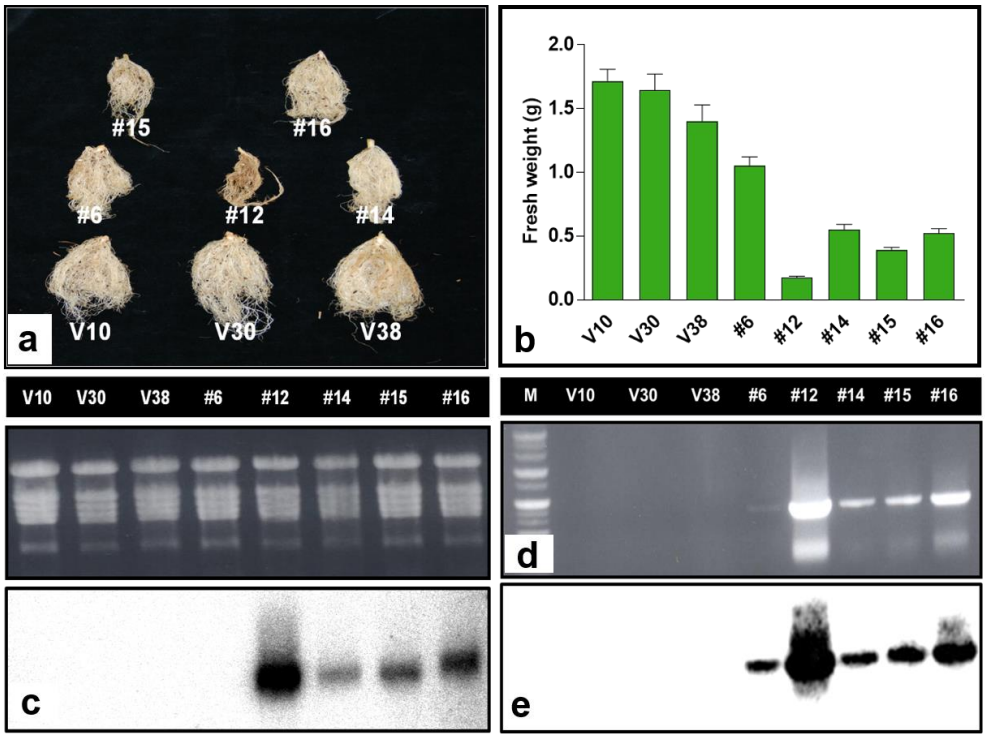

Figure 13. Phenotype and root development of the *CaRZFP1*-transgenic lettuce and vector-only plants. a. Typical roots of T_3 transgenic lettuce plant lines #6, #12, #14, #15 and #16 and lettuce plants carrying only the vector after 4 weeks since seed imbibition. **b.** Comparison of root mass of the plants in **a**. **c.** RNA blot hybridization results for the plants in **a. d.** RT-PCR results for the same samples in **a**. **e.** RT-PCR results in **d** was further confirmed by DNA blot analysis with the ^{32}P-labeled *CaRZFP1* probe. M, size marker. Error bars show standard deviation.

III.7. *CaRZFP1*-transgenic lettuce plants were shorter at full growth and flowering was delayed

The weak growth of *CaRZFP1*-transgenic lettuce plants continued late in development, in contrast to vector-only plants, which appeared normal from the vegetative phase to flowering. At full growth, *CaRZFP1*-transgenic lettuce was shorter than vector-only plants (Figure 14a). Additionally, vector-only plants began to flower at 115 d after sowing (DAS), whereas *CaRZFP1*-transgenic lettuce began to flower 123 to 130 DAS (Figure 14b). Inflorescence size was smaller in transgenic lettuce than in vector-only plants (Figure 14c). Flower size did not differ significantly between the transgenic and control lines, but the former head significantly fewer flowers per inflorescence, a characteristic that was again correlated with *CaRZFP1* transcript levels. Transgenicity at full growth was again confirmed with RNA blot hybridization for most lines and with RT-PCR and DNA blot analysis for line #6 (Figure 14d, e and f). Seed development in each flower appeared normal in transgenic lettuce (Figure 14g, h and i), although the total seed number per inflorescence was negatively correlated with *CaRZFP1* expression levels. Seed size, morphology, and weight in the transgenic lettuce lines did not differ significantly from those in the vector-only plants (Figure 14g, h, i and j). We next selected four *CaRZFP1*-transgenic lettuce lines (#6, #12, #14, and #16) for further investigation.

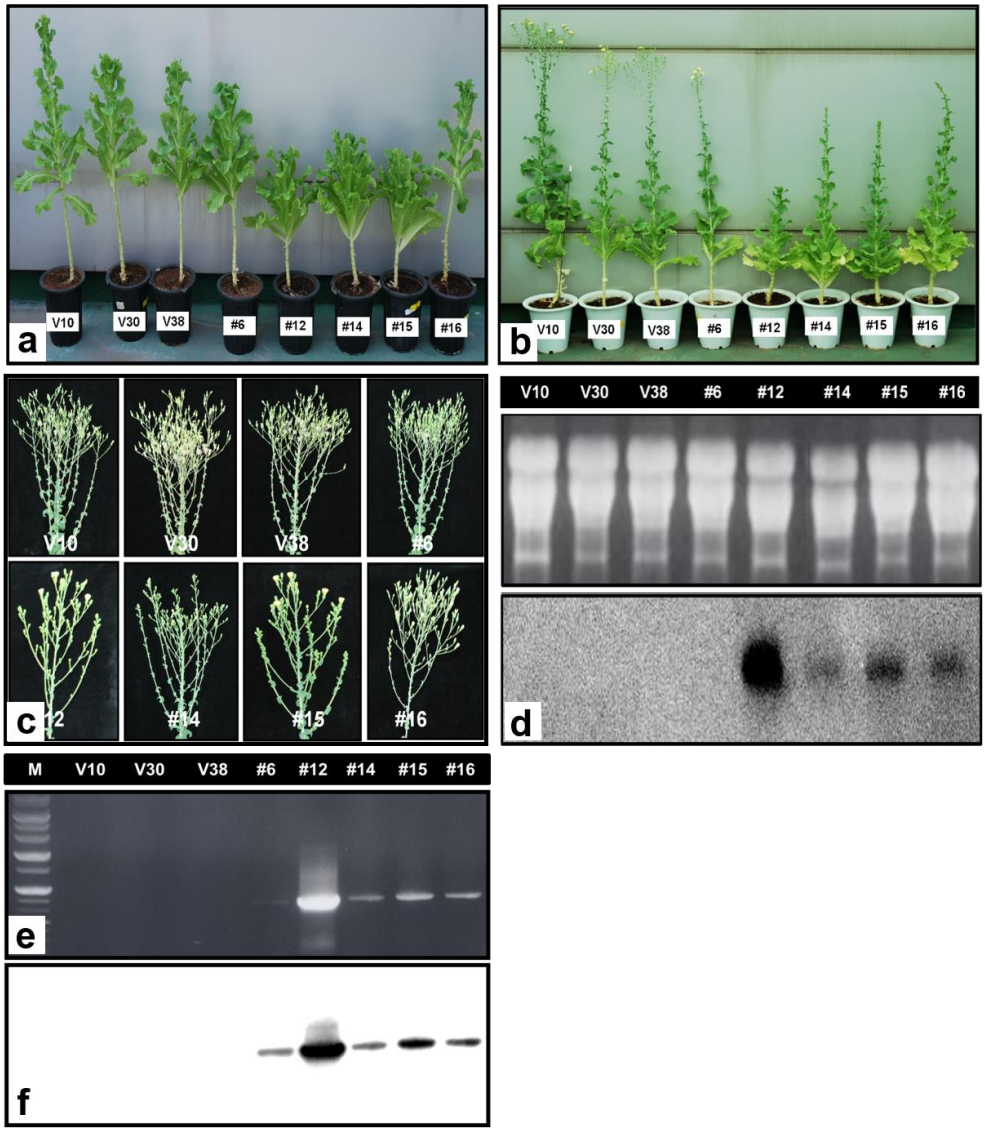
a
V10
V30
V38
#6
#12
#14
#15
#16
b
V10
V30
V38
#6
#12
#14
#15
#16
c
V10
V30
V38
#6
#12
#14
#15
#16
V10 V30 V38 #6 #12 #14 #15 #16
d
M V10 V30 V38 #6 #12 #14 #15 #16
e
f

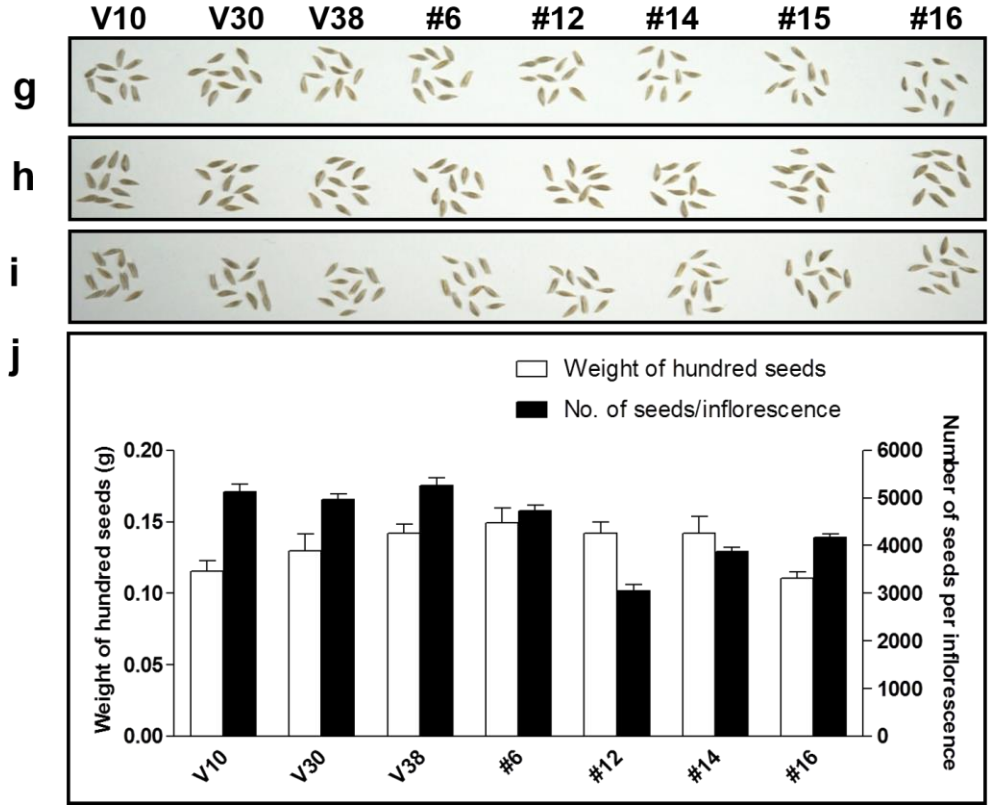
V10
V30
V38
#6
#12
#14
#15
#16
g
h
i
j
Weight of hundred seeds
No. of seeds/inflorescence
Weight of hundred seeds (g)
0.20
0.15
0.10
0.05
0.00
Number of seeds per inflorescence
6000
5000
4000
3000
2000
1000
0
V10
V30
V38
#6
#12
#14
#16

Figure 14. Hampered growth and development *CaRZFP1* over-expressing transgenic lettuce plants extended to the reproductive stage. a. Typical examples of T_3 transgenic lettuce plant lines #6, #12, #14, #15 and #16 and lettuce plants carrying only the vector at the full growth. **b.** Typical examples of T_3 transgenic lettuce plant lines and vector-control lines at the flowering stage. **c.** Fully developed inflorescences. **d.** RNA blot hybridization results for the plants in **b**. **e**. RT-PCR results for the same samples in **d**. **f.** RT-PCR results in **e** was further confirmed by DNA blot analysis with the ^{32}P-labeled *CaRZFP1* probe. M, size marker. **g.** Typical examples of mature T_2 generation seeds. **h.** Typical examples of mature T_3 generation seeds. **i.** Typical examples of mature T_4 generation seeds. **j.** The average weight of 100 mature seeds and number of seeds per inflorescence of *CaRZFP1*-transgenic and vector-only lettuce lines from T_2, T_3 and T_4 generation. Error bars show standard deviation.

III.8. Development of endodermis and vascular bundle was impaired in the *CaRZFP1*-transgenic lettuce roots

To examine the retarded growth of *CaRZFP1*-transgenic lettuce and the robust growth of *CaRZFP1*-transgenic tobacco (Zeba *et al.,* 2009) at the cellular level, we analyzed leaf, stem, and root sections of both plants and compared them with vector-only controls. Leaves of transgenic lettuce and vector-only lettuce were not distinguishable in terms of morphology, cell size, or tissue organization. Cross sections of transgenic and control lines revealed basically identical mesophyll cell size and number, vascular bundle structure, chloroplast distribution in the mesophyll cells, as well as epidermal cell size and morphology (Figure 15a). Top views of epidermal cells and stomata of transgenic and vector-only lettuce did not reveal any differences in epidermal cell size, stomatal size, or stomatal density (Figure 15b, c, and d). Likewise, stem morphology, cell size, and tissue organization in transgenic versus vector-only lettuce were indistinguishable (Figure 15e).

Significant defects in endodermis and vascular bundle development were observed in *CaRZFP1*-transgenic lettuce roots. The internal structure of vector-only lettuce roots was typical and well defined; visible structures included the surrounding epidermal layer, parenchyma cells inside the epidermis, endodermal layer, and pericycle surrounding the internal vascular bundles, as well as radially lined vessel elements and phloem between the xylem elements (Figure 15f and g). The internal root structures of transgenic lettuce plants significantly deviated from typical. In the line with the strongest *CaRZFP1* expression (#12), the endodermis and pericycle was barely defined, vessel elements were not compactly structured and sometimes even disconnected, while the xylem element did not appear to be formed at the root center (Figure 15f and g). These root-development defects

were also present in other transgenic lettuce lines to a lesser extent and were strongly correlated with *CaRZFP1* expression levels; stronger *CaRZFP1* expression resulted in greater impairment in endodermis, pericycle, and vascular bundle structure. However, *CaRZFP1* expression did not seem to affect root cortex cells; parenchymal cell size and overall shape were normal in *CaRZFP1*-transgenic lettuce (Figure 15f and g).

To identify spatial *CaRZFP1* expression patterns in *CaRZFP1*-transgenic and vector-only lettuce roots, we performed *in situ* hybridization assays. The antisense probe of *CaRZFP1* detected the transcript strongly from the roots of line #12, at medium levels from lines #14 and #16, and at low levels from line #6; however, *CaRZFP1* mRNA was expressed equally within all root cell types in every transgenic plant. In the vector-only plants, no significant signal could be detected (Figure 15h). Hybridization of the root sections with the *CaRZFP1* sense probe found no significant signal over background, failing to distinguish between the transgenic and vector-only roots (data not shown). Previously, we engineered transgenic lines of tobacco overexpressing *CaRZFP1* under the control of CaMV 35S promoter. These *CaRZFP1*-transgenic tobacco plants exhibited robust growth and abiotic stress tolerance (Zeba *et al.,* 2009). When these *CaRZFP1*-transgenic tobacco plants were examined for the development of roots at the cellular level, the overall root cell structure, tissue patterns, or morphology, including the endodermis and vascular bundle, did not differ from vector-only plants (Figure 15i, j and k).

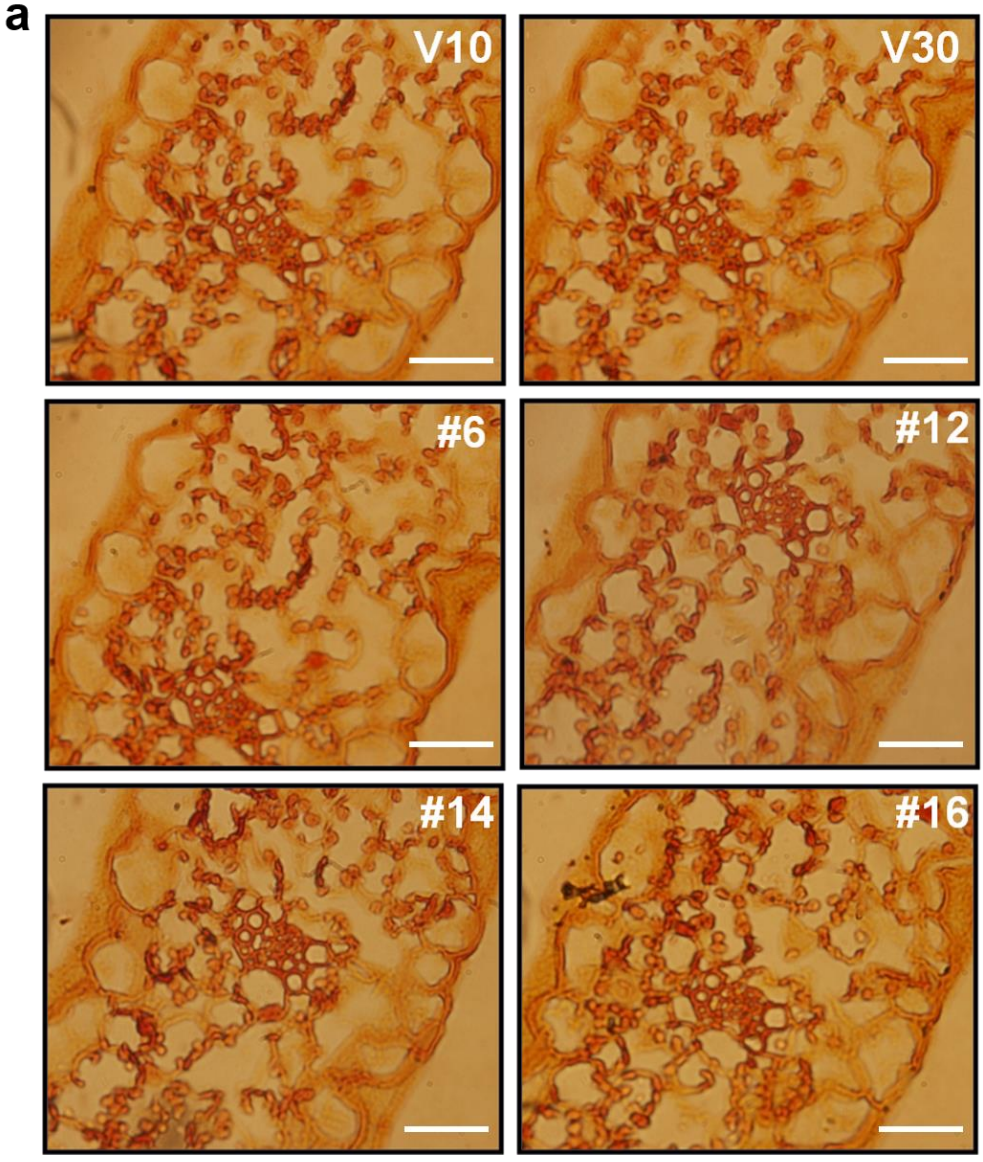
a
V10
V30
#6
#12
#14
#16

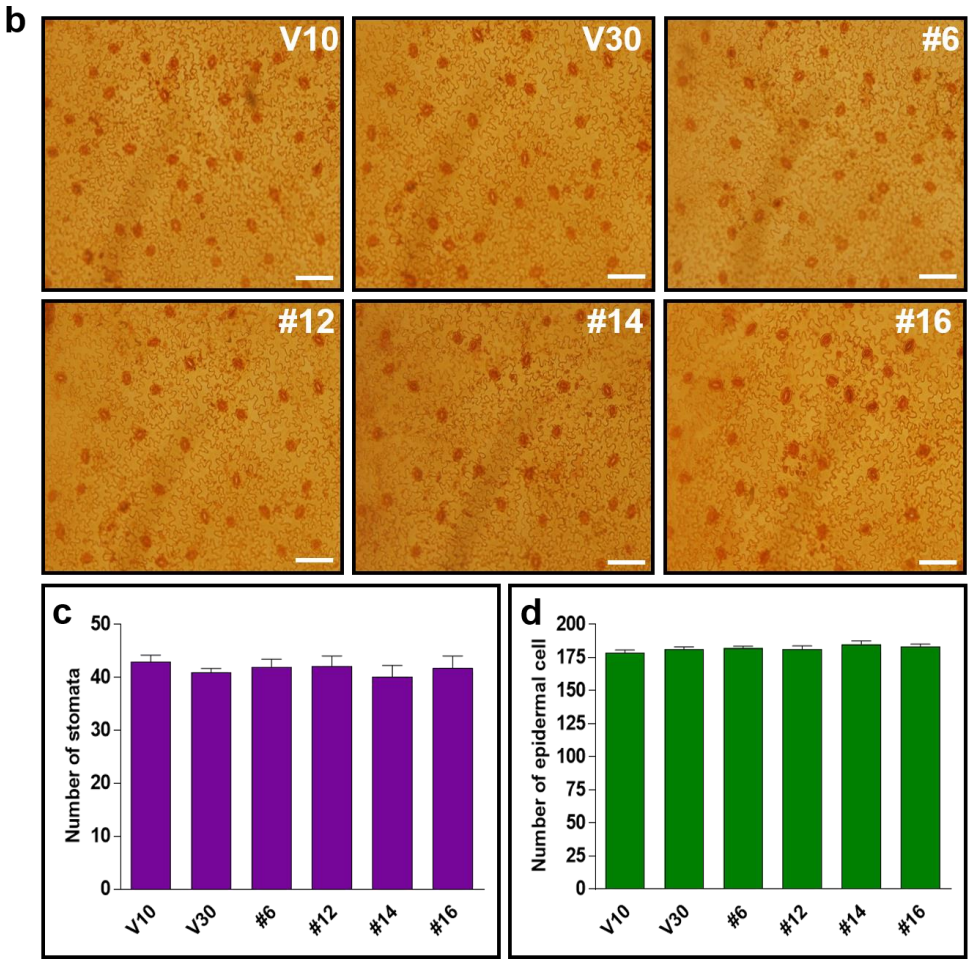
b
V10
V30
#6
#12
#14
#16
c
Number of stomata
0
10
20
30
40
50
V10
V30
#6
#12
#14
#16
d
Number of epidermal cell
0
25
50
75
100
125
150
175
200
V10
V30
#6
#12
#14
#16

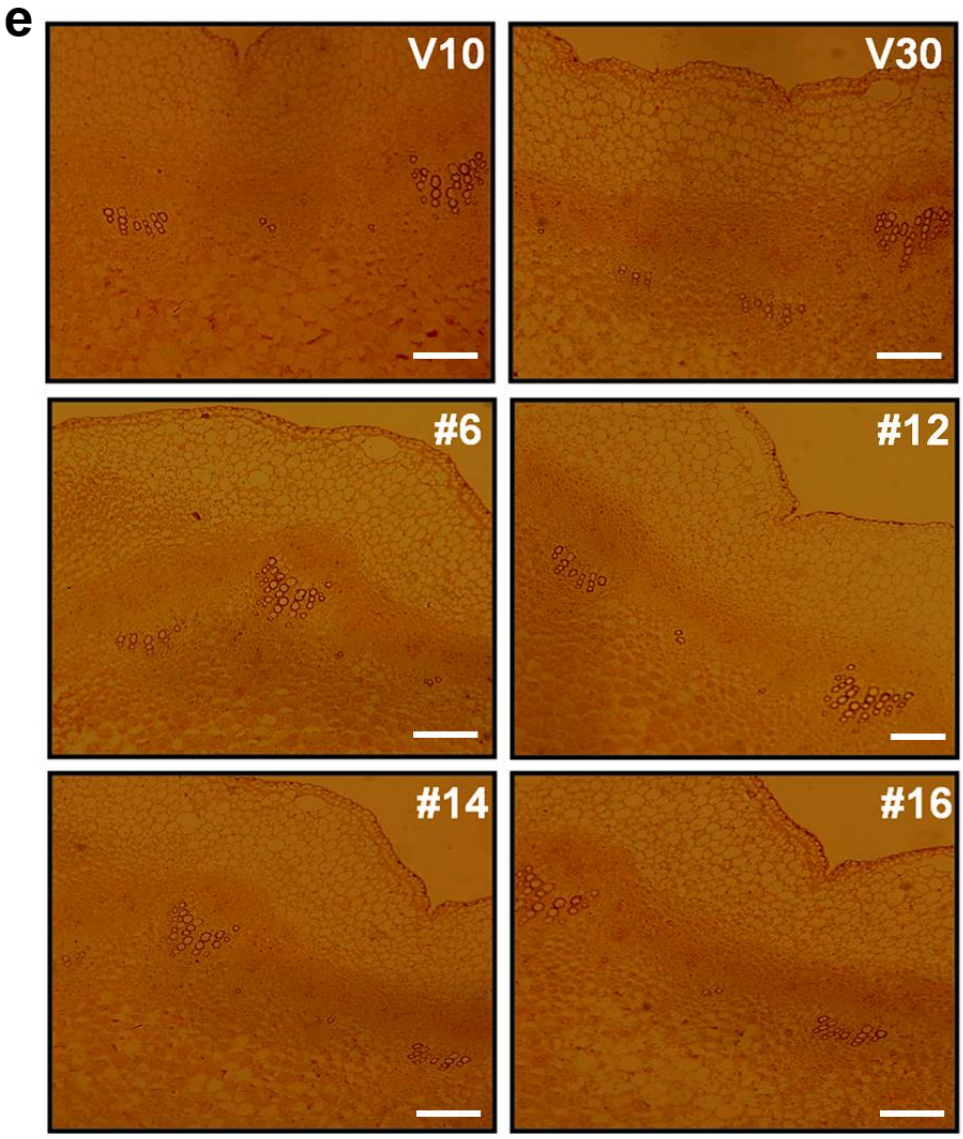
e
V10
V30
#6
#12
#14
#16

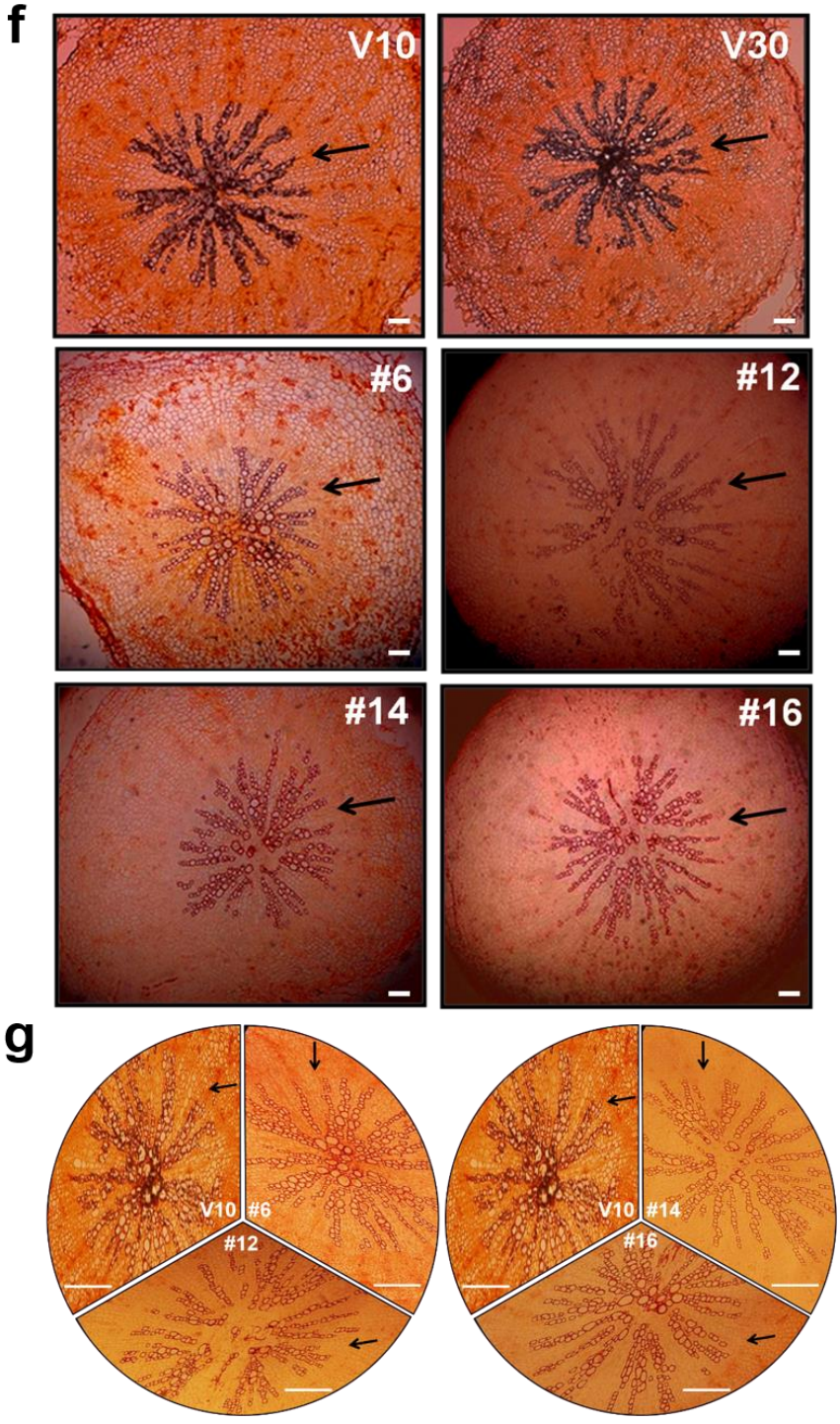
f
V10
V30
#6
#12
#14
#16
g
V10
#6
#12
V10
#14
#16

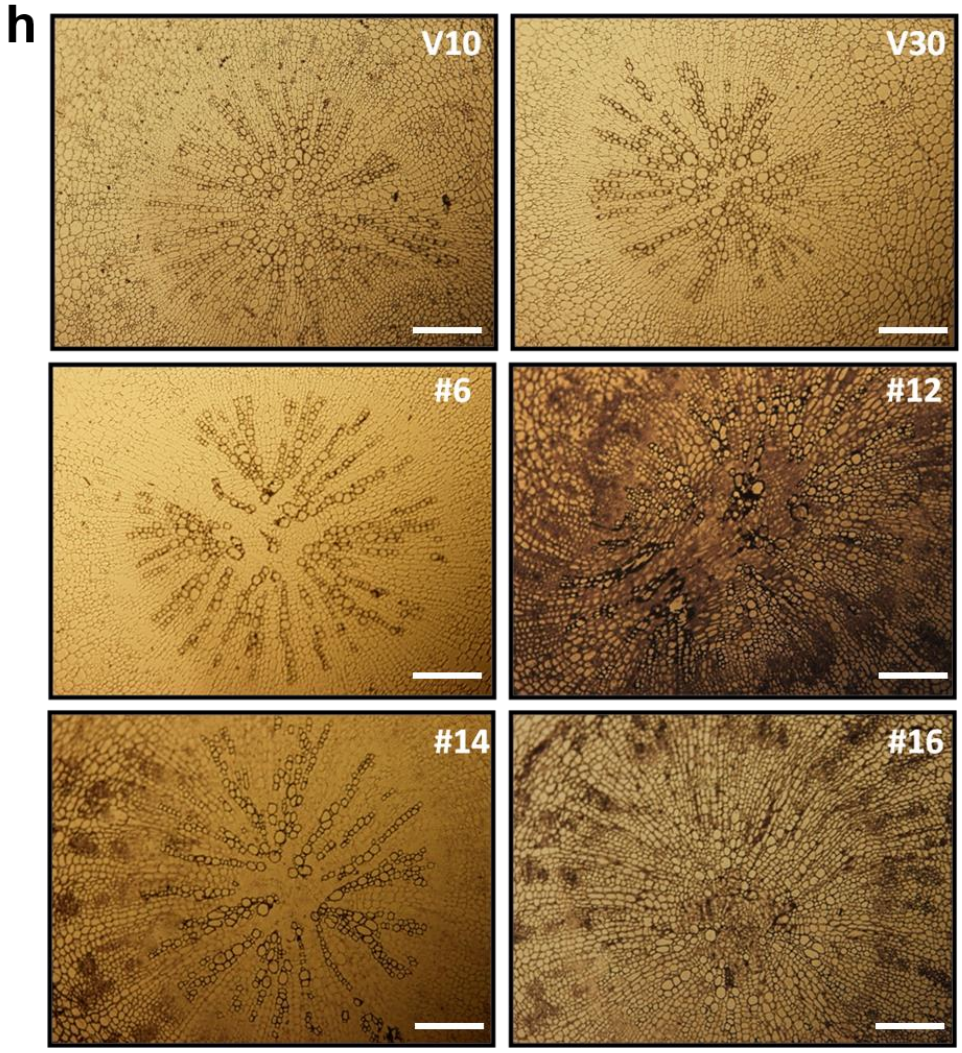
h
V10
V30
#6
#12
#14
#16

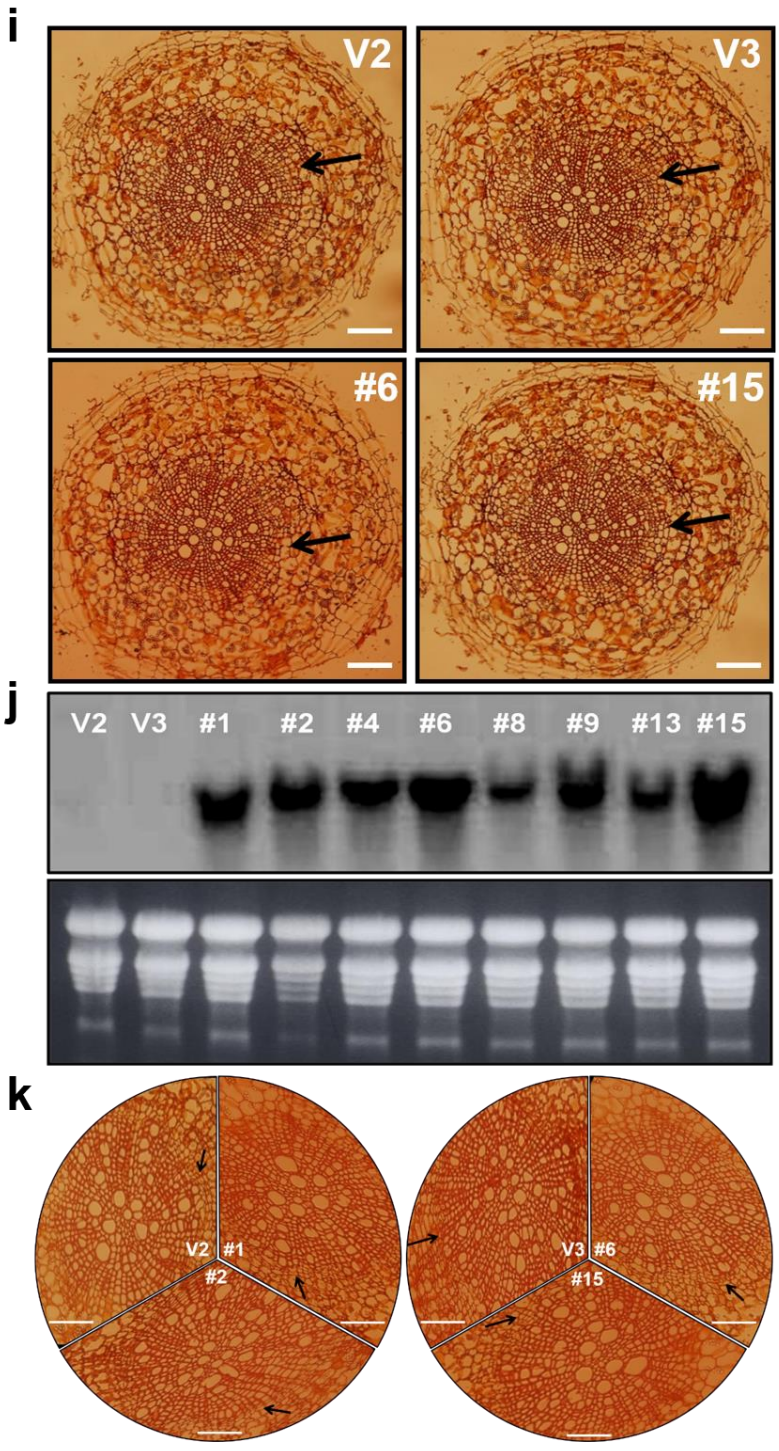
i
V2
V3
#6
#15
j
V2 V3 #1 #2 #4 #6 #8 #9 #13 #15
k
V2 #1
#2
V3 #6
#15

Figure 15. Cytological comparisons of *CaRZFP1*-transgenic and vector-only lettuce plants. **a**. Leaf cross sections of *CaRZFP1*-transgenic lettuce and vector-only lettuce. Scale bar is 10 μm. **b.** Leaf epidermal layer with stomata. Scale bar is 25 μm. **c.** Number of stomata in *CaRZFP1*-transgenic lettuce lines and vector-only lettuce lines. **d.** Number of epidermal cells in *CaRZFP1*-transgenic lettuce lines and vector-only lines. Error bars show standard deviation. **e.** Stem cross sections of *CaRZFP1*-transgenic lettuce lines and vector-only lines. Scale bar is 25 μm. **f.** Root cross sections of *CaRZFP1*-transgenic lettuce lines and vector-only lines. Arrows point endodermis layer. Scale bar is 25 μm. **g.** Magnified view of **f**. Scale bar is 25 μm. **h.** *In situ* localization of *CaRZFP1* transcript in *CaRZFP1*-transgenic lettuce plant roots. Cross sections of roots were hybridized with digoxigenin-labeled *CaRZFP1* antisense RNA probes. Scale bar is 25 μm. **i**. Roots of *CaRZFP1*-transgenic tobacco plants showed normal internal structure. Cross sections of the vector-only control lines, V2 and V3, and *CaRZFP1*-transgenic lines, #6 and #15. **j**. RNA blot hybridization results for several transgenic tobacco lines for the *CaRZFP1* transcript. **k**. Magnified view of the root cross sections of the vector-only lines and the *CaRZFP1*-transgenic lines. Scale bars are for 25 μm.

III.9. *CaRZFP1*-transgenic lettuce plants were intolerant to abiotic stresses

Expression of *CaRZFP1* was not detected under normal physiological conditions and quickly induced under diverse abiotic stresses, not only under high-temperature stress in hot pepper. And these results led us to hypothesize that *CaRZFP1* might have functioned in the tolerance mechanism against abiotic stresses in hot pepper, and possibly in other plant species phylogenitically close that happened to be the case in tobacco (Zeba *et al*., 2009). Thus, *CaRZFP1* over-expression effect on the abiotic stress tolerance in *CaRZFP1*-transgenic lettuce plants was examined, even though the *CaRZFP1*-transgenic lettuce plants showed much reduced growth under normal conditions. First, the high-temperature tolerance of transgenic lettuce and vector-only plants that had been incubated at 44°C for 1, 2, and 4 h. However, no significant differences were observed between the transgenic lettuce and vector-only plants. All transgenic lettuce and vector-only plants died after exposure to high-temperature stress treatment (Figure 16a and b). Secondly, the cold tolerance assay was performed, transgenic lettuce and vector-only plants that had been incubated at 4°C for 4 days and returned to the normal temperature (25°C) for recovery. However, no noticeable differences were observed between the transgenic lettuce and vector-only plants after being exposed to cold treatment (Figure 16c and d). Finally, we compared the capacity of the transgenic lettuce and vector-only plants to respond to dehydration. Dehydration sensitivity was recorded as the capacity of plants to resume growth after water stress, when returned to normal conditions. The growth assay was performed with transgenic lettuce and vector-only plants that had been stressed by withholding water for 4 weeks. After re-watering for two weeks, no meaningful differences were observed between the

transgenic lettuce and vector-only plants (Figure 16e and f). All these experiments were repeated three times and the results obtained from these experiments were consistent. Therefore, from all the stress treatment conditions, no significant differences were observed between the transgenic lettuce and vector-only plants in abiotic stresses tolerance. These results indicate that function of *CaRZFP1* in lettuce may not have been linked to the abiotic stress response-related functional networks.

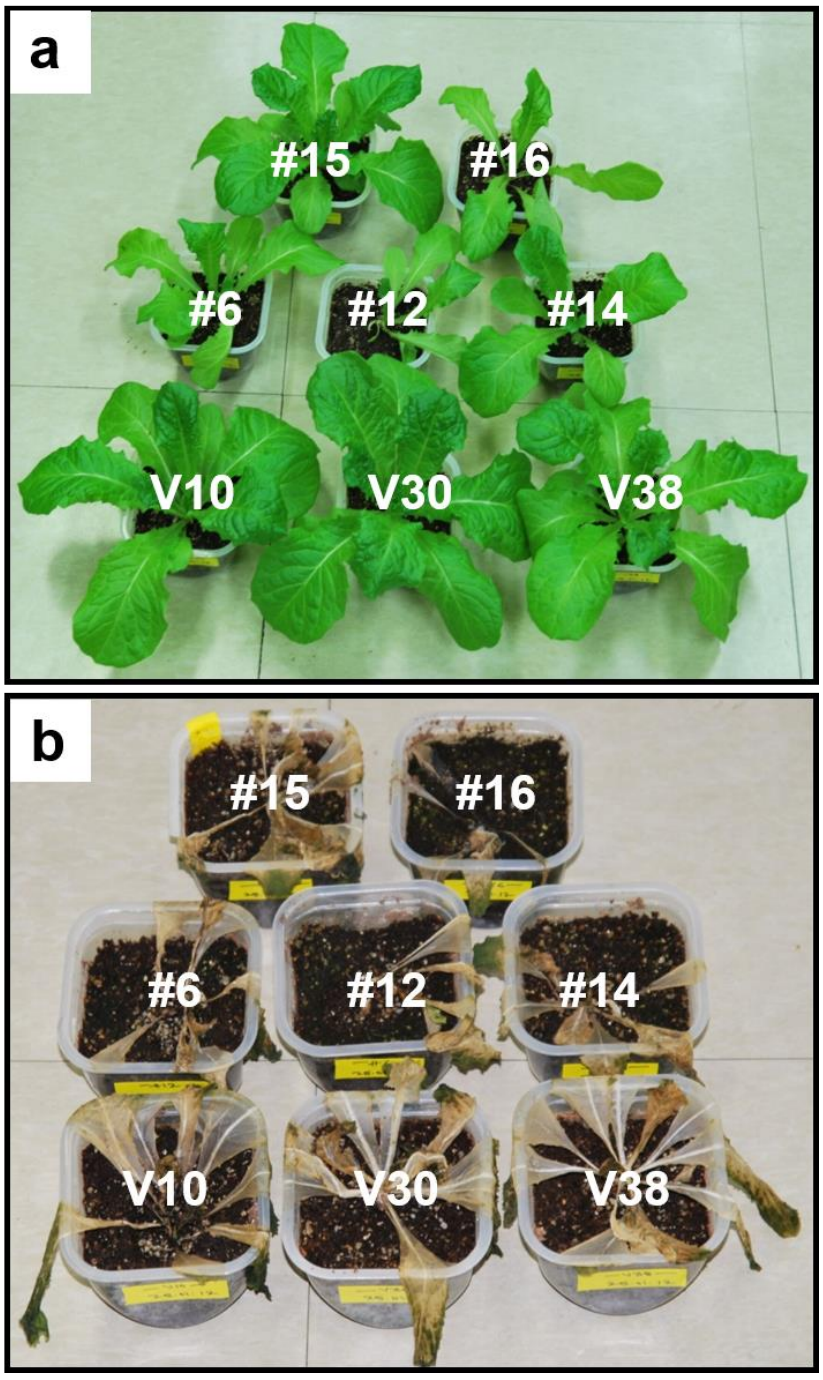
a
#15
#16
#6
#12
#14
V10
V30
V38
b
#15
#16
#6
#12
#14
V10
V30
V38

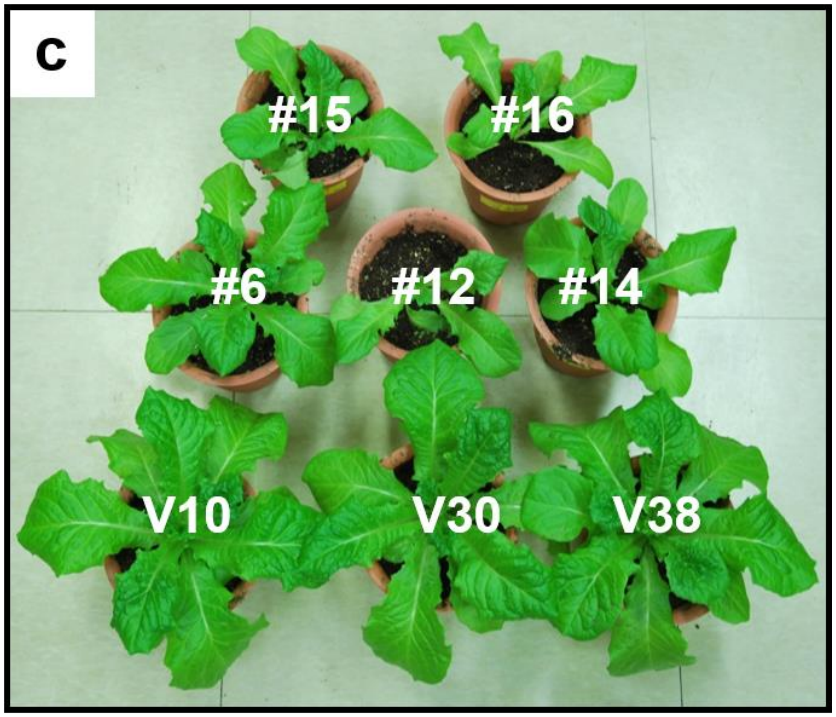
c
#15
#16
#6
#12
#14
V10
V30
V38


d
#15
#16
#6
#12
#14
V10
V30
V38

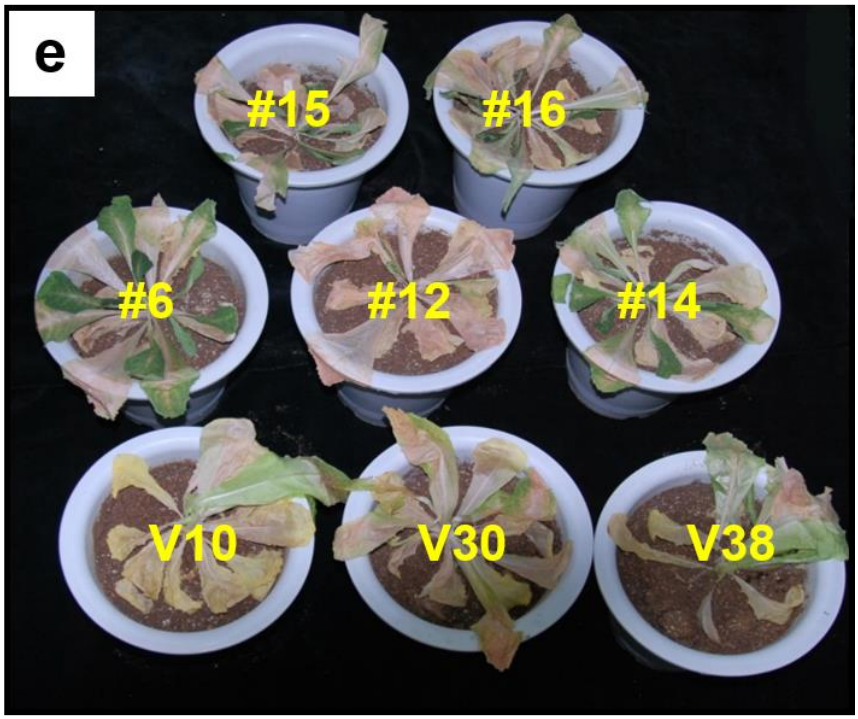
e
#15
#16
#6
#12
#14
V10
V30
V38


f
#15
#16
#6
#12
#14
V10
V30
V38

Figure 16. Abiotic tolerance assay of transgenic lettuce plants. a. A typical representative picture of thermotolerance assay of T_3 transgenic lettuce and vector-only plants. Young plants of about 7-8 fully expanded leaves of T_3 transgenic lettuce and vector-only plants were exposed to high-temperature at 44°C for 1, 2, 4 h and returned to the normal temperature (25°C) for recovery. **b**. A representative picture taken after 1 week. **c**. Cold tolerance assay of T_3 transgenic lettuce and vector-only plants. Young plants of about 7-8 fully expanded leaves of T_3 transgenic lettuce and vector-only plants were exposed at 4°C for 4 days and returned to the normal temperature (25°C) for recovery. After 1 week photographs were taken. A representative picture is shown **d**. **e.** Drought tolerance assay of T_3 transgenic lettuce and vector-only plants. Phenotype of T_3 transgenic lettuce and vector-only plants at 4 weeks after the cessation of water. **f.** A representative picture is shown, their recovery after 2 weeks of re-watering.

III.10. Transcriptome profiles of *CaRZFP1*-transgenic lettuce plants

What explains the strong correlation between *CaRZFP1* expression levels and diminished growth and development in lettuce plants? To elaborate on the potential underlying genes, whole transcriptome profiling was performed on transgenic lettuce that differed in *CaRZFP1* transcript levels (low, moderate, and high; lines #6, #12, #14, #16) and the vector-only lettuce. Three plants per line were used. Agilent Arabidopsis GE 4 X 44K microarray was used for the transcriptome profiling of the lettuce lines because a lettuce microarray was unavailable and our previous work on tobacco also used the Arabidopsis microarray (Zeba *et al.*, 2009). Differentially expressed (either up- or down-regulated) transcripts between line #12 (with the strongest *CaRZFP1* expression) and control lines were determined via a 2-fold change threshold ($P < 0.05$). Among 87 genes identified as significantly differentially expressed, 73 were up-regulated (Table 2) and 14 were down-regulated (Table 3). These genes could be categorized into several groups according to their putative functions: regulation of cell cycle and DNA processing; transcription factors; growth and cell wall proteins; metabolic proteins; signal transduction proteins; defense response; transport; protein folding, modification, and destination; plus an unannotated group (Table 2, and 3).

Differentially expressed genes in transgenic line #12 were again screened for the correlation between *CaRZFP1* expression and growth impairment in lines #14, #16 (medium *CaRZFP1* expression), and #6 (low *CaRZFP1* expression). This analysis verified the presence of the correlative change in fold values from highest in line #12 to the lowest in vector-only lines (Table 2, and 3). I separated the up- and down-regulated genes into two groups:

"Group 1" included genes with correlative changes in expression level among four transgenic lettuce lines (#6, #14, #16 and #12) (Figure 17a), while "Group 2" included only genes with significant expression-level changes mainly in line #12 (Figure 17b).

Group 1 contained the following up-regulated putatively annotated genes: cell division protease ftsH-11 (*FTSH11*), timeless family protein (*ATIM*), indeterminate-domain 7 protein (*IDD7*), Arabidopsis response regulator 10 (*ARR10*), BES1-interacting MYC-like 1 (*BIM1*), membrane insertion protein, OxaA/YidC with tetratricopeptide repeat domain-containing protein, extensin 3 (*EXT3*), peroxidase 45, glucose-1-phosphate adenylyltransferase small subunit (*ADG1*), NADH dehydrogenase (ubiquinone) flavoprotein 1 (*CI51*), FMN-binding protein, serine/threonine-protein kinase (*ATM*), Hs1pro-1 protein, nodulin MtN3-like protein, Sec24-like transport protein (*ERMO2*), glutamate receptor 2.1 (*GLR2.1*), auxin efflux carrier family protein, pentatricopeptide repeat-containing protein, cysteine/histidine-rich C1 domain-containing protein, conserved peptide upstream open reading frame 24 (*CPuORF24*), putative ubiquitin-conjugating enzyme E2 18 (*UBC18*), armadillo/beta-catenin-like repeats-containing protein, F-box associated ubiquitination effector family protein, development and cell death domain protein (*DCD*), and six uncharacterized genes (Table 2). Additionally, Group 1 contained the following down-regulated genes: Rm1C-like cupins super family protein, amidohydrolase family protein (*LAF3*), indole-3-acetate beta-D-glucosyltransferase (*IAGLU*), serine/threonine-protein kinase Nek5 (*NEK6*), NSP-interacting kinase 3 (*NIK3*), transducin family protein/WD40 repeat family protein, tRNA-Ser and one uncharacterized gene (Table 3).

Putative annotation of up-regulated genes in Group 2 was as follows: 1 genes in “Cell cycle and DNA processing,” 4 genes in “Transcription factor,” 3 genes in “Growth-related cell wall proteins,” 6 genes in “Metabolism,” 6 genes in “Signal transduction,” 1 gene in “Defense response,” 10 genes in “Transport facilitation,” 8 genes in “Protein folding, modification and destination,” and 4 uncharacterized genes. Only six putatively annotated of down-regulated genes in Group 2: 1 gene in “Transcription factor,” 1 gene in “Metabolism,” 2 genes in “Protein folding, modification and destination,” and 2 uncharacterized genes (Figure 18). Group 1 contained 24 up-regulated putatively annotated genes, 7 up-regulated unannotated genes, 7 down-regulated putatively annotated genes, and 1 down-regulated unannotated gene (Figure 18; Table 2 and 3). Group 2 contained 39 up-regulated putatively annotated genes, 3 up-regulated unannotated genes, 4 down-regulated putatively annotated genes, and 2 down-regulated unannotated genes (Figure 18; Table 2 and 3).

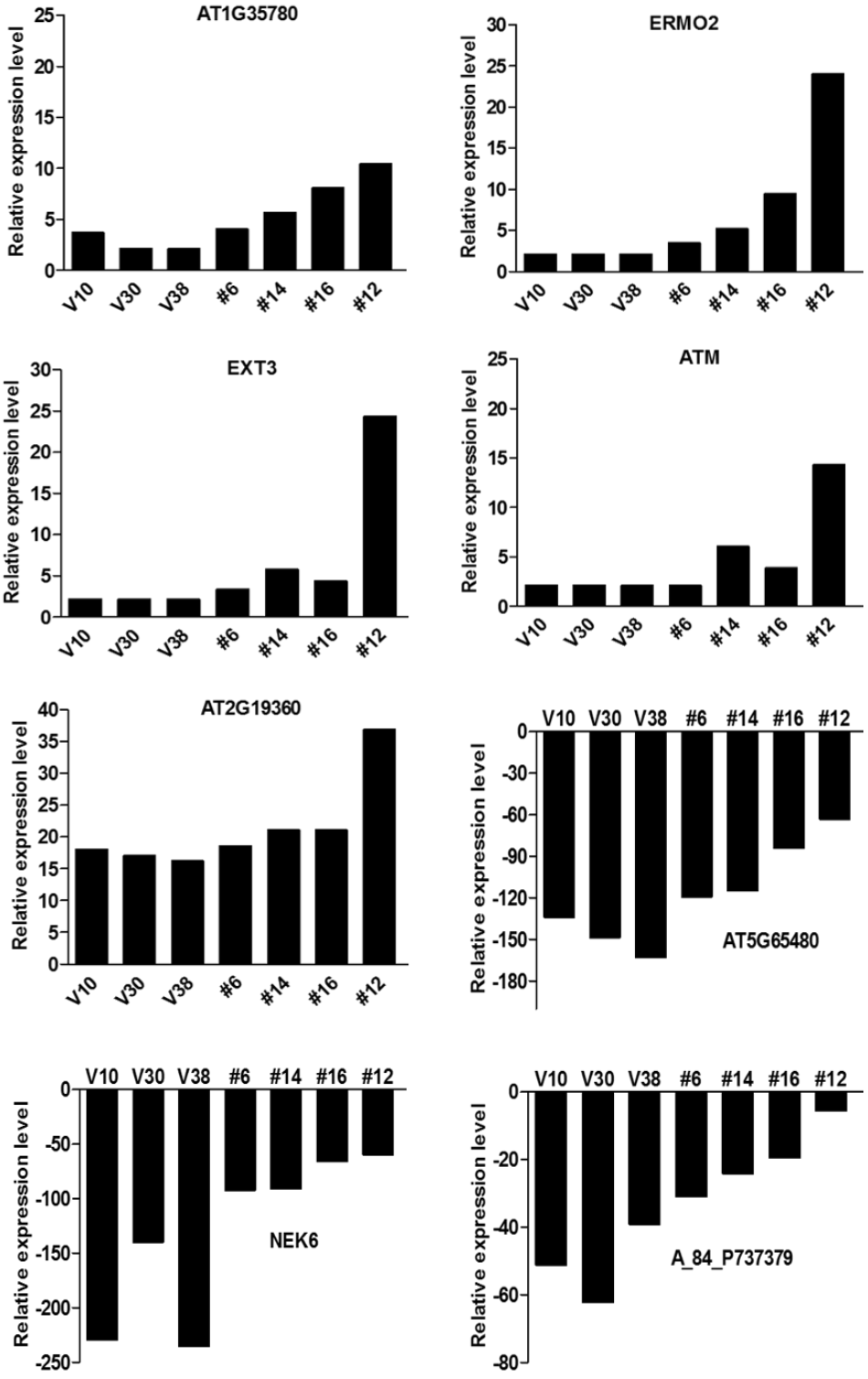
AT1G35780
Relative expression level
25
20
15
10
5
0
V10 V30 V38 #6 #14 #16 #12
ERMO2
Relative expression level
30
25
20
15
10
5
0
V10 V30 V38 #6 #14 #16 #12
EXT3
Relative expression level
30
25
20
15
10
5
0
V10 V30 V38 #6 #14 #16 #12
ATM
Relative expression level
25
20
15
10
5
0
V10 V30 V38 #6 #14 #16 #12
AT2G19360
Relative expression level
40
35
30
25
20
15
10
5
0
V10 V30 V38 #6 #14 #16 #12
V10 V30 V38 #6 #14 #16 #12
Relative expression level
0
-30
-60
-90
-120
-150
-180
AT5G65480
V10 V30 V38 #6 #14 #16 #12
Relative expression level
0
-50
-100
-150
-200
-250
NEK6
V10 V30 V38 #6 #14 #16 #12
Relative expression level
0
-20
-40
-60
-80
A_84_P737379

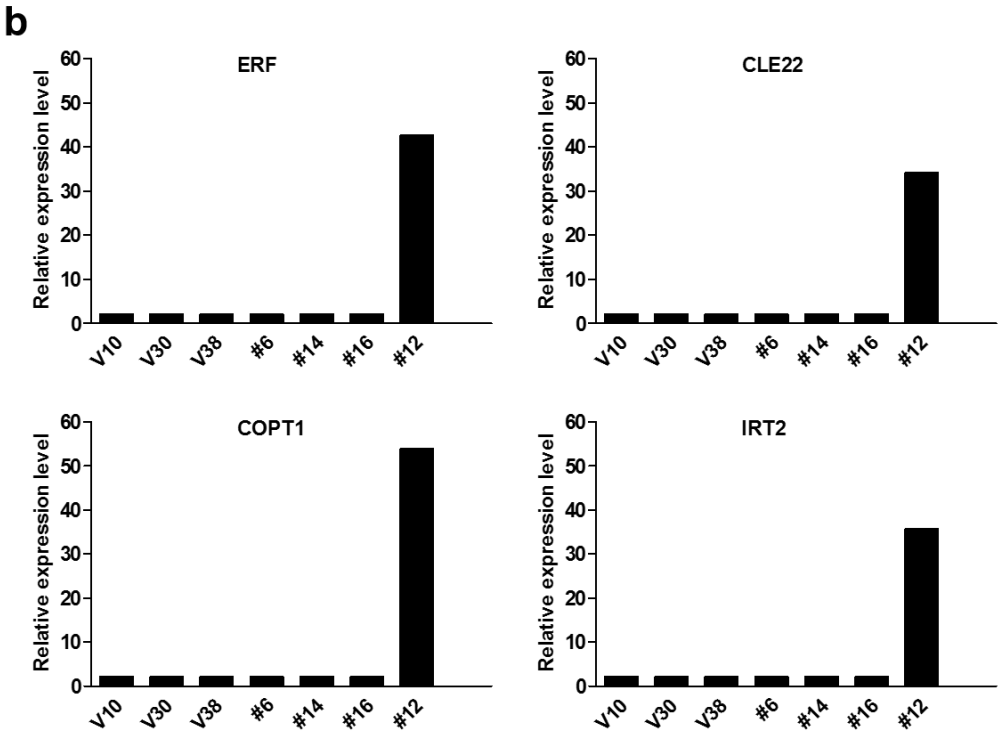

Figure 17. Comparison of relative expression levels of transcripts induced or suppressed in *CaRZFP1*-transgenic lettuce and vector-only lines. The x-axes are representing the *CaRZFP1*-transgenic and vector-only lettuce lines and y-axes are scales of relative expression levels of transcripts induced or suppressed in transcriptome profile. **a.** Group 1 genes with correlative changes in expression among the four *CaRZFP1*-transgenic lettuce lines **b.** Group 2 genes expression mainly changes in line #12.

Table 2. Genes up-regulated in *CaRZFP1*-overexpressing T_4 generation lettuce plants.

Agilent probe set ID	Gene symbol	Gene description	Expression level					*CaRZFP1*-transgenic lettuce lines/vector controls (log_2 fold change)				*p*-value
			Average of vector control lines	#6	#14	#16	#12	#6	#14	#16	#12	
Cell cycle and DNA processing												
A_84_P11226	**At5g53170**	**Cell division protease ftsH-11 (FTSH11)**	**2.13**	**2.60**	**2.78**	**5.49**	**11.02**	**0.28**	**0.38**	**1.36**	**2.36**	**7.40E-03**
A_84_P833412	**At5g52910**	**Timeless family protein (ATIM)**	**2.13**	**2.13**	**3.06**	**2.87**	**21.83**	**0**	**0.52**	**0.42**	**3.35**	**1.67E-02**
A_84_P11445	At1g08260	DNA polymerase epsilon subunit 1 (TIL1)	2.13	2.13	2.13	2.13	21.78	0	0	0	3.35	6.40E-03
Transcription factor												
A_84_P824828	At1g80490	Topless-related protein 1 (TPR1)	4.38	6.20	7.40	5.66	43.56	0.50	0.75	0.37	3.31	2.50E-02
A_84_P62920	**At1g55110**	**Indeterminate-domain 7 protein (IDD7)**	**2.64**	**2.70**	**6.66**	**4.49**	**22.56**	**0.03**	**1.33**	**0.76**	**3.09**	**9.50E-02**
A_84_P16708	**At4g31920**	**Arabidopsis response regulator 10 (ARR10)**	**2.15**	**2.16**	**2.65**	**2.33**	**21.49**	**0.00**	**0.30**	**0.11**	**3.31**	**7.60E-03**
A_84_P19621	**At5g08130**	**BES1-interacting MYC-like 1 (BIM1)**	**2.13**	**2.13**	**2.45**	**2.42**	**18.06**	**0**	**0.20**	**0.18**	**3.08**	**4.80E-03**
A_84_P18116	At1g80580	Ethylene-responsive factor (ERF)	2.13	2.13	2.13	2.13	42.73	0	0	0	4.32	1.30E-03
A_84_P751359	At1g08465	Putative axial regulator YABBY 2 (YAB2)	2.13	2.13	2.13	2.13	134.4	0	0	0	5.97	2.00E-04

A_84_P854322	At1g20910	ARID/BRIGHT DNA-binding domain-containing protein	2.13	2.13	2.13	2.13	44.69	0	0	0	4.38	3.80E-03
Growth related cell wall protein genes												
A_84_P226209	**At3g44370**	**Membrane insertion protein, OxaA/YidC with tetratricopeptide repeat domain-containing protein**	**2.12**	**2.46**	**4.99**	**4.28**	**13.66**	**0.21**	**1.23**	**1.01**	**2.68**	**1.59E-02**
A_84_P786204	**At1g21310**	**Extensin 3 (EXT3)**	**2.13**	**3.55**	**5.79**	**4.35**	**24.22**	**0.73**	**1.44**	**1.02**	**3.50**	**1.25E-02**
A_84_P829356	At4g33610	Glycine-rich protein	2.13	2.13	2.13	2.13	18.07	0	0	0	3.08	4.40E-03
A_84_P594615	At3g28550	Proline-rich extensin-like family protein	2.13	2.13	2.13	2.13	17.64	0	0	0	3.04	7.50E-03
A_84_P568734	At3g24860	Hydroxyproline-rich glycoprotein family protein	2.13	2.13	2.13	2.13	16.53	0	0	0	2.95	4.10E-03
Metabolism												
A_84_P857567	**At4g30170**	**Peroxidase 45**	**2.13**	**2.33**	**5.40**	**3.80**	**13.43**	**0.12**	**1.34**	**0.83**	**2.65**	**1.27E-02**
A_84_P20665	**At5g48300**	**Glucose-1-phosphate adenylyltransferase small subunit (ADG1)**	**2.12**	**2.15**	**2.54**	**2.82**	**14.70**	**0.02**	**0.26**	**0.41**	**2.79**	**6.10E-03**
A_84_P813705	**At5g08530**	**NADH dehydrogenase (ubiquinone) flavoprotein 1(CI51)**	**2.13**	**2.16**	**4.97**	**6.17**	**17.29**	**0.02**	**1.22**	**1.53**	**3.02**	**1.06E-02**
A_84_P258550	**At3g03890**	**FMN binding protein**	**2.52**	**6.64**	**7.63**	**10.71**	**21.99**	**1.39**	**1.59**	**2.08**	**3.12**	**1.20E-03**
A_84_P2	At4g10	Sucrose-phosphate	2.13	2.13	2.13	2.13	11.61	0	0	0	2.44	4.30E-03

1361	120	synthase										
A_84_P156385	At5g66230	Chalcone-flavanone isomerase family protein	2.13	2.13	2.13	2.13	43.43	0	0	0	4.34	1.50E-03
A_84_P833808	At1g17420	Lipoxygenase 3 (LOX3)	2.13	2.13	2.13	2.13	52.15	0	0	0	4.60	1.70E-02
A_84_P15837	At5g08100	Isoaspartyl peptidase/L-asparaginase 1 subunit beta	2.13	2.13	2.13	2.13	53.24	0	0	0	4.63	1.00E-03
A_84_P790164	At5g41080	Glycerophosphoryl diester phosphodiesterase family protein	2.13	2.13	2.13	2.13	36.63	0	0	0	4.10	3.60E-03
A_84_P831419	At1g54620	Pectin methylesterase inhibitor superfamily protein	2.13	2.13	2.13	2.13	42.20	0	0	0	4.30	5.60E-03
Signal transduction												
A_84_P852024	At1g06700	Protein kinase domain-containing protein	2.29	3.25	3.20	2.39	38.83	0.50	0.48	0.06	4.08	5.00E-03
A_84_P18426	**At3g48190**	**Serine/threonine-protein kinase (ATM)**	**2.13**	**2.13**	**6.05**	**3.88**	**14.3**	**0.00**	**1.50**	**0.86**	**2.74**	**2.92E-02**
A_84_P212118	At4g04960	L-type lectin receptor kinase VII.1 (LECRK-VII.1)	2.13	2.13	2.13	2.13	42.65	0	0	0	4.31	3.00E-03
A_84_P14571	At3g20860	NIMA-related kinase 5 (NEK5)	2.13	2.13	2.13	2.13	11.65	0	0	0	2.44	1.58E-02
A_84_P791547	At3g24540	Proline-rich extensin-like receptor kinase (PERK)	2.13	2.13	2.13	2.13	23.59	0	0	0	3.46	5.10E-03

A_84_P570789	At5g11360	Interleukin-1 receptor-associated kinase 4 protein	2.13	2.13	2.13	2.13	21.50	0	0	0	3.33	7.70E-03
A_84_P302670	At5g12235	CLAVATA3/ESR-related 22 protein (CLE22)	2.13	2.13	2.13	2.13	34.13	0	0	0	3.99	8.70E-03
Defense Response												
A_84_P16568	**At3g55840**	**Hs1pro-1 protein**	**2.68**	**3.91**	**6.01**	**4.93**	**66.14**	**0.54**	**1.16**	**0.87**	**4.62**	**3.20E-03**
A_84_P761276	At3g61185	Defensin-like (DEFL) family protein	2.13	2.13	2.13	2.13	92.58	0	0	0	5.43	**8.00E-04**
Transport facilitation												
A_84_P827818	**At4g10850**	**Nodulin MtN3-like protein**	**2.13**	**2.67**	**2.83**	**2.81**	**22.46**	**0.32**	**0.40**	**0.39**	**3.39**	**1.20E-02**
A_84_P818490	**At3g07100**	**Sec24-like transport protein (ERMO2)**	**2.13**	**3.44**	**5.17**	**9.43**	**24.02**	**0.69**	**1.27**	**2.14**	**3.49**	**3.10E-03**
A_84_P11158	**At5g27100**	**Glutamate receptor 2.1 (GLR2.1)**	**2.13**	**2.24**	**2.52**	**8.41**	**12.28**	**0.06**	**0.24**	**1.97**	**2.52**	**8.20E-02**
A_84_P793674	**At5g01990**	**Auxin efflux carrier family protein**	**5.37**	**9.83**	**14.6**	**15.03**	**26.93**	**0.87**	**1.44**	**1.48**	**2.32**	**7.80E-03**
A_84_P808620	At3g26520	Tonoplast intrinsic protein 2 (TIP2)	2.13	2.13	2.13	2.13	15.61	0	0	0	2.86	4.10E-03
A_84_P21005	At2g39890	Proline transporter 1 (PROT1)	2.13	2.13	2.13	2.13	20.66	0	0	0	3.27	1.12E-02
A_84_P70864	At5g51710	K(+) efflux antiporter 5 (KEA5)	2.13	2.13	2.13	2.13	11.84	0	0	0	2.47	1.91E-02
A_84_P609485	At1g79520	Cation efflux family protein	2.13	2.13	2.13	2.13	11.87	0	0	0	2.47	4.18E-02
A_84_P750326	At3g55740	Proline transporter 2 (PROT2)	2.13	2.13	2.13	2.13	12.51	0	0	0	2.55	1.85E-02

A_84_P814453	At1g80300	Nucleotide transporter 1 (NTT1)	2.13	2.13	2.13	2.13	26.69	0	0	0	3.64	3.30E-03
A_84_P18458	At1g23910	Polyketide cyclase/dehydrase and lipid transport superfamily protein	2.13	2.13	2.13	2.13	58.51	0	0	0	4.77	8.30E-03
A_84_P18546	At4g19680	Fe(2+) transport protein 2 (IRT2)	2.13	2.13	2.13	2.13	35.68	0	0	0	4.06	6.90E-03
A_84_P21721	At5g59030	Copper transporter 1 (COPT1)	2.13	2.13	2.13	2.13	53.89	0	0	0	4.65	6.10E-03
A_84_P21354	At4g08290	Nodulin MtN21 /EamA-like transporter family protein	2.13	2.13	2.13	2.13	63.14	0	0	0	4.88	1.60E-03
Protein fate (folding, modification, destination)												
A_84_P12483	**At1g31920**	**Pentatricopeptide repeat-containing protein**	**4.09**	**4.51**	**10.7**	**10.03**	**55.64**	**0.14**	**1.39**	**1.29**	**3.76**	**4.70E-03**
A_84_P833611	**At2g17600**	**Cysteine/histidine-rich C1 domain-containing protein**	**11.43**	**15.8**	**17.5**	**16.04**	**78.29**	**0.46**	**0.62**	**0.48**	**2.77**	**3.10E-03**
A_84_P17816	**At5g45428**	**Conserved peptide upstream open reading frame 24 (CPuORF24)**	**20.54**	**29.6**	**29.9**	**31.92**	**193.3**	**0.53**	**0.54**	**0.63**	**3.23**	**1.00E-04**
A_84_P12134	**At5g42990**	**Putative ubiquitin-conjugating enzyme E2 18 (UBC18)**	**5.89**	**7.15**	**10.1**	**11.88**	**26.55**	**0.27**	**0.77**	**1.01**	**2.17**	**1.06E-02**
A_84_P18897	**At1g71410**	**Armadillo/beta-catenin-like repeats-containing protein**	**2.14**	**3.62**	**7.93**	**8.86**	**18.3**	**0.75**	**1.88**	**2.04**	**3.09**	**5.50E-03**

A_84_P589334	**At4g01640**	**F-box associated ubiquitination effector family protein**	**2.14**	**2.21**	**3.39**	**3.75**	**158.9**	**0.04**	**0.66**	**0.80**	**6.21**	**6.00E-02**
A_84_P866419	**At2g35140**	**Development and cell death domain protein (DCD)**	**2.13**	**2.13**	**2.65**	**3.95**	**24.72**	**0**	**0.31**	**0.88**	**3.53**	**1.98E-02**
A_84_P22756	At1g31090	F-box domain-containing protein	2.13	2.13	2.13	5.13	16.75	0	0	1.26	2.97	3.70E-03
A_84_P845356	At4g03510	E3 ubiquitin-protein ligase (RMA1)	2.13	2.13	2.13	8.86	23.73	0	0	2.05	3.47	3.40E-03
A_84_P24164	At3g62940	Cysteine proteinases family protein	2.13	2.13	2.13	2.41	56.35	0	0	0.17	4.72	4.60E-03
A_84_P760418	At3g26805	Aspartic protease family protein	2.13	2.13	2.13	2.13	47.46	0	0	0	4.47	5.70E-03
A_84_P21429	At4g30020	PA-domain containing subtilase family protein	2.13	2.13	2.13	2.13	68.07	0	0	0	4.99	2.30E-03
A_84_P162213	At1g06630	F-box domain-containing protein	2.13	2.13	2.13	2.13	23.16	0	0	0	3.43	1.75E-02
A_84_P238183	At3g23880	F-box/kelch-repeat protein	2.13	2.13	2.13	2.13	27.59	0	0	0	3.69	1.40E-02
A_84_P581169	At3g11000	Development and cell death domain protein (DCD)	2.13	2.13	2.13	2.13	75.02	0	0	0	5.13	6.00E-04
Unannotated genes												
A_84_P595309	**At2g18970**	**Uncharacterized gene**	**2.13**	**3.79**	**8.09**	**4.14**	**22.63**	**0.83**	**1.92**	**0.95**	**3.40**	**1.23E-02**
A_84_P794936	**At5g04550**	**Uncharacterized gene**	**2.70**	**2.91**	**7.33**	**8.62**	**26.57**	**0.11**	**1.43**	**1.67**	**3.29**	**6.60E-03**
A_84_P11270	**At1g55160**	**Uncharacterized gene**	**2.20**	**3.41**	**4.82**	**7.99**	**25.63**	**0.63**	**1.13**	**1.86**	**3.54**	**8.10E-03**

A_84_P756169	**At2g11630**	**Uncharacterized gene**	**2.13**	**2.17**	**2.51**	**3.23**	**140.6**	**0.02**	**0.23**	**0.59**	**6.04**	**5.00E-04**
A_84_P756837	**At2g24755**	**Uncharacterized gene**	**2.13**	**2.13**	**2.67**	**3.04**	**67.12**	**0**	**0.32**	**0.51**	**4.97**	**3.70E-03**
A_84_P766236	**At5g26775**	**Uncharacterized gene**	**2.13**	**2.13**	**4.36**	**7.01**	**225.1**	**0**	**1.02**	**1.71**	**6.71**	**4.00E-04**
A_84_P508404	**At3g11300**	**Uncharacterized gene**	**2.13**	**2.13**	**2.13**	**4.56**	**40.86**	**0**	**0**	**1.09**	**4.25**	**1.40E-03**
A_84_P752460	At1g43195	Uncharacterized gene	2.13	2.13	2.13	2.13	39.57	0	0	0	4.21	4.60E-03
A_84_P513598	At2g22122	Uncharacterized gene	2.13	2.13	2.13	2.13	47.61	0	0	0	4.47	4.30E-02
A_84_P105846	At1g63610	Uncharacterized gene	2.13	2.13	2.13	2.13	44.73	0	0	0	4.38	3.20E-02

Group 1 genes are in bold.

Table 3. Genes down-regulated in *CaRZFP1*-overexpressing T_4 lettuce plants.

Agilent probe set ID	Gene symbol	Gene description	Expression level					*CaRZFP1*-transgenic lettuce lines/vector controls (log_2 fold change)				*p*-value
			Average of vector control lines	#6	#14	#16	#12	#6	#14	#16	#12	
Transcription factor												
A_84_P824704	At2g47850	Zinc finger CCCH domain-containing protein 32	64.18	34.29	44.06	47.61	5.18	-0.90	-0.54	-0.43	-3.62	1.26E-02
Metabolism												
A_84_P850432	**At4g10300**	**RmlC-like cupins super family protein**	**1632**	**902.8**	**857.9**	**503.8**	**400.2**	**-0.85**	**-0.92**	**-1.69**	**-2.02**	**4.45E-02**
A_84_P723766	**At3g55850**	**Amidohydrolase family protein (LAF3)**	**2079**	**1910**	**1810**	**1459**	**335**	**-0.12**	**-0.19**	**-0.51**	**-2.63**	**2.40E-03**
A_84_P18637	**At4g15550**	**Indole-3-acetate beta-D-glucosyltransferase (IAGLU)**	**34.19**	**32.85**	**35.78**	**31.59**	**3.19**	**-0.05**	**-0.15**	**-0.11**	**-3.41**	**1.02E-02**
A_84_P13059	At5g37600	Glutamine synthetase cytosolic isozyme 1-1 (GSR1)	42.68	13.24	17.14	11.78	4.57	-1.68	-1.31	-1.85	-3.22	6.00E-03
Signal transduction												

A_84_P830423	**At3g44200**	**Serine/threonine-protein kinase Nek5 (NEK6)**	**250**	**92.17**	**90.86**	**65.86**	**59.65**	**-1.44**	**-1.46**	**-1.92**	**-2.06**	**4.08E-02**
A_84_P23660	**At1g60800**	**NSP-interacting kinase 3 (NIK3)**	**25.15**	**10.19**	**10.02**	**8.07**	**3.21**	**-1.30**	**-1.32**	**-1.63**	**-2.96**	**7.50E-03**
Protein fate (folding, modification, destination)												
A_84_P95886	**At2g47990**	**Transducin family protein/WD-40 repeat family protein**	**40.71**	**26.96**	**21.51**	**12.9**	**10.12**	**-0.59**	**-0.92**	**-1.65**	**-2.00**	**6.40E-03**
A_84_P13790	At4g08950	Phosphate-responsive 1 family protein (EXO)	47.50	19.30	18.56	22.29	2.13	-1.29	-1.35	-1.09	-4.47	1.93E-02
A_84_P830642	At3g02490	Pentatricopeptide repeat (PPR) superfamily protein	24.5	9.24	14.56	13.95	2.83	-1.40	-0.75	-0.81	-3.11	8.90E-03
Protein synthesis												
A_84_P829794	**AtCG00290**	**tRNA-Ser**	**4125**	**3663**	**2464**	**2464**	**657**	**-0.17**	**-0.74**	**-.074**	**-2.64**	**5.50E-03**
Unannotated genes												
A_84_P737379	**At5g37650**	**Uncharacterized gene**	**50.87**	**30.94**	**24.18**	**19.51**	**5.62**	**-0.71**	**-1.07**	**-1.38**	**-3.17**	**1.86E-02**
A_84_P762480	At3g52742	Uncharacterized gene	15.14	20.19	7.06	13.85	3.43	-0.41	-1.10	-0.12	-2.14	3.81E-02
A_84_P762419	At3g15518	Uncharacterized gene	54.62	11.36	12.52	16.43	3.52	-2.26	-2.12	-1.73	-3.95	3.58E-02

Group 1 genes are in bold.

I also determined the level of overlap differentially expressed genes between *CaRZFP1*-transgenic lettuce lines. These analyses revealed that remarkable degree of overlap was found in up- and down-regulated differentially expressed gene sets between *CaRZFP1*-transgenic lettuce line #6, #14 and 12 (Figure 19a and b). A hierarchical clustering tree also revealed that ectopic expression of *CaRZFP1* dramatically modulated the expression profile of numerous genes in *CaRZFP1*-transgenic lettuce compared with the vector-only plants (Figure 19c). These genes might be involved in the diminishing growth of *CaRZFP1*-transgenic lettuce plants. Based on the previously reported functions of these up- and down-regulated genes, I made a possible working model is proposed in Figure 20 to depict the mechanism of *CaRZFP1* function in the impeded development of endodermis, pericycle, vascular bundle and retarded growth and development of *CaRZFP1*-trasgenic lettuce plants. This model demonstrates that ectopic expression of *CaRZFP1* might dergulate the genes involved in ubiquitin-mediated protein degradation which later affects the phytohormone signaling resulting in impaired endodermis and vascular bundle development. The group 1 genes showed the correlative expression change among the four transgenic lines and the arrested development of endodermis and the vascular bundle is closely correlated with *CaRZFP1* expression level, thus, group 1 genes considered more likely to linked with *CaRZFP1* expression in transgenic lettuce. However, all up- and down-regulated group 1 and 2 genes together might be leading to composite negative effects on growth and development of *CaRZFP1*-transgenic lettuce plants.

To validate the transcriptome analysis results, total RNA from the same transgenic lettuce lines used for transcriptome experiments was subjected to RNA blot analyses with oligonucleotides corresponding to those on the microarray. Nine genes that were either significantly up- or down-regulated

in transgenic lettuce lines were randomly selected for analysis. The genes encoded an FMN-binding protein, Hs1pro-1 protein, *EXT3*, *F-box*, auxin efflux carrier protein, *ERMO2*, *ATM*, *NIK3*, and *NEK6* (Table 4). Although some variation existed between the microarray and RNA blot results, trends in the differentially expressed genes were generally consistent across the two different approaches (Figure 21). Therefore, collectively these results showed that *CaRZFP1*-transgenic lettuce plants constitutively overexpressing *CaRZFP1* exhibited poorer growth and delayed flowering including weakened leaf growth, shorter plant height, diminish and stunted root growth compared with vector-only plants. I found a strong negative-correlation between the growth impairment and the transcript level of *CaRZFP1*. The ectopic expression of *CaRZFP1* significantly affects the endodermis, pericycle and vascular bundle development in *CaRZFP1*-transgenic lettuce roots. Overall, growth of *CaRZFP1*-transgenic lettuce plants was dramatically impeded by *CaRZFP1* expression in a dose-dependent fashion. This study also demonstrated that the same gene can result in a totally different outcome depending on the host species it is moved into.

Table 4. Oligonucleotides used in RNA blot analyses to confirm transcriptome profile data produced by microarray analysis in the *CaRZFP1*-transgenic and vector-only lettuce plants.

Agilent probe set ID	Gene description	Nucleotide sequence
A_84_P258550	FMN binding protein	5′-CTCTTCCATCTGAATCCTGCTACAACAAGAAAAGCTTCCTCCAATACACATTTTATCTTA-3′
A_84_P16568	Hs1pro-1 protein	5′-CGAATGCAAATAGAACGGTGGCGAATCACGAGTCCTATGATTCACTGACTCAGGTGTTTA-3′
A_84_P786204	Extensin 3 (Ext3)	5′-CACGGAGAACACGATGTACACAAGAAGACAAAGACAAGACGAAACCAGTACTGGTGATTG-3′
A_84_P589334	F-box	5-′ACGATGACGACGAGGACTACGACGACATTAGTATTATTTGTCAAGGCAACAACAACACTA -3′
A_84_P793674	Auxin efflux carrier protein	5′-AATATCATCTCAGAGACTCCGATTCTCTCTGTTTCTCCTCCACTTTTCAACCCAAGTCCA-3′
A_84_P818490	Sec24-like transport protein (ERMO2)	5′-CGGCCTTCTTCCTTGGGCCATAATGTGTTGTTTTGGATAAAGAAGTGCTACTTTTTGATT-3′
A_84_P18426	Serine/threonine-protein kinase (ATM)	5-′CAGGCACAGCAACTAATACAAGACGCAATTGACACAGATCGTTTGTCCCATATGTTCCCT-3′
A_84_P23660	NSP-interacting kinase 3 (NIK3)	5′-ATGGTGAGTTCTTCGCCGCGTGTGAGGTATTACTCGGATTATATTCAGGAATCGTCTCTT-3′
A_84_P830423	Serine/threonine-protein kinase Nek5 (NEK6)	5′-TCCTTAGGCTGTTGTATATATGAGATGGCTGCGTATCGACCTGCTTTCAAAGCTTTTGAT-3′

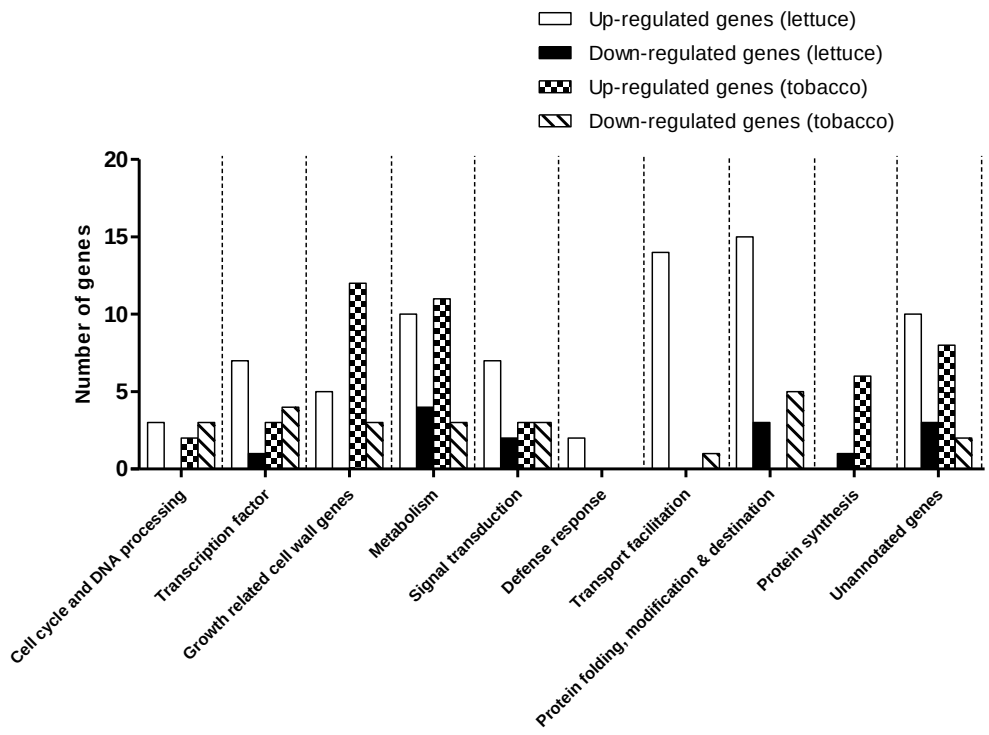

Figure 18. Differentially expressed genes in *CaRZFP1*-transgenic lettuce and *CaRZFP1*-transgenic tobacco plants were categorized into several groups according to their putative functions. The x-axis shows putative functional categories, and the y-axis shows the number of genes altered in expression.

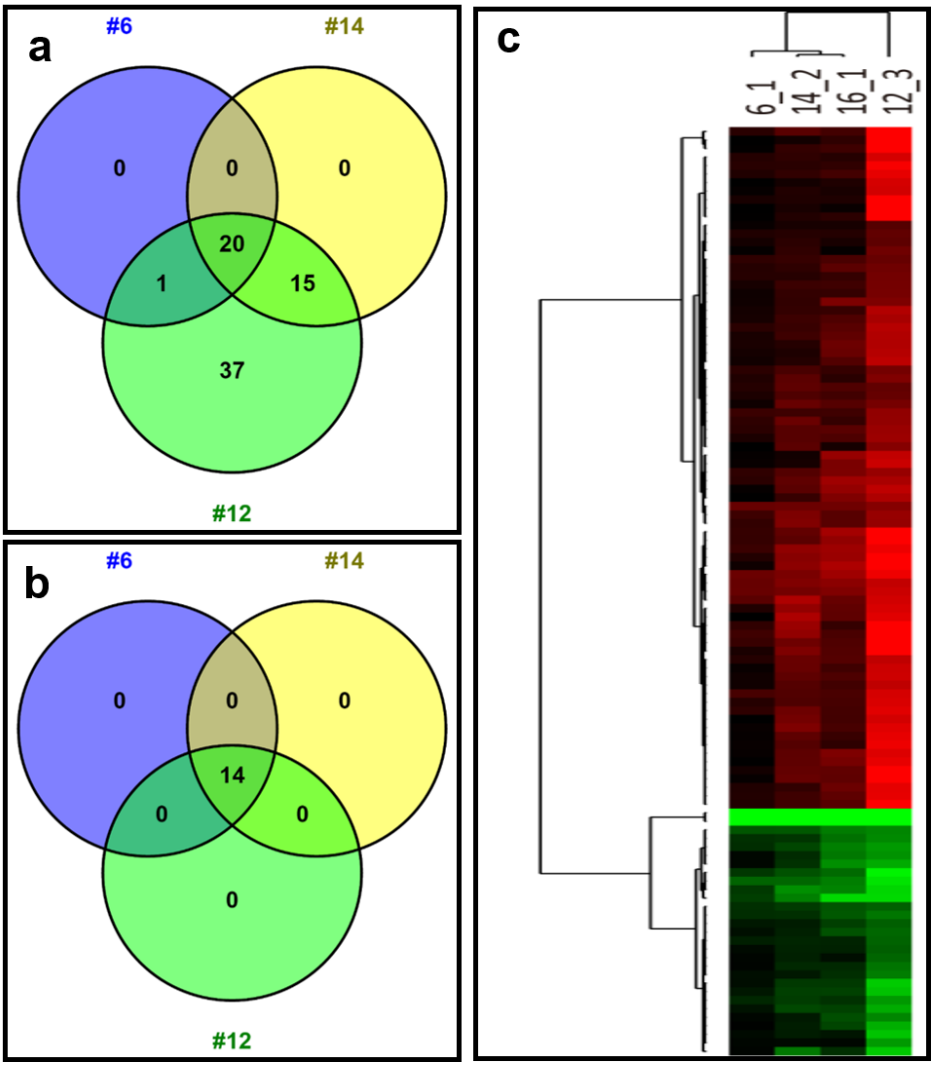

Figure 19. Overlap of differentially expressed genes in *CaRZFP1*-transgenic lettuce line #6, #14 and #12. a. Venn diagram showing significant overlapping of up-regulated genes in transcriptome analyses among *CaRZFP1*-transgenic lettuce lines. **b.** Overlapping of down-regulated **c.** Hierarchical clustering analysis. Red and green colors represent up- and down-regulated genes, respectively. The Venn diagram was generated using Venny (87).

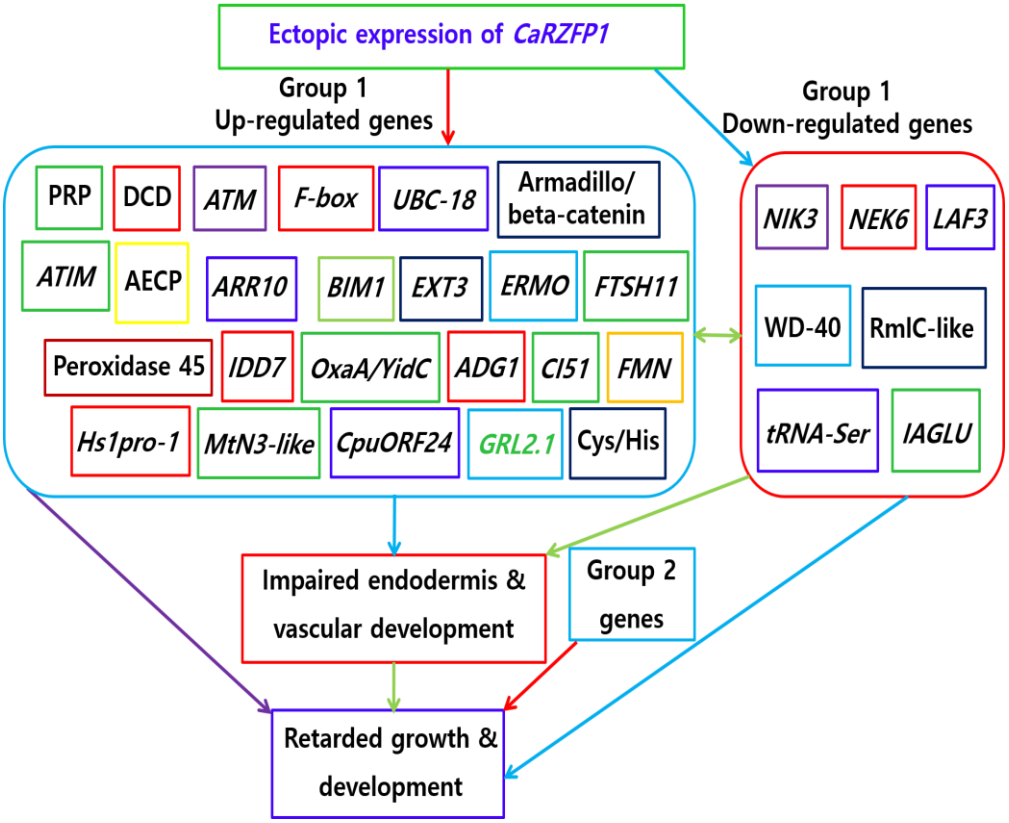

Figure 20. Possible function of *CaRZFP1* in impaired development of endodermis, pericycle, vascular bundle and retarded growth of *CaRZFP1*-transgenic lettuce plants. The group 1 genes closely correlated with *CaRZFP1* expression level and arrested development of endodermis and the vascular bundle among the four transgenic lines while all up- and down-regulated group 1 and 2 genes together might be involved in retarded growth and development of *CaRZFP1*-transgenic lettuce plants.

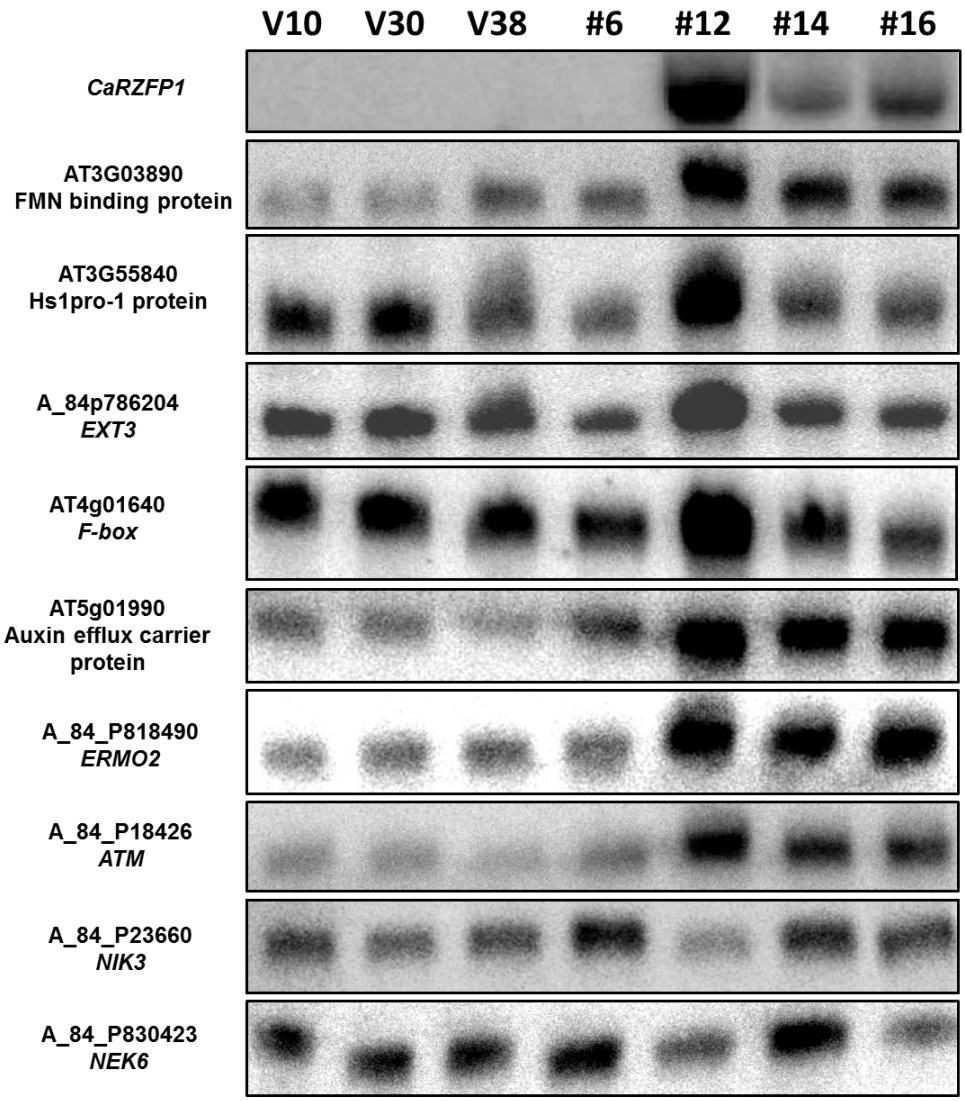
V10
V30
V38
#6
#12
#14
#16
CaRZFP1
AT3G03890
FMN binding protein
AT3G55840
Hs1pro-1 protein
A_84p786204
EXT3
AT4g01640
F-box
AT5g01990
Auxin efflux carrier
protein
A_84_P818490
ERMO2
A_84_P18426
ATM
A_84_P23660
NIK3
A_84_P830423
NEK6

Figure 21. RNA blot hybridization results using oligonucleotides for the differentially expressed transcripts in the *CaRZFP1*-transgenic and vector-only lettuce plants to confirm transcriptome profile data produced by microarray analysis. Nine up- and down-regulated genes from the microarray results were randomly chosen, the genes encoded an FMN-binding protein, Hs1pro-1 protein, *EXT3*, *F-box*, auxin efflux carrier protein, *ERMO2*, *ATM*, *NIK3*, and *NEK6*. Oligonucleotide sequences corresponding to the genes on the microarray array chips were labeled with ^{32}P, and used for RNA blot analysis. Total RNAs from three vector-only control lines and four *CaRZFP1*-transgenic lines, #6, #12, #14, and #16, were separated by electrophoresis on an agarose gel, blotted to a membrane, and hybridized with^{32}P -labeled oligonucleotides.

CHAPTER IV
DISCUSSION

I characterized abiotic stress inducible *Capsicum annuum RING Zinc Finger Protein 1*, named *CaRZFP1*, encoding a C3HC4-type RING zinc finger protein gene from hot pepper. C3HC4-type RING motif has consensus sequence Cys-X2-Cys-X9-39-Cys-X1-3-His-X2-3-Cys/His-X2-Cys-X4-48-Cys-X2-Cys where Cys, represent cysteine; His, histidine; X can be any amino acid. Amino sequence alignments of *CaRZFP1* revealed that *CaRZFP1* shares a highly conserved C3HC4-type RING zinc finger domains (Figure 6) in plants, insects and animals. It has been reported that Arabidopsis and Rice genome contain a large number of genes encoding RING finger proteins that are highly conserved across the eukaryotes (Vierstra, 2009), which suggests that evolutionarily important function of *CaRZFP1* in plant developmental processes (Figure 7). The development of multicellular organisms depends on cellular growth and morphogenesis, involving the expression of numerous genes and intricate gene regulatory networks. RING zinc-finger proteins have been closely and repeatedly implicated in the development of multiple organisms (Laity *et al.,* 2001; Krishna *et al.,* 2003; Gamsjaeger *et al.,* 2007; Matthews *et al.,* 2009; Font & Mackay, 2010), but cases reported in plants are comparatively few (Zhang *et al.,* 2005; Joseph *et al.,* 2014; Shi *et al.,* 2014; Yang *et al.,* 2014; Liu *et al.,* 2016). To investigate the *in vivo* function of *CaRZFP1*, we mobilized and ectopically expressed *CaRZFP1* into tobacco (*Nicotiana tabacum*). The *CaRZFP1*-transgenic tobacco plants showed enhanced growth and tolerance to abiotic stresses (Zeba *et al.,* 2009). In this study, I mobilized and over-expressed *CaRZFP1* in lettuce (*Lactuca sativa*) to further analyze the effect of *CaRZFP1* ectopic expression in a heterologous host plant (Figure 11). To the opposite of tobacco, *CaRZFP1*-transgenic lettuce displayed impaired growth (weakened leaf growth, stunted root growth, shorter plant height, and delayed flowering) compared with vector-only plants. The ectopic expression of *CaRZFP1* dramatically impeded the growth and development

of *CaRZFP1*-transgenic lettuce plants. *CaRZFP1*-transgenic lettuce plants displayed significant differences in their developmental progression. I noticed that *CaRZFP1*-transgenic lettuce plants exhibited pleiotropic developmental changes during all phases of *CaRZFP1*-transgenic lettuce plant development. The ectopic expression of *CaRZFP1* hampered the growth and development of *CaRZFP1*-transgenic lettuce plants with a different degree of severity, even though, *CaRZFP1* expression was driven under the control of CaMV 35S promoter (Figure 11). I observed a strong negative-correlation between the growth impairment and the transcript level of *CaRZFP1*, i.e. stronger expression of *CaRZFP1* tightly associated with the severe retarded in growth, suggesting that *CaRZFP1* plays a negative regulatory role during growth and development of *CaRZFP1*-transgenic lettuce plants. It seems that variable levels of *CaRZFP1* transcript clearly diminishing the growth of *CaRZFP1*-transgenic lettuce plants in a dose-dependent manner (Figure 12). These results suggest that CaRZFP1 may possess an important biological function. CaRZFP1 might be actively participating in the cellular and metabolic processes by effectively altering a subset gene which plays critical role in plant growth and development. The heterologous expression of *CaRZFP1* impeded the primary root growth and lateral root formation in *CaRZFP1*-transgenic lettuce plants. Transgenic root length was drastically shortened, but root diameter was not significantly changed. This negative-correlation was also extended to the root growth. *CaRZFP1* transcript level hampered the root growth and development in a concentration-dependent manner (Figure 13). Overall root size, mass, and branching in transgenic lettuce were reduced considerably with rising *CaRZFP1* expression levels. In addition, the weaken growth of *CaRZFP1*-transgenic lettuce plants were continued to the late stage of development and the transcript level of *CaRZFP1* was always correlated with the negative phenotypic effect on the

CaRZFP1-transgenic lettuce plants. *CaRZFP1*-transgenic lettuce plants were shorter in height, delayed flower and size of flowers were smaller (Figure 14a, b and c), while seed size and morphology was similar to those of vector-only plants. However, inflorescence development was dramatically affected by the *CaRZFP1* expression, with overall size decreasing with increasing *CaRZFP1* expression. Yet transgenic flowers did not differ from control plants, although flower number per inflorescence was drastically reduced. Likewise, while transgenic seeds exhibited normal morphology, their total number per inflorescence decreased drastically with increasing *CaRZFP1* expression (Figure 14g, h i and j). Therefore, collectively these results demonstrated that *CaRZFP1* might have pleiotropic functions in various developmental processes of *CaRZFP1*-transgenic lettuce plants in a dose-dependent manner by negatively regulating the expression of several key genes involved in growth and development. The ectopic expression of rice CCCH zinc finger gene, *OsDOS*, exhibited several pleiotropic phenotypes such as delayed growth, shorter stature, abnormally developed panicles, deferred heading and severe sterility, as well as delayed leaf senescence (Kong *et al.,* 2006). In Arabidopsis plants over-expressing Q-type C2H2 genes such as *ZAT12* (Vogel *et al.,* 2005), *ZAT6* (Devaiah *et al.,* 2007), retarded the growth and development of transgenic plants. RNAi suppression of *ZAT6* was lethal, suggesting a key role of ZAT6 in regulating plant growth and development. Over-expression of *ZFP10* and *ZFP11* in Arabidopsis and tobacco (*Nicotiana tabacum*) resulted in dwarf plants with abnormal morphology and reduced fertility (Dinkins *et al.,* 2012). *PROG1* gene encodes a zinc-finger with transcriptional activity and mapped onto chromosome 7. *OsTZF1*, a CCCH-type transcription factor and belong to the zinc finger gene family in rice (*Oryza sativa*). Expression of *OsTZF1* was induced by drought, high-salt stress, hydrogen peroxide, abscisic acid, methyl jasmonate, and salicylic acid.

Constitutive expression of *OsTZF1* also showed pleiotropic phenotypes in rice development such as delayed seed germination, growth retardation at the seedling stage, and delayed leaf senescence (Jan *et al.*, 2013). The ectopic expression of *PtaZFP2* negatively regulate the stem growth and gene expression responsiveness to external mechanical loads in poplar (Martin *et al.*, 2014). AtC3H17, a non-tandem CCCH zinc finger protein, over-expression of *AtC3H17* caused pleiotropic effects on vegetative development, flowering and seed development in Arabidopsis (Seok *et al.*, 2016).

When the poor growth phenotype was investigated at the tissue and cellular level, *CaRZFP1* expression led to specific effects in lettuce. Although overall height of transgenic lettuce decreased parallel to *CaRZFP1* expression, the development of shoot internal structure was not significantly hampered. Shoot and leaf cross sections also exhibited normal development overall, as did vascular bundles, mesophyll cells, and epidermal cells (Figure 15a, b, c and d). Transgenic lettuce roots were strongly affected by the *CaRZFP1* expression, increasing in disorganization of vascular bundles as *CaRZFP1* expression levels rose. Remarkably, we observed a strong correlation, albeit negative, between the expression level of *CaRZFP1* and the degree of disruption in root internal morphology. *CaRZFP1*-transgenic lettuce plant roots showed the significant deterioration of these structures as well as the formation of endodermis layer as the expression level of *CaRZFP1* increased. Moreover, the xylem ray became irregular and disconnected, while the endodermis and pericycle were ill-defined and eventually unidentifiable. However, cells in root ground tissue were unaffected (Figure 15f and g). In contrast, *CaRZFP1*-transgenic tobacco plant exhibited enhanced growth including larger primary root, more lateral root, larger hypocotyls and bigger leaf size, resulting in heavier fresh weight. *CaRZFP1*-transgenic tobacco plant roots showed normal development of endodermis and vascular bundle

(Figure 15i, j and k). These results demonstrated that the over-expression of *CaRZFP1* may negatively regulate genes have been implicated in endodermis and vascular development in *CaRZFP1*-transgenic lettuce plant.

What could be the molecular link between *CaRZFP1* and endodermis, vascular bundle and root development? The cell specification of initials leading to endodermal cells is regulated by the interaction between GRAS-type transcription factors, SHORTROOT (SHR) and SCARECROW (SCR), play key roles in the formation and maintenance of the root endodermis. SHR proteins are expressed in the stele and move into the cortex/endodermal initial cell. In this layer, SHR interacts with SCR forming a transcription activation complex, which activates the transcription of several target genes that together trigger the periclinal division of cortex–endodermal initials leading to the formation of the endodermis and the cortex (Miyashima *et al.*, 2013). AtMYB93 transcription factor negatively regulates the lateral root development in Arabidopsis. Interestingly, AtMYB93 expression is highly restricted to the few endodermal cells overlying developing lateral root primordia, suggesting that this transcriptional regulator might play a key role in mediating the effect of the endodermis on lateral root development (Rybel *et al.*, 2016). The *Arabidopsis* ERECTA (ER) receptor kinase is known to regulate the architecture of inflorescence stems. *ER* and its paralogue, *ER-LIKE1*, were redundantly involved in the procambial development of inflorescence stems. Interestingly, their activity in the phloem was sufficient for vascular regulation. Two endodermis-derived peptide hormones, EPFL4 and EPFL6, were redundantly involved in such regulation. It has been previously reported that EPFL4 and EPFL6 act as ligands of phloem-expressed ER for stem elongation. Therefore, these findings indicate that cell–cell communication between the endodermis and the phloem plays an important role in procambial development as well as stem elongation (Uchida

and Tasaka, 2013). These facts suggest that crosstalk between a subset of genes regulate the plant root development might have been altered by ectopic expression of *CaRZFP1* in transgenic lettuce plants, resulting in the phenotypic alterations that I observed in these transgenic lettuce plants. CaRZFP1 may critical for the establishment and maintenance of endodermis and vascular bundle (Figure 15). At this point, it is not clear, how CaRZFP1 does regulate the genes involved in endodermis cell fate determination, vascular bundle and root development.

Hot pepper (*Capsicum annuum*) economically important crop that is intensively cultivated throughout the world. The Asian people use hot pepper extensively in their foods, dishes and well known for hot spicy flavors. Hot pepper can acclimate in diverse abiotic stresses owing to its numerous genes, which play a crucial role in tolerance mechanism. Although, many genes are reported that have been involved to abiotic stresses response in hot pepper (Cho *et al.,* 2006; Seong and Wang 2008; Choi *et al.,* 2011; Chen *et al.,* 2014; Park *et al.,* 2017), however, only handful of RING zinc finger documented so far (Seoung *et al.,* 2007; Seong and Wang 2008; Zeba *et al.,* 2009). Here also I demonstrated that several abiotic stress treatments induced the early expression of the *CaRZFP1* transcript in different tissues of hot pepper. Furthermore, the expression profile of *CaRZFP1* showed that *CaRZFP1* induced under most of the abiotic stresses (high-temperature, dehydration, high salinity and cold) exposed here. The transcript of *CaRZFP1* was typically not detected under normal physiological conditions, however, *CaRZFP1* expression was quickly and strongly induced in response to diverse abiotic stresses (Figure 9). Thus, it would be reasonable to speculate that *CaRZFP1* may be functional in different tissues simultaneously in response to multiple abiotic stresses during early stages of the tolerance event to deal with effective plant adaption process in hot pepper.

Recent studies also revealed that some members of ZFPs in plants, such as *CaRma1H1*, *Atrzf1*, *AtAIRP3/LOG2*, *OsZFP36*, *GmZF1*, *AtZAP6*, *AtZat10*, *AtZat12*, *AtZat7*, *AtZat6*, *OsZFP6*, and *VuSTOP1*, have been implicated in the responses of plants to diverse abiotic stresses (Lee *et al.*,2009; Guan *et al.,* 2014; Kim and Kim, 2013; Kielbowicz-Matuk, 2012; Shi and Chan, 2014; Yu *et al.,* 2014; Zhang *et al.,* 2014; Fan *et al.,* 2015). Here, I have shown that the expression of *CaRZFP1* transcript was also induced by various abiotic stresses in different tissues of hot pepper (Figure 9). Thus, CaRZFP1 may have a crucial function in hot pepper in response to multiple abiotic stresses. *CaRZFP1*-transgenic tobacco showed enhanced abiotic stress tolerance by *CaRZFP1*-overexpresssion (Zeba *et al.,* 2009). I tempted to bring the similar effect of *CaRZFP1*-ectopic expression in lettuce. However, no meaningful differences were observed between the *CaRZFP1*-transgenic lettuce plants and vector control under diverse abiotic stress conditions (Figure 16). CaRZFP1 may produce a very low concentration of signaling proteins in *CaRZFP1*-transgenic lettuce plants, which might be insufficient to activate the key downstream signaling pathways related to the abiotic stress response functional networks. CIPK (CBL-interacting protein kinases) genes (*OsCIPK01*–*OsCIPK30*) were surveyed for their transcriptional responses to various abiotic stresses in rice. The results showed that 20 *OsCIPK* genes were differentially induced by at least one of the stresses, including drought, salinity, cold, polyethylene glycol, and abscisic acid treatment. The ectopic expression of *OsCIPK03*, *OsCIPK12*, and *OsCIPK15* showed significantly improved tolerance to cold, drought, and salt stress in transgenic rice plants, however, no significant effect on improving tolerance to other abiotic stresses (Xiang *et al.,* 2007). Therefore, these results suggest that the response of a gene to biotic and abiotic stresses at the transcriptional or translational level does not mean that these genes must have the significant effect in conferring

tolerance to these stresses.

Transcriptome profiling of transgenic lettuce revealed many differentially expressed genes that could be separated into two groups: Group 1 with correlative changes among the four selected transgenic lines (#6, #12, #14, #16), and Group 2 with significant changes mainly in line #12, which showed the highest *CaRZFP1* expression (Figure 18a and b). I concentrated on Group 1 genes because the correlative change in expression among the four transgenic lines was considered most likely to be linked with *CaRZFP1* expression in transgenic lettuce. Among Group 1 genes, cell division protease ftsH-11 (FTSH11) has been implicated in housekeeping proteolysis of membrane proteins (Wagner *et al.,* 2005). Timeless family protein (ATIM) regulates circadian rhythm mechanism in the files (Rosato *et al.,* 2006). Indeterminate-domain (IDD) protein family members have been implicated in auxin production, gravitropism and lateral organ differentiation, heat stress responses, regulation of sugar transporter regulation, as well as the promotion of seed germination (Cui *et al.,* 2013). In maize and rice, the *ID1* gene, a member of IDD family, acts as a master switch for transitioning from the vegetative to the reproductive phase. Plants with loss-of-function *id1* remain in a prolonged state of vegetative growth and form aberrant flowers (Park *et al.,* 2008). Flowering time and inflorescence development were significantly altered in *CaRZFP1*-transgenic lettuce. Therefore, these results imply that the CaRZFP1 may play an essential role in regulating signaling pathways that modulate the timing of the floral transition and flowering time in *CaRZFP1*-transgenic lettuce plants (Figure 14b and c). Arabidopsis response regulator 10 (ARR10) has been implicated in the cytokinin signaling (To *et al.,* 2007). BES1-interacting MYC-like 1 (BIM1) played an essential role in brassinosteroid signaling (Xing *et al.,* 2013). The ectopic expression of *CaRZFP1* may regulate phytohormone signaling and

subsequently affect the growth and development of *CaRZFP1*-transgenic lettuce plants (Figure 12, 13 and 14). OxaA/YidC is essential for protein insertion into bacterial and mitochondrial inner membranes, as well as thylakoid membranes of chloroplasts (Hennon *et al.,* 2015). Extensin 3 (EXT3) expression was also up-regulated over 3-fold in *CaRZFP1*-transgenic lettuce; these proteins are critical structural components of the cell wall during plant growth and development (Lamport *et al.,* 2011). Peroxidases are among the largest protein families; they function in the cross-linking of cell wall proteins, lignin biosynthesis, suberization, auxin catabolism, oxidative stress, and defense responses (Hiraga *et al.,* 2001; Tognolli *et al.,* 2002; Cosio *et al.,* 2009; Marjamaa *et al.,* 2009). Glucose-1-phosphate adenylyltransferase small subunit (ADG1) is a key regulatory enzyme in the plant starch and bacterial glycogen biosynthesis pathway (Bahaji *et al.,* 2011). NADH:ubiquinone oxidoreductase in the Complex I of the electron transport chain is a central component in cellular respiration, the main process providing energy in most heterotrophic eukaryotes and in autotrophic organisms during their heterotrophic phase (Kuhn *et al.,* 2015). Complex I deficiencies have dramatic effects on cellular physiology, numerous plant growth defects and human diseases have been associated with the defect in complex I, especially, the catalytic core subunit NADH dehydrogenase (ubiquinone) flavoprotein 1 (NDUFV1) (Lazarou *et al.,* 2009). FMN binding proteins are critical in the electron transport process. Over-expression of FMN-binding protein (AtHal3) altered growth rates while improving salt and drought tolerance in Arabidopsis (Espinosa-Ruiz *et al.,* 1999). The ectopic expression of *CaRZFP1* may deregulate genes involved in vital metabolic processes and affects the *CaRZFP1*-transgenic lettuce plant growth and development (Figure 12, 13 and 14).

Transcriptome analysis also showed that many genes with known

function in plant development were altered in the *CaRZFP1*-transgenic lettuce. A serine/threonine-protein kinase (ATAXIA-TELANGIECTASIA MUTATED, ATM) that is important in DNA damage response (Liu *et al.,* 2015; Wang *et al.,* 2016) was also elevated in *CaRZFP1*-transgenic lettuce plants. The up-regulated Hs1pro-1 gene has been implicated in defense response in plants (Yuan *et al.,* 2008). Nodulin MtN3-like protein is the member of SWEETs (Sugars Will Eventually be Exported Transporters) family, that are essential for the maintenance of animal blood glucose levels, plant nectar production, plant seed and pollen development (Chandran, 2015). Another significantly up-regulated gene in transgenic lettuce encoded sec24-like transport protein (ERMO2); *SEC24A* encodes a coat protein complex II vesicle coat subunit involved in endoplasmic reticulum-to-Golgi trafficking during the early secretory pathway (Qu *et al.,* 2014). The secretory pathway is critical for cells to maintain membrane homeostasis, protein localization and production of vital cellular constituents such as lipids, sugars and proteins that enable cells to communicate with the external environment. In plants, secretory pathway defects often lead to cell division defects (Sylvester, 2000; Faso *et al.,* 2009). Therefore, it is possible that the ectopic expression of *CaRZFP1* perturbed the novel mechanism underlying membrane trafficking pathway which subsequently affects the growth and development of *CaRZFP1*-transgenic lettuce plants (Figure 12, 13 and 14). Glutamate receptor 2.1 (GLR2.1) is a member of ligand-gated ion channel family, and it functions in coordination of mitotic activity during root development, sensing carbon-to-nitrogen status, cellular calcium ion homeostasis, response to light, regulation of plant hormone biosynthesis, and signaling pathways (Tapken *et al.,* 2013; Weiland *et al.,* 2016). A knockout of *OsGLR3.1* affects the whole root system including primary, lateral and adventitious roots and causes a shortening of the primary roots (Li *et al.,* 2006). Moreover, because an optimum auxin

concentration is required for shoot and root growth, lateral root development, and differentiation of vascular strands (Spiegelman *et al.,* 2015; Aremu *et al.,* 2016), excessive expression of auxin efflux carrier family genes could harm for plant growth and development. Pentatricopeptide repeat proteins function in multiple processes as modular RNA-binding proteins that mediate gene expression through altering RNA sequence, turnover, and processing (Schmitz-Linneweber and Small, 2008). They exhibit profound effects on organelle biogenesis and function; consequently, they are influential in major plant processes, including photosynthesis, respiration, development, and environmental responses (Small and Peeters, 2000; Manna, 2015). The ectopic expression of *CaRZFP1* may misregulate the genes involved in vital metabolic processes. In turn, secondary effects may be triggered in other metabolic pathways that are critical to plant growth and development (e.g., photosynthesis, electron transport, cellular respiration) (Figure 12, 13 and 14). Cysteine/histidine-rich C1 domain-containing protein also has been implicated for its important role in regulating plant growth and development (Hwang *et al.,* 2014). Conserved peptide upstream open reading frame 24 (CPuORF24) regulates polyamine and sucrose concentrations in response to starvation (Hayden & Jorgensen, 2007). Ubiquitin-conjugating enzyme E2 18 (UBC18), armadillo/beta-catenin-like repeats-containing protein (ARM), F-box associated ubiquitination effector family protein, and development and cell death domain protein (DCD), all have been implicated in ubiquitin-mediated protein degradation. ARM repeat proteins may serve as adaptors in signaling networks; numerous Arabidopsis ARM repeat proteins are implicated in protein degradation pathways as E3 ubiquitin ligases (Mudgil *et al.,* 2004). Notably, plant genome contains a large number of genes encoding ZFPs (Ciftci-Yilmaz and Mittler, 2008; Yuan *et al.,* 2013; Li *et al.,* 2014) and the RING-zinc finger proteins tend to possess E3 ubiquitin

ligase activity (Stone *et al.,* 2005; Vierstra, 2009; Jang *et al.,* 2015). Ubiquitin-mediated protein degradation plays a key regulatory role in plant growth and development, as well as being implicated in plant hormone signaling (Dharmasiri *et al.,* 2013; Furniss and Spoel, 2014; Sharma *et al.,* 2016). Thus, these facts suggest that CaRZFP1 might also function at the post-translational level in various developmental processes through ubiquitin-dependent protein degradation. It is reasonable to speculate that the CaRZFP1 may repress gene expression by ubiquitylating other regulators of the transcriptional machinery through proteasome-mediated protein degradation processes (Figure 12, 13 and 14).

Some genes were significantly down-regulated (<2-fold) in *CaRZFP1*-transgenic lettuce compared with vector-only plants. RmlC-like cupin super family proteins have both enzymatic and non-enzymatic functions, the former including decarboxylases, isomerases, epimerases, oxidoreductases, disomerases, dioxygenases, and hydrolases, the latter including auxin binding, seed storage, and nuclear transcription factors (Agarwal *et al.,* 2009; Iyer *et al.,* 2010; Uberto & Moomaw, 2013). Amidohydrolase family protein (LAF3) is involved in phytochrome A signal transduction (Hare *et al.,* 2003). Indole-3-acetate beta-D-glucosyltransferase (IAGLU) plays a crucial role in auxin conjugation pathway and auxin metabolism (Jackson *et al.,* 2002). The NIMA-related Kinase 6 (NEK6) in Arabidopsis organizes microtubules, thus regulating cellular expansion, directional growth of roots and hypocotyls, petiole elongation, cell file formation, and morphogenesis (Motose *et al.,* 2011; Takatani *et al.,* 2015). NSP-interacting kinase 3 (NIK3) is involved in plant defense response and developmental processes (Zorzatto *et al.,* 2015). WD40 domains are present in eukaryotic proteins linked to scaffolding, cooperative assembly, chaperoning other proteins, and regulation of multi-cellular processes (Gibson, 2009; Stirnimann *et al.,* 2010; Gachomo *et al.,* 2014). WD40

repeat protein NEDD1 regulates microtubule development during mitotic cell division in Arabidopsis (Zeng *et al.,* 2009). Several WD40 proteins such as LRWD1, WDR5, RbBP4/7, NURF55, and WDR77 are classified as chromatin readers because they can recruit chromatin modifiers to specific sites on the chromosome by direct interaction with histone (Migliori *et al.,* 2012; Kumar *et al.,* 2013). The flax lines overexpressing LuWD40-1 had delayed flowering, severely reduced pollen viability, branching and growth (Kumar *et al.,* 2013). The transcript level of tRNA-Ser was also significantly repressed in *CaRZFP1*-transgenic lettuce plants.

These 24 up-regulated genes and seven down-regulated Group 1 genes are all necessary for plant growth and development. Thus, the negative phenotypic results related to *CaRZFP1* expression in lettuce are probably caused by the imbalance among growth and development regulators. Ectopically expressed CaRZFP1 induced and suppressed various genes in lettuce, leading to composite negative effects on growth and development, especially in the root and floral meristem division in the inflorescence. Although root endodermal development was significantly hampered in the CaRZFP1-transgenic lettuce plants, none of the annotated genes exhibited a direct relationship in their regulation with suberin biosynthetic processes, except one peroxidase that was expressed, albeit not significantly. We note that among Group 1, seven uncharacterized genes were correlatively up-regulated and one, correlatively down-regulated; it is impossible to speculate on their functions at present (Table 2 and 3). In Group 2, 43 genes were strongly overexpressed and six genes strongly down-regulated in the line #12 (Table 2 and 3). Because the regulation of these genes was not correlated with *CaRZFP1* expression in the lines #14, #16, and #6, their overexpression and suppression in the line #12 were likely the result of composite effects from the biased expression of Group 1 genes, rather than due directly to *CaRZFP1*

expression.

Ectopic expression of *CaRZFP1* in tobacco enhanced plant growth (larger leaves, longer hypocotyls, longer primary roots, and increased lateral roots), leading to heavier fresh weight (Zeba *et al.,* 2009). Transcriptome analysis revealed that growth-related genes were widely altered, i.e., 37 up-regulated and 22 down-regulated annotated genes, in *CaRZFP1*-overexpressing transgenic tobacco (Table 5 and 6). Up-regulated ADP-ribosylation factors are important in regulating intracellular membrane trafficking, a process linked to root development and the polar localization of PIN-FORMED (PIN) family auxin efflux facilitators (Yoo *et al.,* 2008; Yuan *et al.,* 2015). Dramatic elevation (up to 6-fold) was observed in the expression of growth-related cell wall proteins, four of which were arabinogalactan proteins (AGPs) (Schultz *et al.,* 2000; Knoch *et al.,* 2014; Showalter & Basu, 2016). These results suggest that CaRZFP1 activates and positively regulates cell-wall protein expression to modify cell wall plasticity, effectively promoting the growth of transgenic tobacco plants. Proline-rich proteins are important in Arabidopsis root-hair formation (Bernhardt and Tierney, 2000; Boron *et al.,* 2014), and transcriptome analysis revealed that four proline-rich protein genes were up-regulated in *CaRZFP1*-transgenic tobacco, and *CaRZFP1*-transgenic tobacco plants exhibited more developed root hairs (Zeba *et al.,* 2009). Plant ABC transporter family proteins experienced an over 7-fold up-regulation; these proteins are implicated in chlorophyll biosynthesis, Fe-S cluster formation, stomatal movement, and ion fluxes (Schulz and Kolukisaoglu, 2006; Hwang *et al.,* 2016). Gibberellin-responsive proteins were also highly induced in transgenic tobacco; these proteins have been implicated in hypocotyl and stem elongation (Achard *et al.,* 2007). Ectopic expression of *CaRZFP1* in tobacco also down-regulated two dozens of genes, but to a lesser degree than the up-regulation experienced by the genes

described above (Table 6). Finally, eight up- and two down-regulated genes were unannotated in *CaRZFP1*-transgenic tobacco (Table 5 and 6), and their possible effects on tobacco growth and development are not feasible to be suggested.

Table 5. Up-regulated genes in *CaRZFP1*-overexpressing T_2 tobacco plants·.

Affymetrix probe set ID	Gene symbol	Gene description	*CaRZFP1*-transgenic tobacco lines / vector controls (log_2 fold change)	*p*-value
Cell cycle and DNA processing				
248105_at	At5g55280	Cell division protein ftsZ	2.21	2.78E-01
256238_at	At3g12400	Tumour susceptibility gene 101 (tsg101) family protein	3.21	8.79E-02
Transcriptional factor				
260305_at	At1g70490	ADP-ribosylation factor	6.88	1.63E-02
256069_at	At1g13740	ABI five binding protein 2	5.80	5.23E-02
249468_at	At5g39650	DUO1-activated unknown 2 (DUO2)	2.03	4.13E-01
Growth related cell wall protein genes				
250437_at	At5g10430	Arabinogalactan-protein (agp4)	4.42	1.17E-01
247279_at	At5g64310	Arabinogalactan-protein (agp1)	2.52	1.44E-01
253050_at	At4g37450	Arabinogalactan-protein (agp18)	3.50	1.89E-03
266552_at	At2g46330	Arabinogalactan-protein (agp16)	2.87	8.11E-02
	At5g49080	Proline-rich extensin-like family protein	2.18	4.35E-01
252253_at	At3g49300	Proline-rich family protein	1.78	4.66E-01
	At3g49305	Hypothetical protein contains proline-rich extensin domains	2.17	1.72E-01
252971_at	At4g38770	Proline-rich family protein (prp4)	6.05	1.88E-02
255138_at	At4g08380	Proline-rich extensin-like family protein	2.48	2.06E-01
245967_at	At5g19800	Hydroxyproline-rich glycoprotein family protein	2.72	1.56E-01
263046_at	At2g05380	Glycine-rich protein(grp3)	3.71	2.39E-02
261826_at	At1g11580	Pectin methylesterase	2.32	1.65E-01
Metabolism				
264474_at	At5g38410	Ribulose bisphosphate carboxylase small chain 3b	3.49	3.16E-01
256865_at	At3g23820	NAD-dependent epimerase	2.21	2.28E-01
257816_at	At3g25140	Glycosyl transferase family 8 protein	2.86	1.26E-01
	At4g15233	ABC transporter family protein	7.31	1.47E-01
264394_at	At1g11860	Aminomethyltransferase	2.72	7.98E-02
247843_at	At5g58050	Glycerophosphoryl diester phosphodiesterase family protein	2.43	1.95E-01
254802_at	At4g13090	Xyloglucan:xyloglucosyl transferase/xyloglucan Endotransglycosylase	2.27	1.33E-01
251174_at	At3g63200	Patatin-like protein 9	4.88	2.43E-02
260284_at	At1g80380	Phosphoribulokinase/uridine kinase-related	2.51	2.03E-01
253090_at	At4g36360	Beta-galactosidase	4.55	3.33E-02

266716_at	At2g46820	Curvature thylakoid 1B (CURT1B)	3.07	1.97E-01
Signal transduction				
260221_at	At1g74670	Gibberellin-responsive protein	4.46	4.71E-02
266867_at	At2g45770	Signal recognition particle receptor protein/ chloroplast (ftsY) similar to cell division protein	3.06	1.60E-01
265073_at	At1g55480	Plant protein family containing a PDZ, a K-box, and a TPR motif (ZKT)	2.61	1.48E-01
Protein synthesis				
248655_at	At5g48760	60s ribosomal protein L13A (RPL13aD)	1.89	5.01E-01
251487_at	At3g59760	Cysteine synthase c/O-acetylserine (thiol)-lyase isoform c	2.22	2.97E-01
264849_at	At2g17360	40s ribosomal protein s4 (rps4a)	2.32	3.01E-01
262117_at	At1g02780	60s ribosomal protein	3.31	2.86E-01
250256_at	At5g13650	Elongation factor family protein	2.38	1.36E-01
253333_at	At4g33510	3-deoxy-D-arabino-heptulosonate-7-phosphate 2 (dahp2)	2.58	1.11E-01
Unannotated genes				
247241_at	At5g64680	Uncharacterized gene	2.23	2.51E-01
249681_at	At5g36070	Uncharacterized gene	5.56	1.49E-02
	At3g43684	Uncharacterized gene	2.58	7.40E-02
263840_at	At2g36885	Uncharacterized gene	4.09	9.03E-02
	At2g05752	Uncharacterized gene	4.38	1.29E-01
251038_at	At5g02240	Uncharacterized gene	3.00	2.64E-01
245198_at	At1g67700	Uncharacterized gene	1.99	5.09E-01
254656_at	At4g18070	Uncharacterized gene	2.28	2.71E-01

Table 6. Down-regulated genes in *CaRZFP1*-overexpressing T_2 tobacco plants.

Affymetrix probe set ID	Gene symbol	Gene description	*CaRZFP1*-transgenic tobacco lines / vector controls (log_2 fold change)	*p*-value
Cell cycle and DNA processing				
264399_at	At1g61780	Postsynaptic protein-related	-1.94	2.41E-01
247598_at	At5g60870	Regulator of chromosome condensation (rcc1) family protein	-2.43	6.68E-02
256273_at	At3g12090	Tetraspanin gene family (TET6)	-2.43	6.02E-02
Transcription factor				
247125_at	At5g66070	Zinc finger (C3HC4-type ring finger) family protein	-2.03	2.39E-01
263152_at	At1g54060	Trihelix DNA binding protein family	-1.80	2.17E-01
255495_at	At4g02720	Ortholog of NKAP (NF-kB activating protein) proteins	-2.22	1.48E-01
250974_at	At5g02820	Brassinosteroid insensitive 5 (BIN5)	-2.55	2.03E-02
Growth related cell wall protein genes				
256964_at	At3g13520	Arabinogalactan-protein (agp12)	-2.36	1.52E-01
265511_at	At2g05540	Glycine-rich protein	-1.69	7.32E-02
260840_at	At1g29050	Trichome birefringence-like 38	-2.25	2.57E-01
Metabolism				
266072_at	At2g18700	Trehalose phosphatase/synthase 11 (TPS11)	-2.40	1.78E-01
265926_at	At2g18600	Rub1-conjugating enzyme	-2.23	1.32E-01
252395_at	At3g47950	ATPase	-2.03	2.57E-01
Signal transduction				
257043_at	At3g19700	Leucine-rich repeat transmembrane protein kinase	-2.17	1.10E-01
247306_at	At5g63870	Serine/threonine protein phosphatase (pp7)	-2.16	8.73E-02
248017_at	At5g56460	Protein kinase	-2.86	2.62E-02
Transport facilitation				
247632_at	At5g60460	Sec61-beta subunit family protein	-2.78	2.12E-02
Protein fate (folding, modification, destination)				
265960_at	At2g37470	Histone h2b	-3.19	9.00E-02
253826_at	At4g27960	Ubiquitin-conjugating enzyme 9 (ubc9)	-2.35	2.24E-01
258954_at	At3g01400	Armadillo/beta-catenin repeat family protein	-2.89	3.11E-03
247107_at	At5g66040	Protein with thiosulfate sulfurtransferase/rhodanese activity (STR16)	-1.91	1.79E-01
258979_at	At3g09440	Heat shock protein 70 (hsp70)	-1.83	2.08E-01
Unannotated genes				
265457_at	At2g46550	Uncharacterized gene	-2.66	2.06E-01
260320_at	At1g63930	Uncharacterized gene	-2.72	2.79E-01

The expression profiles, either significantly up-regulated or significantly down-regulated, of lettuce and tobacco plants overexpressing *CaRZFP1* were dissimilar. Transgenic lettuce and tobacco did not share any genes with significantly altered expression (Table 2 and 3; Table 5 and 6). And, overall expression profiles, either significantly up-regulated or significantly down-regulated, were largely different between transgenic lettuce and tobacco. In transgenic tobacco, more genes involved in protein synthesis and growth-related cell wall proteins experienced altered expression than in lettuce. However, transgenic lettuce contained more highly altered genes that were involved in transcription factors, transport facilitation, as well as protein folding, modification, and destination (Figure 18; Table 2 and 3; Table 5 and 6).

The commercial microarrays are only available for model crop plants; however, transcriptome profiling in non-model crop plants remains a challenge because of the development costs is prohibitive for the most of the research groups. Several researchers have been demonstrated the use of the heterologous microarray to compare the gene expression between distantly related species and establish this technique as a tool for comparative functional genomics in multiple species (Renn *et al.,* 2004; Davey *et al.,* 2009; Degletagne *et al.,* 2010; Ruiz-Laguna *et al.,* 2016). To identify differentially expressed transcripts via heterologous microarray depends on the degree of similarity between the target and probe sequences. The adequate sequence identity exists in numerous genes within related phylogenetic groups. The number of spots detected by heterologous microarray decline with increasing phylogenetic distance as sequence mismatches and affect the outcome of the experiments. Heterologous microarray efficiency also depends upon the nature and length of the probes employed, for instance, short oligonucleotide

probes (Affymetrix) is more sensitive to sequence mismatches than the longer probes (Agilent). It cannot be ruled out that many genes failed to hybridize due to sequence variation across species but maintaining low stringency in hybridization conditions can detect a maximum number of spots. Moreover, number of detected spots does not translate into information of fold changes in expression level. The quantitative real-time PCR and oligo-RNA blotting can also provide another layer of quality control and help strengthen the results obtained by heterologous microarrays. cDNA microarray constructed targeting to ~4500 genes from a brain-specific cDNA library for the African cichlid fish. Heterologous hybridization was performed with eight different fish species. The expression profiling demonstrated the consistent hybridization for closely related taxa (65 million years divergence time) while the lesser extent with very distantly related species (200 million years divergence time) (Renn *et al.,* 2004). RNA of control and drought stressed leaves of the *Musa* cultivar 'Cachaco' were hybridized to the Affymetrix Rice Genome Array, total 2,810 differentially expressed transcript with a >2-fold change in expression levels were identified. These drought-responsive transcripts included many functional classes associated with plant biotic and abiotic stress responses, as well as a range of regulatory genes known to be involved in coordinating abiotic stress responses. Fifty-two *Musa* transcripts were homologous to genes underlying QTLs for drought and cold tolerance in rice (Davey *et al.,* 2009).

In-depth studies are necessary to clearly understand the basis of the described differences in *CaRZFP1*-transgenic lettuce and tobacco. However, several possible explanations can be proposed. Because tobacco is closely related to hot pepper (both Solanaceae), hot-pepper-derived CaRZFP1 was likely expressed in a similar genetic environment when mobilized to tobacco. In contrast, CaRZFP1 in lettuce was probably expressed in a very different

genetic environment, likely even interacting with proteins that are not normal counterparts or binding at a DNA domain that is extremely dissimilar from any in hot pepper or tobacco. These new interactions probably caused the expression of unexpected downstream genes. Because signal transduction pathways are complex and extensively interconnected (Larrieu & Vernoux, 2015), unpredictable outcomes may result once novel interactions trigger a different network of signal transductions or gene sets.

CONCLUSION

This study provides important insight into the function of C3HC4-type RING finger proteins in lettuce. I provided candidate genes downstream of the ectopically expressed *CaRZFP1* in lettuce that specifically affected root development, especially of the endodermis, pericycle, and vascular structures. I also provided strong evidence that the same gene can yield completely different outcomes depending on its host species. Advances in molecular biology have improved crops through transferring genes from one organism to new hosts. These results are significant because unexpected outcomes of gene mobilization to improve crops are a major safety concern. In addition to the extreme cares to control the unwanted and uncontrolled spread of transgenes between closely related wild species and the newly introduced transgenic crops through pollen diffusion, the results in this report asks for another level of concerns due to the chance of occurring unexpected phenotype appearance from the gene transfer or there could be consequences no one thought or scientists cannot test yet. Likewise, the concern can be extended to the general molecular approach to decipher the function of a genetic component. Scientific researches heavily rely on a model system, for an example Arabidopsis, to decipher the function of a gene/protein, pathways and networks in plants. If different plant species carry quite different scaffolding network for a protein or gene, the outcome can be quite different. Since plasticity of development is one important nature in plants, we tempt to see the much heavier emphasis on each plant species as a host for the common and for the specificity. Therefore, collectively these results demonstrated that developmental plasticity is an important trait in plants that probably reflects flexibility in new gene accommodation, and thus analysis for the unexpected outcome seemed to be important in plant gene manipulation that can be done by closely following tracks of gene introduced.

REFERENCES

Achard, P., Liao, L., Jiang, C., Desnos, T., Bartlett, J., Fu, X., and Harberd, N. P. 2007. DELLAs contribute to plant photomorphogenesis. Plant Physi ol. 143: 1163-1172.

Agarwal, G., Rajavel, M., Gopal, B., and Srinivasan, N. 2009. Structure-base d phylogeny as a diagnostic for functional characterization of proteins with a cupin fold. PLoS One 4: e5736.

Alam, I., Yang, Y.Q., Wang, Y., Zhu, M.L., Wang, H.B., Chalhoub, B., and Lu, Y.H. 2017. Genome-wide identification, evolution and expression anal ysis of RING finger protein genes in *Brassica rapa*. Sci Rep. 7: 40690.

Anderson, W.F., Ohlendorf, D.H., Takeda, Y., and Matthews, B.W. 1981. Str ucture of the cro repressor from bacteriophage lambda and its interact ion with DNA. Nature 290: 754–758.

Andreini, C., Banci, L., Bertini, I., and Rosato, A. 2006. Counting the zinc-pr oteins encoded in the human genome. J Proteome Res. 5: 196–201.

Ansieau, S., and Leutz, A. 2002. The conserved Mynd domain of BS69 binds c ellular and oncoviral proteins through a common PXLXP motif. J Biol Chem. 277 : 4906–10.

Bahaji, A., Li, J., Ovecka, M., Ezquer, I., Muñoz, F.J., Baroja-Fernández, E., R omero, J.M., Almagro, G., Montero, M., Hidalgo, M., Sesma, M.T., a nd Pozueta-Romero, J. 2011. *Arabidopsis thaliana* mutants lacking ADP -glucose pyrophosphorylase accumulate starch and ADP-glucose: furt her evidences for the occurrence of important sources, other than ADP -glucose pyrophosphorylase, of ADP-glucose linked to leaf starch bios ynthesis. Plant Cell Physiol. 52: 1162–1176.

Baou, M., Jewell, A., and Murphy, J.J. 2009. TIS11 family proteins and their r oles in posttranscriptional gene regulation. J Biomed Biotechnol. 63452

0 .

Basu, M., Sengupta, I., Khan, W., Srivastava, D.K., Chakrabarti, P., Roy, S., and Das, C. 2017. Dual histone reader ZMYND8 inhibits cancer cell in vasion by positively regulating epithelial genes. Biochem J. 9: 23-29.

Berg, J.M., and Shi, Y. 1996. The galvanization of biology: a growing apprecia tion for the roles of zinc. Science 271: 1081-1085.

Bernhardt, C., and Tierney, M.L. 2000. Expression of AtPRP3, a proline-rich s tructural cell wall protein from Arabidopsis, is regulated by cell-type-specific developmental pathways involved in root hair formation. Pla nt Physiol. 122: 705-714.

Blackshear, P. J. 2002. Tristetraprolin and other CCCH tandem zinc-finger pr oteins in the regulation of mRNA turnover. Biochem Soc Trans. 30: 94 5-52.

Blobel, G. A. 2000. CREB-binding protein and p300: molecular integrators of hematopoietic transcription. Blood 95**:** 745-755.

Boron, A. K., Van Orden, J., Nektarios Markakis, M., Mouille, G., Adriaens en, D., Verbelen, J.P., Hofte, H., and Vissenberg, K. 2014. Proline-ric h protein-like PRPL1 controls elongation of root hairs in *Arabidopsis th aliana*. J. Exp. Bot. 65: 5485-5495.

Brewer, P. B., Heisler, M. G., Hejatko, J., Friml, J. and Benkova, E. 2006. *In si tu* hybridization for mRNA detection in Arabidopsis tissue sections. N at. Protoc. 1: 1462-1467.

Brown, J. 1994. Bootstrap hypothesis tests for evolutionary trees and other de ndrograms. Proc Natl Acad Sci USA. 91: 12293-12297.

Brown, R. S. 2005. Zinc finger proteins: getting a grip on RNA. Curr Opin Str uct Biol 15: 94-8.

Burglin, T.R., and Affolter, M. 2016. Homeodomain proteins: an update. Chr omosoma 125: 497–521.

Chandran, D. 2015. Co-option of developmentally regulated plant SWEET tra

nsporters for pathogen nutrition and abiotic stress tolerance. IUBMB L ife 67: 461–471.

Chen, R., Guo, W., Yin, Y., and Gong, Z.H. 2014. A novel F-box protein CaF-box is involved in responses to plant hormones and abiotic stress in pe pper (*Capsicum annuum* L.). Int J Mol Sci. 15: 2413-30.

Cho, S.K., Kim, J.E., Park, J.A., Eom, T.J., and Kim, W.T. 2006. Constitutive e xpression of abiotic stress-inducible hot pepper CaXTH3, which encod es a xyloglucan endotransglucosylase/ hydrolase homolog, improves drought and salt tolerance in transgenic Arabidopsis plants. FEBS Lett 580: 3136–3144.

Choi, J.Y., Seo, Y.S., Kim, S.J., Kim, W.T., and Shin, J.S. 2011. Constitutiv e expression of *CaXTH3*, a hot pepper xyloglucan endotransglucosyl ase/hydrolase, enhanced tolerance to salt and drought stresses with out phenotypic defects in tomato plants (*Solanum lycopersicum* cv. Do taerang). Plant Cell Rep 30: 867.

Choo, Y., and Klug, A. 1993. A role in DNA binding for the linker sequences of the first three zinc fingers of TFIIIA. Nucleic Acids Res 21: 3341-6.

Ciftci-Yilmaz, S., and Mittler, R. 2008. The zinc finger network of plants. Cell Mol Life Sci. 65: 1150-1160.

Cosio, C., Vuillemin, L., De Meyer, M., Kevers, C., Penel, C., and Dunand, C. 2009. An anionic class III peroxidase from zucchini may regulate hy pocotyl elongation through its auxin oxidase activity. Planta 229: 823-8 36.

Cui, P., Liu, H., Ruan, S., Ali, B., Gill, R.A., Ma, H., Zheng, Z., and Zhou, W. 2017. A zinc finger protein, interacted with cyclophilin, affects root de velopment via IAA pathway in rice. J Integr Plant Biol. 23: 1-7.

Cui, D., Zhao, J., Jing, Y., Fan, M., Liu, J., Wang, Z., Xin, W., and Hu, Y. 2013. The Arabidopsis IDD14, IDD15, and IDD16 cooperatively regulate lat eral organ morphogenesis and gravitropism by promoting auxin biosy

nthesis and transport. PLoS Genet. 9: e1003759.

De Rybel, B., Mahonen, A.P., Helariutta, Y., and Weijers, D. 2016. Plant vasc ular development: from early specification to differentiation. Nat Rev Mol Cell Biol 17, 30–40.

Devaiah, B.N., Karthikeyan, A.S., and Raghothama, K.G. 2007. WRKY75 tra nscription factor is a modulator of phosphate acquisition and root dev elopment in Arabidopsis. Plant Physiol 143 1789–1801 .

Dharmasiri, S., Jayaweera, T., and Dharmasiri, N. 2013. Plant hormone signa lling: current perspectives on perception and mechanisms of action. C eylon J Sci Biol Sci 42: 1–17.

Dinkins, R.D., Tavva, V.S., Palli, S.R., and Collins, G.B. 2012. Mutant and o verexpression analysis of a C2H2 single zinc finger gene of Arabidopsi s. Plant Mol Biol Rep 30: 99–110.

Doyle, J.M., Gao, J., Wang, J., Yang, M., and Potts, P.R. 2010. MAGE-RING p rotein complexes comprise a family of E3 ubiquitin ligases. Mol. Cell 3 9: 963–974.

Duggan, A., Madathany, T., De Castro, S.C., Gerrelli, D., Guddati, K., and Garcia-Anoveros, J. 2008. Transient expression of the conserved zinc f inger gene INSM1 in progenitors and nascent neurons throughout em bryonic and adult neurogenesis. J Comp Neurol. 507: 1497-1520.

Dul, B. E., and Walworth, N.C. 2007. The plant homeodomain fingers of fissi on yeast Msc1 exhibit E3 ubiquitin ligase activity. J. Biol. Chem. 282**:** 1 8397–18406.

Espinosa-Ruiz, A., Belles, J.M., Serrano, R., and Culianez-Macia, F.A. 1999. *Arabidopsis thaliana* AtHAL3: a flavoprotein related to salt and osmotic tolerance and plant growth. Plant J. 20: 529-539.

Fairall, L., Schwabe, J.W., Chapman, L., Finch, J.T., and Rhodes, D. 1993. Th e crystal structure of a two zinc-finger peptide reveals an extension to

the rules for zinc-finger/DNA recognition. Nature 366: 482-487.

Fan, W., Lou, H.Q., Gong, Y.L., Liu, M.Y., Cao, M.J., Liu, Y., Yang, J.L., and Zheng, S.J. 2015. Characterization of an inducible C2H2 -type zinc fin ger transcription factor VuSTOP1 in rice bean (*Vigna umbellata*) reveals differential regulation between low pH and aluminum tolerance mech anisms. New Phytol. 208: 456-468.

Faso, C., Chen, Y.N., Tamura, K., Held, M., Zemelis, S., Marti, L., Saravanan, R., Hummel, E., Kung, L., and Miller, E. 2009. A missense mutation i n the Arabidopsis COPII coat protein Sec24A induces the formation of clusters of the endoplasmic reticulum and Golgi apparatus. Plant Cell 21: 3655-3671.

Feng, H., Pyykko, I., and Zou, J. 2016. Involvement of ubiquitin-editing pro tein A20 in modulating inflammation in rat cochlea associated with s ilver nanoparticle-induced CD68 upregulation and TLR4 activation. Nanoscale Res Lett. 11: 240.

Font, J., and Mackay, J.P. 2010. Beyond DNA: zinc finger domains as RNA-bi nding modules. Methods Mol Biol. 649: 479-491.

Frassinetti, S., Bronzetti, G., Caltavuturo, L., Cini, M., and Croce, C.D. 2006 The role of zinc in life: a review. J Environ Pathol Toxicol Oncol. 25: 59 7–610.

Freemont, P.S., Hanson, I.M., Trowsdale, J. 1991. A novel cysteine-rich seque nce motif. Cell 64**:** 483–484.

Fu, M., and Blackshear, P.J. 2017. RNA-binding proteins in immune regulatio n: a focus on CCCH zinc finger proteins. Nat Rev Immunol. 17: 130–14 3.

Furniss, J.J., and Spoel, S.H. 2014. Cullin-RING ubiquitin ligases in salicylic a cid-mediated plant immune signaling. Front Plant Sci. 6: 154-154.

Gachomo, E.W., Jimenez-Lopez, J.C., Baptiste, L.J., and Kotchoni, S.O. 2014. GIGANTUS1 (GTS1), a member of Transducin/WD40 protein superfa

mily, controls seed germination, growth and biomass accumulation th rough ribosome-biogenesis protein interactions in *Arabidopsis thaliana*. BMC Plant Biol. 14: 37.

Gamsjaeger, R., Liew, C.K., Loughlin, F.E., Crossley, M., and Mackay, J.P. 2 007. Sticky fingers: zinc-fingers as protein-recognition motifs. Trends Biochem. Sci. 32: 63-70.

Gehring, W.J., Affolter, M., and Burglin, T. 1994. Homeodomain proteins. A nnu Rev Biochem. 63: 487–526.

Gibson, T.J. 2009. Cell regulation: determined to signal discrete cooperation. Trends Biochem. Sci. 34: 471-482.

Guan, Q.J., Wang, L.F., Bu, Q.Y., and Wang, Z.Y. 2014. The rice gene OsZFP6 functions in multiple stress tolerance responses in yeast and Arabidop sis. Plant Physiol Biochem 82: 1-8.

Guddat, U., Bakken, A.H., and Pieler, T. 1990. Protein-mediated nuclear exp ort of RNA: 5S rRNA containing small RNPs in *Xenopus oocytes*. Cell 6 0: 619-28.

Guerra, D.D., Pratelli, R., Kraft, E., Callis, J., and Pilot, G. 2013. Functional c onservation between mammalian MGRN1 and plant LOG2 ubiquitin l igases. FEBS Lett. 587: 3400-5.

Hare, P. D., Moller, S.G., Huang, L.F., and Chua, N.H. 2003. LAF3, a novel fa ctor required for normal phytochrome A signaling. Plant Physiol. 133: 1592-1604.

Hematy, K., Bellec, Y., Podicheti, R., Bouteiller, N., Anne, P., Morineau, C., Haslam, R.P., Beaudoin, F., Napier, J.A., Mockaitis, K., Gagliardi, D., Vaucheret, H., Lange, H., Faure, J.D. 2016. The zinc-finger protein SO P1 is required for a subset of the nuclear exosome functions in Arabid opsis. PLoS Genet. 12: e1005817.

Hennon, S.W., Soman, R., Zhu, L., and Dalbey, R.E. 2015. YidC/Alb3/Oxa1 family of invertases. J. Biol. Chem. 290: 14866–14874.

Hiraga, S., Sasaki, K., Ito, H., Ohashi, Y., and Matsui, H. 2001. A large famil y of class III plant peroxidases. Plant Cell Physiol. 42: 462-468.

Horsch, R.B., Fry, J.E., Hoffmann, N.L., Eichholtz, D., Rogers, S.G., and Fral ey, R.T. 1985. A simple and general method for transferring genes into plants. Science 227: 1229-1231.

Houbaviy, H.B., Usheva, A., Shenk, T., and Burley, S.K. 1996. Cocrystal stru cture of YY1 bound to the adeno-associated virus P5 initiator. Proc Na tl Acad Sci USA. 93: 13577-13582.

Houben, K., Wasielewski, E., Dominguez, C., Kellenberger, E., Atkinson, R. A., Timmers, H.T., Kieffer, B., and Boelens, R. 2005. Dynamics and m etal exchange properties of C4C4 RING domains from CNOT4 and the p44 subunit of TFIIH. J Mol Biol. 349: 621-637.

Howard, M.L., and Davidson, E.H. 2004. cis-Regulatory control circuits in de velopment. Dev Biol**.** 271: 109-18.

Hua, Z., and Vierstra, R.D. 2011. The cullin-RING ubiquitin-protein ligases. Annu Rev Plant Biol. 62: 299-334.

Hwang, J.U., Song, W.Y., Hong, D., Ko, D., Yamaoka, Y., Jang, S., Yim, S., Le e, E., Khare, D., Kim K., Palmgren, M., Yoon, H.S., Martinoia, E., and Lee, Y. 2016. Plant ABC transporters enable many unique aspects of a terrestrial plant's lifestyle. Mol Plant 9: 338-355.

Iyer, L.M., Abhiman, S., de Souza, R.F., and Aravind, L. 2010. Origin and ev olution of peptide-modifying dioxygenases and identification of the w ybutosine hydroxylase/hydroperoxidase. Nucleic Acids Res. 38: 5261-5279.

Jackson, R.G., Kowalczyk, M., Li, Y., Higgins, G., Ross, J., Sandberg, G., an d Bowles, D.J. 2002. Over-expression of an Arabidopsis gene encodin g a glucosyltransferase of indole-3-acetic acid: Phenotypic characteriza tion of transgenic lines. Plant J. 32: 573–583.

Jan, A., Maruyama, K., Todaka, D., Kidokoro, S., Abo, M., Yoshimura, E., S

hinozaki, K., Nakashima, K., and Yamaguchi-Shinozaki, K. 2013. Os TZF1, a CCCH-tandem zinc finger protein, confers delayed senescenc e and stress tolerance in rice by regulating stress-related genes Plant P hysiol. 161: 1202– 1216.

Jang, K., Lee, H.G., Jung, S.J., Paek, N.C., and Seo, P.J. 2015. The E3 ubiquiti n ligase COP1 regulates thermosensory flowering by triggering GI de gradation in Arabidopsis. Sci Rep. 5: 12071.

Joseph, M.P., Papdi, C., Kozma-Bognar, L., Nagy, I., Lopez-Carbonell, M., R igo, G., Koncz, C., and Szabados, L. 2014. The Arabidopsis ZINC FIN GER PROTEIN3 Interferes with Abscisic Acid and Light Signaling in S eed Germination and Plant Development. Plant Physiol. 165: 1203-122 0.

K, M.J., and Laxmi, A. 2014. DUF581 is plant specific FCS-like zinc finger inv olved in protein-protein interaction. PLoS One 9: e99074.

Kadrmas J.L., and Beckerle, M.C. 2004. The LIM domain: From the cytoskelet on to the nucleus. Nat. Rev. Mol. Cell Biol. 5: 920–931.

Kielbowicz-Matuk, A. 2012. Involvement of plant C2H2-type zinc finger tran scription factors in stress responses. Plant Sci. 185-186: 78-85.

Kim, W.C., Kim, J.Y., Ko, J.H., Kang, H., Kim, J., and Han, K.H. 2014. AtC3H 14, a plant-specific tandem CCCH zinc-finger protein, binds to its targ et mRNAs in a sequence-specific manner and affects cell elongation in Arabidopsis thaliana. Plant J. 80: 772-784.

Kong, Z., Li, M., Yang, W., Xu, W., and Xue, Y. 2006. A novel nuclear-localize d CCCH-type zinc finger protein, OsDOS, is involved in delaying leaf senescence in rice. Plant Physiol. 141: 1376-1388.

Klug, A. 2010. The discovery of zinc fingers and their applications in gene reg ulation and genome manipulation Annu. Rev. Biochem. 79: 213–231.

Klumper, W., and Qaim, M. 2014. A meta-analysis of the impacts of genetical

ly modified crops. PLoS One 9: e111629.

Knoch, E., Dilokpimol, A., and Geshi, N. 2014. Arabinogalactan proteins: foc us on carbohydrate active enzymes. Front Plant Sci. 11: 198.

Krishna, S.S., Majumdar, I., and Grishin, N.V. 2003. Structural classification of zinc fingers: survey and summary. Nucleic Acids Res. 31: 532-550.

Kuhn, K., Obata, T., Feher, K., Bock, R., Fernie, A.R., and Meyer, E.H. 2015. Complete mitochondrial complex I deficiency induces an up-regulatio n of respiratory fluxes that is abolished by traces of functional comple x I. Plant Physiol. 168: 1537-1549.

Kumar, S., Jordan, M.C., Datla, R., and Cloutier, S. 2013. The LuWD40-1 gen e encoding WD repeat protein regulates growth and pollen viability in flax (*Linum usitatissimum* L.). PLoS One 8: e69124.

Laity, J.H., Lee, B.M., and Wright, P.E. 2001. Zinc finger proteins: new insight s into structural and functional diversity. Curr. Opin. Struct. Biol. 11: 3 9-46.

Lamport, D.T., Kieliszewski, M.J., Chen, Y., and Cannon, M.C. 2011. Role of the extension superfamily in primary cell wall architecture. Plant Phys iol. 156: 11-19.

Larrieu, A., and Vernoux, T. 2015. Comparison of plant hormone signalling s ystems. Essays Biochem. 58: 165-181.

Lazarou, M., Thorburn, D.R., Ryan, M.T., and McKenzie, M. 2009. Assembl y of mitochondrial complex I and defects in disease. Biochim. Biophys. Acta 1793: 78–88.

Lee, H.K., Cho, S.K., Son, O., Xu, Z., Hwang, I., and Kim, W.T. 2009. Drough t stress-induced Rma1H1, a RING membrane-anchor E3 ubiquitin liga se homolog, regulates aquaporin levels via ubiquitination in transgeni c Arabidopsis plants. Plant Cell 21: 622-641.

Lee, T.I., and Young, R.A. 2000. Transcription of eukaryotic protein-coding g enes. Annu Rev Genet. 34: 77–137.

Li, J., Zhu, S., Song, X., Shen, Y., Chen, H., Yu, J., Yi, K., Liu, Y., Karplus, V. J., and Wu, P. 2006. A rice glutamate receptor–like gene is critical for t he division and survival of individual cells in the root apical meristem. Plant Cell 18: 340-349.

Li, W.T., Chen, W.L., Yang, C., Wang, J., Yang, L., He, M., Wang, J.C., Qin, P., Wang, Y.P., and Ma, B.T. 2014. Identification and network constructi on of zinc finger protein (ZFP) genes involved in the rice-*Magnaporthe oryzae* interaction. Plant Omics 7: 540.

Lin, A.W., and Man, H.Y. 2013. Ubiquitination of neurotransmitter receptors and postsynaptic scaffolding proteins Neural Plast 2013: 432057.

Lim, S.D., Cho, H.Y., Park, Y.C., Ham, D.J., Lee, J.K., and Jang, C.S. 2013.The rice RING finger E3 ligase, OsHCI1, drives nuclear export of multiple substrate proteins and its heterogeneous overexpression enhances acq uired thermotolerance J. Exp. Bot. 64: 2899–2914.

Linnen, J.M., Bailey, C.P., and Weeks, D.L. 1993. Two related localized mRN As from *Xenopus laevis* encode ubiquitin-like fusion proteins. Gene 12 8: 181–8.

Littlewood, T.D., and Evan, G.I. 1995. Transcription factors 2: helix-loop-heli x. Protein Profile 2: 621–702.

Liu, C.H., Finke, A., Diaz, M., Rozhon, W., Poppenberger, B., Baubec, T., an d Pecinka, A. 2015. Repair of DNA damage induced by the cytidine a nalog zebularine requires ATR and ATM in Arabidopsis. Plant Cell 2 7: 1788-1800.

Liu, J., Zhang, C., Wei, C., Liu, X., Wang, M., Yu, F., Xie, Q., and Tu, J. 2015. The RING finger ubiquitin E3 ligase OsHTAS enhances heat tolerance by promoting H_2O_2-induced stomatal closure in Rice. Plant Physiol. 17 0: 429-443.

Lovering, R., Hanson, I.M., Borden, K.L., Martin, S., O'Reilly, N.J., Evan, G. I., Rahman, D., Pappin, D.J., Trowsdale, J., and Freemont, P.S. 1993. I dentification and preliminary characterization of a protein motif relate d to the zinc finger. Proc Natl Acad Sci USA 90**:** 2112–2116.

Marjamaa, K., Kukkola, E.M., and Fagerstedt, K.V. 2009. The role of xylem cl ass III peroxidases in lignification. J. Exp. Bot. 60: 367-376.

Martin, L., Decourteix, M., Badel, E., Huguet, S., Moulia, B., Julien, J.L., and Leblanc-Fournier, N. 2014. The zinc finger protein PtaZFP2 negativel y controls stem growth and gene expression responsiveness to externa l mechanical loads in poplar. New Phytol 203: 168-181.

Matthews, J.M., Kowalski, K., Liew, C.K., Sharpe, B.K., Fox, A.H., Crossley, M., and Mackay, J. P. 2000. A class of zinc fingers involved in protein-protein interactions. Eur. J. Biochem. 267: 1030-1038.

Matthews, J.M., and Sunde, M. 2002. Zinc fingers-folds for many occasions. I UBMB Life 54: 351-355.

Matthews, J.M., Bhati, M., Lehtomaki, E., Mansfield, R.E., Cubeddu, L., and Mackay, J.P. 2009. It takes two to tango: the structure and function of LIM, RING, PHD and MYND domains. Curr Pharm Des. 15: 3681-369 6.

McCarty, A.S., Kleiger, G., Eisenberg, D., and Smale, S.T. 2003. Selective di merization of a C2H2 zinc finger subfamily. Mol. Cell 11: 459–470.

McKay, D.B., and Steitz, T.A. 1981. Structure of catabolite gene activator prot ein at 2.9 A resolution suggests binding to left-handed B-DNA. Nature 290: 744–9.

Meyer, S., and Kieffer, B. 2015. *Protein motifs: Zinc fingers*. (John Wiley and S ons, New York).

Migliori, V., Mapelli, M., and Guccione, E. 2012. On WD40 proteins: propelli ng our knowledge of transcriptional control? Epigenetics 7: 815-822.

Miller, J., McLachlan, A.D., and Klug, A. 1985. Repetitive zinc-binding doma

ins in the protein transcription factor IIIA from *Xenopus oocytes*. EMBO J. 4: 1609-1614.

Miyashima S., Sebastian J., Lee J. Y., and Helariutta Y. 2013. Stem cell functi on during plant vascular development. EMBO J. 32: 178–193.

Moldovan J.B., and Moran J.V. 2015. The zinc-finger antiviral protein ZAP in hibits LINE and Alu retrotransposition. PLoS Genet. 11: e1005121.

Montano, G., Cesaro, E., Fattore, L., Vidovic, K., Palladino, C., Crescitelli, R., Izzo, P., Turco, M.C., and Costanzo, P. 2013. Role of WT1–ZNF224 int eraction in the expression of apoptosis-regulating genes. Hum Mol Ge net. 22: 1771-1782.

Motose, H., Hamada, T., Yoshimoto, K., Murata, T., Hasebe, M., Watanabe, Y., Hashimoto, T., Sakai, T., and Takahashi, T. 2011. NIMA-related ki nases 6, 4, and 5 interact with each other to regulate microtubule orga nization during epidermal cell expansion in Arabidopsis thaliana. Pla nt J. 67: 993-1005.

Muto, Y., Pomeranz Krummel, D., Oubridge, C., Hernandez, H., Robinson, C.V., Neuhaus, D., and Nagai, K. 2004. The structure and biochemical properties of the human spliceosomal protein U1C. J Mol Biol 341: 185 -98.

Nakayama, K.I., and Nakayama, K. 2006. Ubiquitin ligases: cell-cycle control and cancer. Nat Rev Cancer 6: 369–81.

Nicolia, A., Manzo, A., Veronesi, F., and Rosellini, D. 2013. An overview of t he last 10 years of genetically engineered crop safety research. Crit. Re v. Biotechnol. 34: 1–12.

Niksic, M., Slight, J., Sanford, J.R., Caceres, J.F., and Hastie, N.D. 2004. Wil ms' tumour protein (WT1) shuttles between nucleus and cytoplasm an d is present in functional polysomes. Hum Mol Genet 13: 463-71.

Nolte, R.T., Conlin, R.M., Harrison, S.C., and Brown, R.S. 1998. Differing rol es for zinc fingers in DNA recognition: structure of a six-finger transcr

iption factor IIIA complex. Proc Natl Acad Sci USA. 95: 2938-2943.

Ogo, O.A., Tyson, J., Cockell, S.J., Howard, A., Valentine, R.A., and Ford, D. 2015. The zinc finger protein ZNF658 regulates the transcription of genes involved in zinc homeostasis and affects ribosome biogenes is through the zinc transcriptional regulatory element. Mol. Cell. Bio l. 35: 977–987.

Ogura, K., Kishimoto, N., Mitani, S., Gengyo-Ando, K., and Kohara, Y. 2003. Translational control of maternal glp-1 mRNA by POS-1 and its intera cting protein SPN-4 in *Caenorhabditis elegans*. Development 130: 2495-2 503.

Pabo, C.O., and Lewis, M. 1982. The operator-binding domain of lambda rep ressor: structure and DNA recognition. Nature 298: 443–7.

Papworth, M., Kolasinska, P. and Minczuk, M. 2006. Designer zinc-finger pr oteins and their applications. Gene 366: 27-38.

Park, C., Lim, W.C., Baek, W., Kim, J.H., Lim, S., Kim, H.S., Kim, K.N., and Lee, C.S. 2017. The pepper WPP domain protein, CaWDP1, acts as a n ovel negative regulator of drought stress via ABA signaling. Plant Cell Physiol. 58: 779-788.

Park, C., Lim, C.W., Baek, W., and Lee, S.C. 2015. RING type E3 ligase CaAI R1 in pepper acts in the regulation of abscisic acid signaling and drou ght stress response. Plant Cell Physiol. 56: 1808-19.

Park, D. S., **Yu, Y. M.**, **Kim, Y. J.**, and **Maeng, P. J.** 2015. Negative regulation of the vacuole-mediated resistance to K(+) stress by a novel C2H2 zinc finger transcription factor encoded by *aslA* in *Aspergillus nidulans*. J. M icrobiol. 53: 100-110.

Park, G.G., Park, J.J., Yoon, J., Yu, S.N., and An, G. 2010. A RING finger E3 li gase gene, *Oryza sativa* Delayed Seed Germination 1 (OsDSG1), contro ls seed germination and stress responses in rice. Plant Mol Biol. 74: 467 -478.

Park, J., Nguyen, K.T., Park, E., Jeon, J.S., and Choi, G. 2013. DELLA protein s and their interacting RING Finger proteins repress gibberellin respo nses by binding to the promoters of a subset of gibberellin-responsive genes in Arabidopsis. Plant Cell 25: 927-943.

Park, S.J., Kim, S.L., Lee, S., Je, B.I., Piao, H.L., Park, S.H., Kim, C.M., Ryu, C.H., Park, S.H., Xuan, Y.H., Colasanti, J., An, G., and Han, C.D. 2008. Rice Indeterminate 1 (OsId1) is necessary for the expression of Ehd1 (Early heading date 1) regardless of photoperiod. Plant J. 56: 1018-1029.

Pavletich, N.P., and Pabo, C.O. 1991. Zinc finger-DNA recognition: crystal str ucture of a Zif268-DNA complex at 2.1 A. Science 252: 809-817.

Pavletich, N.P., and Pabo, C.O. 1993. Crystal structure of a five-finger GLI-D NA complex: new perspectives on zinc fingers. Science 261: 1701-7.

Pearson, H. 2008. The fate of fingers. Nature 455: 160-164.

Pennell, R.I., and Roberts, K. 1990. Sexual development in the pea is presage d by altered expression of arabinogalactan protein. Nature 344: 547-54 9.

Pohlmann, T., Baumann, S., Haag, C., Albrecht, M., and Feldbrugge, M. 201 5. A FYVE zinc finger domain protein specifically links mRNA transp ort to endosome trafficking. eLife **4**.

Ponting, C.P., Blake, D.J., Davies, K.E., Kendrick-Jones, J., and Winder, S. J. 1996. ZZ and TAZ: new putative zinc fingers in dystrophin and othe r proteins. Trends Biochem Sci. 21**:** 11–13.

Qu, J., Kang, S.G., Wang, W., Musier-Forsyth, K., and Jang, J.C. 2014. *Arabid opsis thaliana* tandem zinc finger 1 (AtTZF1) protein in RNA binding a nd decay. Plant J. 78: 452–467.

Qu, X., Chatty, P.R., and Roeder, A.H. 2014. Endomembrane trafficking prote in SEC24A regulates cell size patterning in Arabidopsis. Plant Physiol. 166: 1877-1890.

Rodriguez, M.S., Egana, I., Lopitz-Otsoa, F., Aillet, F., Lopez-Mato, M., Dorr

onroso, A., Lobato-Gil, S., Sutherland, J., Barrio, R., and Trigueros, C. 2014. The ring ubiquitin e3 rnf114 interacts with a20 and modulates nf -κb activity and t-cell activation. Cell Death Dis. 5: e1399.

Rosato, E., Tauber, E., and Kyriacou, C.P. 2006. Molecular genetics of the fru it-fly circadian clock. Eur. J. Hum. Genet. 14: 729–738.

Saitou, N., and Nei, M. 1987. The neighbor-joining method: a new method fo r reconstructing phylogenetic trees. Mol Biol Evol. 4: 406-425.

Sambrook, J., and Russell, D. W. 2001. *Molecular cloning*. Cold spring harbor l aboratory press New York..

Sanchez, R., and Zhou, M.M. 2011**.** The PHD finger: a versatile epigenome re ader. Trends Biochem. Sci. 36: 364–72.

Schmitz-Linneweber, C., and Small, I. 2008. Pentatricopeptide repeat protein s: a socket set for organelle gene expression. Trends Plant Sci. 13: 663-6 70.

Schultz, C.J., Johnson, K.L., Currie, G., Bacic, A. 2000. The classical arabinog alactan protein gene family of Arabidopsis. Plant Cell 12: 1751–1767.

Schulz, B., and Kolukisaoglu, H.U. 2006. Genomics of plant ABC transporter s: the alphabet of photosynthetic life forms or just holes in membrane s? FEBS letters 580: 1010-1016.

Schumann, U., Prestele, J., O'Geen, H., Brueggeman, R., Wanner, G., and Gi etl, C. 2007. Requirement of the C3HC4 zinc RING Wnger of the *Arabi dopsis PEX10* for photorespiration and leaf peroxisome contact with ch loroplasts. Proc Natl Acad Sci USA. 104: 1069–1074.

Seong, E.S., and Wang, M. 2008. A novel CaAbsi1 gene induced by early-abio tic stresses in Pepper. BMB Rep 41: 86–91.

Seong, E.S., Choi, D., Cho, H.S., Lim, C.K., Cho, H.J., Wang, M.H. 2007. Cha racterization of a stress-responsive ankyrin repeat-containing zinc fing er protein of *Capsicum annuum* (CaKR1). J Biochem Mol Biol. 40: 952-8.

Seok, H.Y., Woo, D.H., Park, H.Y., Lee, S.Y., Tran, H.T., Lee, E.H., Vu Nguye

n, L., and Moon, Y.H. 2016. AtC3H17, a non-tandem CCCH zinc finge r protein, functions as a nuclear transcriptional activator and has pleio tropic effects on vegetative development, flowering and seed develop ment in Arabidopsis. Plant Cell Physiol. 57: 603-615.

Sharma, B., Joshi, D., Yadav, P.K., Gupta, A.K., and Bhatt, T.K. 2016. Role of ubiquitin-mediated degradation system in plant biology. Front Plant S ci. 7: 806.

Shen, L., Thong, Z., Gong, X., Shen, Q., Gan, Y., and Yu, H. 2014. The putati ve PRC1 RING-finger protein AtRING1A regulates flowering through repressing MADS AFFECTING FLOWERING genes in Arabidopsis. D evelopment 141: 1303–1312.

Shi, H., Wang, X., Ye, T., Chen, F., Deng, J., Yang, P., Zhang, Y., and Chan, Z. 2014. The Cysteine2/Histidine2-Type Transcription Factor ZINC FIN GER OF ARABIDOPSIS THALIANA6 Modulates Biotic and Abiotic St ress Responses by Activating Salicylic Acid-Related Genes and C-REP EAT-BINDING FACTOR Genes in Arabidopsis. Plant Physiol. 165: 13 67-1379.

Shimberg, G.D., Michalek, J.L., Oluyadi, A.A., Rodrigues, A.V., Zucconi, B. E., Neu, H.M., Ghosh, S., Sureschandra, K., Wilson, G.M., Stemmler, T.L., and Michel, S.L. 2016. Cleavage and polyadenylation specificity factor 30: an RNA-binding zinc-finger protein with an unexpected 2Fe -2S cluster. Proc Natl Acad Sci USA. 113: 4700–4705.

Showalter, A.M., and Basu, D. 2016. Glycosylation of arabinogalactan-protei ns essential for development in Arabidopsis. Commun Integr Biol. 9: e 1177687.

Small, I.D., and Peeters, N. 2000. The PPR motif–a TPR-related motif prevale nt in plant organellar proteins. Trends Biochem Sci. 25: 45-47.

Spadaccini R., Perrin, H., Bottomley, M.J., Ansieau, S., and Sattler, M. 2006. Structure and functional analysis of the MYND domain. J. Mol. Biol. 3

58: 498–508.

Spiegelman, Z., Ham, B.K., Zhang, Z., Toal, T.W., Brady, S.M., Zheng, Y., Fe i, Z., Lucas, W.J., and Wolf, S. 2015. A tomato phloem-mobile protein regulates the shoot-to-root ratio by mediating the auxin response in di stant organs. Plant J. 83: 853-863.

Splettstoesser, T. 2007. Zinc-finger motif of proteins based on X-ray structure of 1A1L.

Stirnimann, C.U., Petsalaki, E., Russell, R.B., and Muller, C.W. 2010. WD40 proteins propel cellular networks. Trends Biochem Sci. 35: 565-574.

Stone, S.L., Hauksdóttir, H., Troy, A., Herschleb, J., Kraft, E., and Callis, J. 2 005. Functional analysis of the RING-type ubiquitin ligase family of A rabidopsis. Plant Physiol. 137: 13-30.

Stumpo, D.J., Broxmeyer, H.E., Ward, T., Cooper, S., Hangoc, G., Chung, Y. J., Shelley, W.C., Richfield, E.K., Ray, M.K., Yoder, M.C., Aplan, P. D., and Blackshear, P.J. 2009. Targeted disruption of Zfp36l2, encodin g a CCCH tandem zinc finger RNA-binding protein, results in defecti ve hematopoiesis. Blood 114: 2401–2410.

Suh, M.C., Hong, C.B., Kim, S.S., and Sim, W.S. 1994. Transgenic tobacco pl ants with *Bacillus thuringiensis* delta-endotoxin gene resistant to Korea n-born tobacco budworms. Mol. Cells 4: 211-219.

Sun, T., Shi, X., Friso, G., Van Wijk, K., Bentolila, S., and Hanson, M.R. 201 5. A zinc finger motif-containing protein is essential for chloroplast R NA editing. PLoS Genet. 11: e1005028.

Sylvester, A.W. 2000. Division decisions and the spatial regulation of cytokin esis. Curr Opin Plant Biol. 3: 58-66.

Takatani, S., Otani, K., Kanazawa, M., Takahashi, T., and Motose, H. 2015. S tructure, function, and evolution of plant NIMA-related kinases: impli cation for phosphorylation-dependent microtubule regulation. J. Plant Res. 128: 875-891.

Takatsuji, H. 1998. Zinc-finger transcription factors in plants. Cell Mol Life Sc i. 54: 582-596.

Takatsuji, H. 1999. Zinc-finger proteins: the classical zinc finger emerges in c ontemporary plant science. Plant Mol Biol. 39: 1073-1078.

Tamura, K., Stecher, G., Peterson, D., Filipski, A., and Kumar, S. 2013. MEG A6: Molecular Evolutionary Genetics Analysis version 6.0. Mol Bio Ev ol. 30: 2725-2729.

Tapken, D., Anschütz, U., Liu, L.H., Huelsken, T., Seebohm, G., Becker, D., and Hollmann, M. 2013. A plant homolog of animal glutamate recept ors is an ion channel gated by multiple hydrophobic amino acids. Sci S ignal. 6: ra47.

To, J.P.C., Deruere, J., Maxwell, B.B., Morris, V.F., Hutchison, C.E., Ferreira, F.J., Schaller, G.E., and Kieber, J.J. 2007. Cytokinin regulates type-A Arabidopsis Response Regulator activity and protein stability via two-component phosphorelay. Plant Cell 19: 3901-3914.

Tognolli, M., Penel, C., Greppin, H., and Simon, P. 2002. Analysis and expre ssion of the class III peroxidase large gene family in Arabidopsis thalia na. Gene 288: 129-138.

Uberto, R., and Moomaw, E.W. 2013. Protein similarity networks reveal relati onships among sequence, structure, and function within the cupin sup erfamily. PLoS One 8: e74477.

Uchida, N., and Tasaka, M. 2013. Regulation of plant vascular stem cells by e ndodermis-derived EPFL-family peptide hormones and phloem-expre ssed ERECTA-family receptor kinases. J Exp Bot 64: 5335–5343.

Venturini, L., Stadler, M., Manukjan, G., Scherr, M., Schlegelberger, B., Stei nemann, D., and Ganser, A. 2015. The stem cell zinc finger 1 (SZF1)/ ZNF589 protein has a human-specific evolutionary nucleotide DNA c hange and acts as a regulator of cell viability in the hematopoietic syst em. Exp Hematol. 44: 257–268.

Vierstra, R.D. 2009. The ubiquitin–26S proteasome system at the nexus of pla nt biology. Nat Rev Mol Cell Biol. 10: 385-397.

Vinson, C., Myakishev, M., Acharya, A., Mir, A.A., Moll, J.R., and Bonovich, M. 2002. Classification of human B-ZIP proteins based on dimerizatio n properties. Mol Cell Biol. 22: 6321–35.

Vogel, J.T., Zarka, D.G., Van Buskirk, H.A., Fowler, S.G., and Thomashow, M.F. 2005. Roles of the CBF2 and ZAT12 transcription factors in config uring the low temperature transcriptome of Arabidopsis. Plant J. 41: 1 95–211.

Wagner, R., von Sydow, L., Aigner, H., Netotea, S., Brugiere, S., Sjogren, L., Ferro, M., Clarke, A., and Funk, C. 2016. Deletion of FtsH11 protease has impact on chloroplast structure and function in *Arabidopsis thalian a* when grown under continuous light. Plant Cell Environ. 39: 2530-25 44.

Waltzer, L., Bataillé, L., Peyrefitte, S., and Haenlin, M. 2016. Two isoforms of Serpent containing either one or two GATA zinc fingers have different roles in Drosophila haematopoiesis. EMBO J. 35: 553-553.

Wang, Z., Schwacke, R., and Kunze, R. 2016. DNA damage-induced transcri ption of transposable elements and long non-coding RNAs in Arabido psis is rare and ATM-dependent. Mol Plant 9: 1142–55.

Wray, G.A., Hahn, M.W., Abouheif, E., Balhoff, J.P., Pizer, M., Rockman, M. V., and Romano, L.A. 2003. The evolution of transcriptional regulatio n in eukaryotes. Mol Biol Evol. 20: 1377–1419.

Weiland, M., Mancuso, S., and Baluska, F. 2016. Signalling via glutamate an d GLRs in *Arabidopsis thaliana*. Funct. Plant Biol. 43: 1-25.

Wigington, C.P., Morris, K.J., Newman, L.E., and Corbett, A.H. 2016. The po lyadenosine RNA binding protein, Zinc Finger Cys3His Protein #14 (Z C3H14), regulates the pre-mRNA processing of a key ATP synthase su bunit mRNA. J Biol Chem. 291: 22442-22459.

Wolfe, S.A., Nekludova, L., and Pabo, C.O. 1999. DNA recognition by Cys2 His2 Zinc finger proteins. Annu. Rev. Biophys. Biomol. Struct. 3: 183-2 12.

Xie, Q., Guo, H.S., Dallman, G., Fang, S., Weissman, A.M., and Chua, N.H. 2002. SINAT5 promotes ubiquitin-related degradation of NAC1 to atte nuate auxin signals. Nature 419: 167-170.

Xiang, Y., Huang, Y., and Xiong L. 2007. Characterization of stress responsive CIPK genes in rice for stress tolerance improvement. Plant Physiol 14 4: 1416–1428.

Xing, S.P., Quodt, V., Chandler, J., Hohmann, S., Berndtgen, R., and Huijser, P. 2013. SPL8 acts together with the brassinosteroid-signaling compon ent BIM1 in controlling *Arabidopsis thaliana* male fertility. Plants 2: 416-428.

Yang, M., May, W.S., and Ito, T. 1999. JAZ requires the double-stranded RN A binding zinc finger motifs for nuclear localization. J Biol Chem 274: 27399-406.

Yang, Y., Ma, C., Xu, Y., Wei, Q., Imtiaz, M., Lan, H., Gao, S., Cheng, L., Wa ng, M., Fei, Z., Hong, B., and Gao, J. 2014. A Zinc Finger Protein Regu lates Flowering Time and Abiotic Stress Tolerance in Chrysanthemum by Modulating Gibberellin Biosynthesis. Plant Cell 26: 2038-2054.

Yoo, C.M., Wen, J., Motes, C.M., Sparks, J.A., and Blancaflor, E.B. 2008. A cl ass I ADP-ribosylation factor GTPase-activating protein is critical for maintaining directional root hair growth in Arabidopsis. Plant Physiol. 147: 1659-1674.

Yu, Y., Xu, W., Wang, J., Wang, L., Yao, W., Yang, Y., Xu, Y., Ma, F., Du, Y., a nd Wang, Y. 2013. The Chinese wild grapevine (*Vitis pseudoreticulata*) E3 ubiquitin ligase *Erysiphe necator*-induced RING finger protein 1 (EI RP1) activates plant defense responses by inducing proteolysis of the VpWRKY11 transcription factor. New Phytol. 200: 834-846.

Yuan, C., Zhou, G., Li, Y., Wang, K., Wang, Z., Li, X., Chang, R., and Qiu, L. 2008. Cloning and sequence diversity analysis of GmHs1 pro-1 in Chi nese domesticated and wild soybeans. Mol. Breed. 22: 593-602.

Yuan, J., Song, J., Ma, H., Song, X., Wei, H., and Liu, Y. 2015. Ectopic express ion a maize ADP-ribosylation factor gene in Arabidopsis, increase pla nt size and growth rate. J. Plant Biochem. Biotechnol. 24: 161-166.

Yuan, X., Zhang, S., Liu, S., Yu, M., Su, H., Shu, H., and Li, X. 2013. Global a nalysis of ankyrin repeat domain C3HC4-type RING finger gene famil y in plants. PLoS One 8: e58003.

Zeba, N., Isbat, M., Kwon, N.J., Lee, M.O., Kim, S.R., and Hong, C.B. 2009. Heat-inducible C3HC4 type RING zinc finger protein gene from *Capsi cum annuum* enhances growth of transgenic tobacco. Planta 229: 861-87 1.

Zeng, C.T., Lee, Y.R.J., and Liu, B. 2009. The WD40 repeat protein NEDD1 fu nctions in microtubule organization during cell division in Arabidopsi s thaliana. Plant Cell 21: 1129-1140.

Zhang, H.W., Cui, F., Wu, Y.R., Lou, L.J., Liu, L.J., Tian, M.M., Ning, Y., Shu, K., Tang, S.Y., and Xie, Q. 2015. The RING finger ubiquitin E3 ligase S DIR1 targets SDIR1-Interacting Protein1 for degradation to modulate t he salt stress response and ABA signaling in Arabidopsis Plant Cell 2 7: 214–227.

Zhang, X., Garreton, V., and Chua, N.H. 2005. The AIP2 E3 ligase acts as a no vel negative regulator of ABA signaling by promoting ABI3 degradati on. Genes Dev. 19: 1532-1543.

Zhou, C.Y., Zha, X.F., Liu, H.W., and Xia, Q.Y. 2016. Zinc finger protein rotu nd deficiency affects development of the thoracic leg in *Bombyx mori*. I nsect science 0: 1-12.

Zorzatto, C., Machado, J.P., Lopes, K.V., Nascimento, K.J., Pereira, W.A., Br ustolini, O.J., Reis, P.A., Calil, I.P., Deguchi, M., Sachetto-Martins,

G., Gouveia, B.C., Loriato, V.A., Silva, M.A., Silva, F.F., Santos, A.A., Chory, J., and Fontes, E.P. 2015. NIK1-mediated translation suppressi on functions as a plant antiviral immunity mechanism. Nature 520: 67 9-682.

Abstract in Korean

하나의 종에서 다른 종으로 유전자를 옮기는 것이 분자생물학적 방법으로 가능해짐에 따라 작물 생산량이 향상되었다. 하지만 이러한 유전공학기술은 환경 문제 등 예상치 못한 부작용에 대한 염려를 일으켰다. 여기서 우리는 특정 기능의 유전자를 다른 종으로 옮긴 경우 원래의 기능과 완전히 다른 결과를 보일 수 있다는 증거를 제시하고자 한다. 본 연구에서 관찰대상인 *Capsicum annuum RING Zinc Finger Protein 1* (*CaRZFP1*) 은 기존에 열 자극을 받은 고추의 cDNA library에서 동정된 C3HC4-type RING zinc finger protein 유전자이다. *CaRZFP1*의 생체 내 기능에 대한 우리 연구실 선행 연구에서, 우리는 이 유전자를 담배 (*Nicotiana tabacum*)에 옮기는 조작이 식물에서의 비생물학적 스트레스에 대한 저항성이 향상됨을 보여준 바 있다. 외부 종에 옮겨져서 발현 유도된 *CaRZFP1*에 대한 후속 연구로 우리는 양상추 (*Lactuca sativa*) 에서 *CaRZFP1*이 발현되게 하였다. 담배의 경우와는 다르게 형질전환 양상추는 대조군에 비하여 덜 성장하고 개화 시기도 늦어짐을 관찰하였다. 이들이 보인 다른 특징으로는 잎 성장 저해, 작은 키, 그리고 짧은 뿌리 등이 있었다. 더불어, 이러한 성장 저해는 *CaRZFP1*과 상당한 상관 관계를 보였다. 또한 *CaRZFP1*이 발현된 양상추에서는 내배엽과 관다발의 발생도 저해되는 것을 확인하였다. 이러한 현상에 관여하는 유전자를 알아내기 위하여 두 종의 형질전환 식물의 전사체를 분석하였고 담배와 양상추에서 다른 결과가 보이게끔

하는 수십 개의 유전자를 알아낼 수 있었다. 특히 *CaRZFP1*과 성장 사이의 뚜렷한 음의 상관관계를 통하여 현상적 차이에 관여할 것으로 생각되는 유전자를 골라낼 수 있었다. 그러한 유전자로는 단백질 인산화효소, 전사인자, 운반 단백질, 호르몬 및 대사 관련 유전자, 기존에 연구되지 않은 유전자 등을 제시할 수 있었다. 양상추와 담배에서 보이는 *CaRZFP1* 발현의 상반된 영향은 종간 형질전환에 의한 예기치 못한 부작용에 대한 연구의 시작점이 될 것으로 기대한다.

Student Number: 2010-31292